SYNTHESIS AND DEVELOPMENT OF LANTADENE CONGENERS AS ANTICANCER AGENTS

Thesis submitted in fulfillment for the requirement of the Degree of

DOCTOR OF PHILOSOPHY

by

SUTHAR SHARAD KUMAR

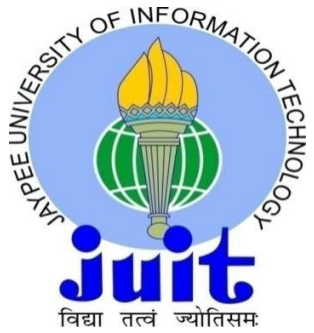

Department of Pharmacy

JAYPEE UNIVERSITY OF INFORMATION TECHNOLOGY

WAKNAGHAT, SOLAN-173234, HIMACHAL PRADESH, INDIA

December 2014

Dedicated to

My Beloved Parents & family

My Supervisor Dr. Manu Sharma &

My Friend Late Mr. Mayur S. Mahajan

ABSTRACT

The cancer is a rapid and uncontrolled growth of the cells, which metastasizes to the other parts of the body via the blood stream and the lymphatic system. Numerous recent studies have revealed the close association between the cancer and inflammation. The chimeric nonsteroidal anti-inflammatory drugs (NSAIDs) are increasingly gaining the ground in recent years as the anticancer agents, since their target protein cyclooxygenase-2 (COX-2) has been found to be actively involved in various malignancies. Lantadenes are the pentacyclic triterpenoids present in the leaves of weed *Lantana camara* Linn. These lantadenes, particularly lantadene A and B have been extensively explored in the last few years for their anticancer potential, predominantly by our group and have shown the remarkable cytotoxicity against the lung cancer cells, while suppressing the cell proliferation and differentiation regulating protein nuclear factor-kappa B (NF-κB). Keeping these accounts in mind, we have synthesized the conjugates of NF-κB inhibitory scaffold lantadene and COX suppressing NSAIDs, as the novel dual acting inhibitors of NF-κB and COX, in the form of lantadene–NSAID hybrid compounds. Along with these lantadene–NSAID conjugates, various other congeners of lantadenes were also synthesized.

The structural modifications were made at the C-3, C-22, and C-28 positions of the lantadenes. Among the esters synthesized at the C-3 position of lantadenes, the cinnamic acid (**50**–**51**) and diclofenac conjugates (**63**–**64**) showed the highest inhibition of inhibitor of nuclear factor-kappa B kinase (IKK) that subsequently suppressed the inhibitor of nuclear factor-kappa B alpha (IκBα) degradation and restrained the NF-κB to transmigrate into the nucleus, thereby stifling the transcription of proteins responsible for oncogenesis. The hydrolysis of C-22 ester side chain as well as synthesis of congeners at C-22 position led to a decrease in the NF-κB and COX inhibitory potentials, indicating the vital

importance of the C-22 ester side chain in the activity. Interestingly, when NSAIDs were conjugated at both the C-3 and C-22 positions of the lantadene (22*β*-hydroxy-oleanolic acid **38**), it dramatically augmented the COX inhibitory activity of the conjugates along with moderately elevating the activity against NF-κB; since, the two NSAID molecules were fused with a lantadene molecule and that in turn better served as a COX inhibitory scaffold. One of such conjugates **79**, bearing diclofenac moieties at both the C-3 and C-22 positions not only displayed the greatest inhibition of COX-2 but also suppressed the IKK and IκBα mediated NF-κB activity to an appreciable degree. The modification or methylation of the C-28 carboxylic group resulted in the complete loss of activity, rendering it a futile attempt.

The synthesized lead lantadene conjugates **50**, **51**, **63**, **64**, and **79** were sufficiently stable in the simulated gastric fluid of pH 2, surviving the artificial gastric conditions, while hydrolyzed at a relatively greater pace in the human blood plasma to fulfill the criteria of a successful prodrug. The molecular docking studies further revealed the possible binding mode of the lead lantadene congeners with the IKK*β*, highlighting the role of Cys-99 residue in covalent Michael addition, apart from the roles of other residues taking part in hydrogen, hydrophobic, and van der Waals interactions.

ACKNOWLEDGEMENTS

The Ph.D. thesis is not a merely an outline of research and time, but it is a summation of all sorts of supports, encouragements, friendships and without them, this thesis would not exist. First and foremost, I acknowledge the almighty for bestowing me with the strength and perseverance that needed to accomplish this research work.

I am greatly indebted to my Ph.D. supervisor **Dr. Manu Sharma** for his invaluable mentoring and guidance, as well as the love and patience he showed towards me throughout this journey, while keeping me on my toes and right path to success. I am indeed deeply inspired by his thrust, enthusiasm, and activeness for research and sometimes, I used to wonder that I have to put some extra hours to match with his pace of working. Moreover, he trusted in me, my abilities, and stood by me in all-weather of this journey. Without this, it would not have been possible for me to achieve this goal. I wish that I can mentor someone in the future with his qualities. At last but not least, I feel fortunate to have chosen him as my supervisor.

I am also grateful to **Dr. R. S. Chauhan**, Professor and Head, Dept. of Biotechnology, Bioinformatics & Pharmacy, for his kind support, making valuable suggestions for the shaping of this task, and providing all the essential amenities for research work.

I convey my earnest gratitude to Vice Chancellor **Prof. (Dr.) S. K. Kak**, Director **Brig. (Retd.) Balbir Singh**, and Dean (A & R) **Prof. (Dr.) T. S. Lamba**, Jaypee University of Information Technology, for their vital remarks during the research and providing all the necessary research facilities to carry out this work.

I would like to thank all my Doctoral Program Monitoring Committee members Dr. Gopal Singh Bisht, Dr. Ghanshyam Singh, and Dr. Saurabh Bansal for their

guidance and warm encouragement throughout the advancement of my Ph.D. program.

Financial assistance from the **Dept. of Science & Technology (DST)**, Govt. of India, is gratefully acknowledged.

Moral support and encouragement from Dr. G. L. Gupta, Dr. Kuldeep Singh, Dr. Udaybhanu, Dr. Poonam Sharma, A. N. Khan, R. K. Tiwari, and Shilpi Chanda, are highly appreciated.

Many thanks are due for my dear friends Sumit Bansal, Varun, Ved, Piyush, Ankush, Ranjan, and Varun Bhardwaj. I would also like to acknowledge the support of my seniors Jeet, Navin, Varun Jaiswal, Mamta Bhatia, and Anshu Aggarwal, my colleagues Arun Chauhan, S. S. Patel, Swapnil, Aseem, Jibesh, Amit, Deepika, Shivani, Manika, Mamta, Kritika, Kanupriya, Charu, Priya, and Sneha, and my juniors Rakesh, Rohit, Tarun, Arun S., Arun P., Lalit, Ishan T., Vaibhav, Ankesh, Nivedita, Deepika, Monika, Manju, Rajnish, Shifa, Simon, and Amisha.

I extend my gratitude to Mr. Ismail Siddiqui, Mr. Ravikant, Mr. Baleshwar, Kamlesh Ji, Mahendra Ji, and Yaswant Ji for their support and helps in the routine functioning of the lab. I would also like to acknowledge the support of Mrs. Somlata Sharma, Mrs. Mamta Mishra, and Sonika Gupta.

I am in debt to Dr. Alex Joseph, Dr. Siddharth S. Kar, and Pankaj Sharma for sharing their keenness, experience, and knowledge in chemistry and their thoughtful discussions and explanations in synthetic skills.

Finally, this dissertation would not have been possible without the support from my parents, brother, sister Rekha, cousins Om, Prem, Mitesh Bhaiyya, and Meenakshi and the rest of the family members.

JAYPEE UNIVERSITY OF INFORMATION TECHNOLOGY

(Established by H.P. State Legislative vide Act No. 14 of 2002)

P.O. Dumehar Bani, Kandaghat, Distt. Solan – 173234 (H.P.) INDIA

Website: www.juit.ac.in

DECLARATION BY THE SCHOLAR

I hereby declare that the work reported in the Ph.D. thesis entitled **"Synthesis and Development of Lantadene Congeners as Anticancer Agents"** submitted at **Jaypee University of Information Technology, Waknaghat, India,** is an authentic record of my work carried out under the supervision of Assistant Professor **Dr. Manu Sharma**. I have not submitted this work elsewhere for any other degree or diploma. I am fully responsible for the contents of my Ph.D. thesis.

(Signature of the Scholar)

Suthar Sharad Kumar

Department of Pharmacy

Jaypee University of Information Technology, Waknaghat, India

Date:

JAYPEE UNIVERSITY OF INFORMATION TECHNOLOGY

(Established by H.P. State Legislative vide Act No. 14 of 2002)

P.O. Dumehar Bani, Kandaghat, Distt. Solan – 173234 (H.P.) INDIA

Website: www.juit.ac.in

SUPERVISOR'S CERTIFICATE

This is to certify that the work reported in the Ph.D. thesis entitled **"Synthesis and Development of Lantadene Congeners as Anticancer Agents"** submitted by **Suthar Sharad Kumar** at **Jaypee University of Information Technology, Waknaghat, India,** is a bonafide record of his original work carried out under my supervision. This work has not been submitted elsewhere for any other degree or diploma.

(Signature of Supervisor)

Dr. Manu Sharma

Department of Pharmacy

Jaypee University of Information Technology, Waknaghat, India

Date:

LIST OF ABBREVIATIONS

NSAIDs	Nonsteroidal anti-inflammatory drugs
NF-κB	Nuclear factor-kappa B
IKK	Inhibitor of nuclear factor-kappa B kinase
IκBα	Inhibitor of nuclear factor-kappa B alpha
COX-2	Cyclooxygenase-2
PGE_2	Prostaglandin E_2
DNA	Deoxyribonucleic acid
K562	Human chronic myeloid leukemia cell line
DLKP	Human lung carcinoma cell line
NADH	Nicotinamide adenine dinucleotide
NADPH	Nicotinamide adenine dinucleotide phosphate
L929	Murine aneuploid fibrosarcoma cell line (From strain L)
MCF-7	Human breast adenocarcinoma cell line (Michigan Cancer Foundation-7)
HT-29	Human colorectal adenocarcinoma cell line
PAHMA	Poly{6-(4-phenylazophenoxy)hexyl methacrylate (AHMA)}
HeLa	Human cervical adenocarcinoma cell line (Henrietta Lacks)
MIA PaCa-2	Human pancreatic carcinoma cell line
SW-620	Human Caucasian colon adenocarcinoma
WI-38	Caucasian fibroblast-like fetal lung cell
HepG2	Human liver hepatocellular carcinoma cell line
LS 180	Intestinal human colon adenocarcinoma cell line
CYP	Cytochrome P450
RNA	Ribonucleic acid
L1210	Mouse lymphocytic leukemia cell line
Molt 4/C8	Human leukemia-derived cell line
CEM	Human T cell lymphoblast-like cell line

H460	Non-small cell lung carcinoma cell line
COLO 320	Human colon adenocarcinoma cell line
DMBA	7,12-dimethylbenz(a)anthracene
TPA	12-*O*-tetradecanoylphorbol-13-acetate
PA III	Rat prostate adenocarcinoma III cells
PC-3M	Human prostate carcinoma cells
HIF-1α	Hypoxia-inducible factor 1-alpha
p-AKT	phospho-Protein kinase B
	(AKR mouse, "T"; transformation capabilities)
Bcl-2	B-cell lymphoma 2
Bax	Bcl-2 associated X protein
A549	Human alveolar lung adenocarcinoma cell line
C26	Murine colon carcinoma cell line
TRAMP-Cl	Transgenic adenocarcinoma of the mouse prostate cells
SKBR-3	Human breast adenocarcinoma cell line (Memorial Sloan–Kettering Cancer Center)
H292	Human lung mucoepidermoid pulmonary carcinoma cells
H522	Human non-small lung adenocarcinoma cells
MDA-MB-468	Human breast adenocarcinoma cell line
IMR90	Human Caucasian fetal lung fibroblast cell line
ERK	Extracellular signal-regulated kinases
c-Src	Proto-oncogene tyrosine-protein kinase Src (Src; sarcoma)
U87-MG	Human glioblastoma-astrocytoma, epithelial-like cell line
NO	Nitric oxide
H_2S	Hydrogen sulfide
T98G	Human Caucasian glioblastoma cell line
HCT 116	Human colorectal carcinoma cell line
PC-3	Human prostate adenocarcinoma cell line
VLA-4	Integrin alpha4beta1 (Very Late Antigen-4)

MDA-MB-231	Human breast adenocarcinoma cell line
DU-145	Human prostate carcinoma cell line
SK-OV3	Human serous ovarian carcinoma cell line
FAP	Familial adenomatous polyposis
FDA	Food and drug administration
TLC	Thin layer chromatography
FT-IR	Fourier transform infra red
KBr	Potassium bromide
cm^{-1}	Per centimeter
NMR	Nuclear magnetic resonance
ppm	Parts per million
$CDCl_3$	Deuterated chloroform
DMSO.d_6	Deuterated dimethyl sulfoxide
Hz	Hertz
MHz	Megahertz
s	Singlet
d	Doublet
dd	Double doublet
t	Triplet
m	Multiplet
br	Broad
Ar-H	Aromatic-hydrogen
ESI-MS	Electrospray ionization mass spectrometry
HR-MS	High-resolution mass spectrometry
eV	Electron volt
Q-T	Quadrupole-time of flight
HPLC	High performance liquid chromatography
PDA	Photodiode array
MeOH	Methanol

THF	Tetrahydrofuran
R_f	Retention factor
$NaBH_4$	Sodium borohydride
HCl	Hydrochloric acid
DCM	Dichloromethane
KOH	Potassium hydroxide
DMSO	Dimethyl sulfoxide
4-DMAP	4-Dimethylaminopyridine
MTT	3-(4,5-Dimethythiazol-2-yl)-2,5-diphenyltetrazolium bromide
HEPES	(4-(2-Hydroxyethyl)-1-piperazineethanesulfonic acid
ATP	Adenosine triphosphate
Sf21	Ovarian cells from *Spodoptera frugiperda* worm
Na_4EDTA	Tetrasodium ethylenediaminetetraacetate
pFASTBAC1	Transposable baculovirus expression vector
PCR	Polymerase chain reaction
RAW	Raschke, Ralph, and Watson cells
DMEM	Dulbecco's modified Eagle's medium
FBS	Fetal bovine serum
ATCC	American type culture collection
3D	Three dimensional
PDB	Protein data bank
Mp	Melting point
DCC	*N*,*N*'-dicyclohexylcarbodiimide
kcal/mol	Kilo calorie per mole
IC_{50}	Half maximal (50%) inhibitory concentration

LIST OF SYMBOLS

δ	Delta
J	Coupling constant
m/z	Mass/charge
Å	Angstrom
nm	Nanometer
µm	Micrometer
mm	Millimeter
ng	Nanogram
µg	Microgram
mg	Milligram
g	Gram
kg	Kilogram
µl	Microliter
ml	Milliliter
L	Liter
min	Minute
h	Hour
%	Percent
w/w	Weight/weight
cm	Centimeter
°C	Degree Centigrade
nmol	Nanomole
µmol	Micromole
mmol	Millimole
mol	Mole
U/ml	Unit per ml

LIST OF FIGURES

LIST OF TABLES

TABLE OF CONTENTS

CHAPTER 1

INTRODUCTION AND REVIEW OF LITERATURE

1.1. Cancer and inflammation

Cancer is the rapid creation of abnormal cells that grow beyond their usual boundaries and which can then invade adjoining parts of the body and spread to other organs [1]. Lung cancer is the most common cancer diagnosed in men worldwide (accounting for 16.5% of all new cases), while breast is the most common cancer diagnosed in women (23% of all new cases) [2]. American cancer society estimated a total of 1,638,910 new cancer cases and 577,190 deaths from cancer in the United States by the end of 2012 [3]. In India, there are 2 to 2.5 million cancer patients at any given point of time with about 0.7 million new cases coming every year and nearly half of them die every year [4]. Tobacco related cancers are most prevalent and accounts for 34% of all cancers in India (50% of all male cancers and 25% of all female cancers) [4]. Current treatments for cancer involve chemotherapy, radiotherapy, and extensive surgery with chemotherapy remains the most noteworthy pharmacological approximation to cancer treatment [5]. Though, the existing anticancer agents suffer from limitations, like toxicity to normal cells and acquired tumor resistance. Therefore, there is an instant need of new anticancer agents with the better selectivity and improved pharmacological profile [5].

It has been well demonstrated that inflammation and cancer are closely related to each other [6]. A growing tumor expresses phenotypes similar to inflammatory cells [7]. Various tumor cells have shown the presence of cytokines and chemokines that play a critical role in the proliferation and differentiation of cancer cells [8,9]. Chronic inflammation plays a major role in the lung carcinogenesis and there are a number of evidences from preclinical

and clinical studies, which showed that persistent inflammation can drive normal lung cells to cancerous cells [10]. The inflammation may be involved in several stages of carcinogenesis, from tumor initiation to tumor promotion and even in the metastatic progression through various mechanisms involving genomic instability, epigenetic modifications, localized immunosuppression, and angiogenesis [11]. Based on these pro-tumor effects, inflammation has been identified as one of the key targets of cancer prevention and treatment strategies [6].

1.2. Role of NF-κB and COX-2 in cancer

Nuclear factor-kappa B (NF-κB) is one of the important targets of anticancer drugs currently being developed. It regulates inflammatory response and apoptotic pathways and remains inactive in the cytoplasm because of its complex formation with an inhibitor of nuclear factor-kappa B alpha (IκBα) [12–15]. In response to inflammatory stimuli, IKK (inhibitor of nuclear factor-kappa B kinase) phosphorylates IκBα, leading to its degradation and release of NF-κB from the NF-κB–IκBα complex [13–15]. The free NF-κB then translocates to the nucleus and binds with specific sequences of DNA; thereby regulating the transcription of target genes [13–15]. The expression of the majority genes that are involved in inflammation or in cellular proliferation (*e.g.* cyclin D1) are regulated by NF-κB.

In response to various external stimuli, such as pro-inflammatory cytokines, bacterial lipopolysaccharides, ultraviolet rays, reactive oxygen species, and phorbol ester, the cyclooxygenase-2 (COX-2) becomes elevated in certain tissues [16,17]. Abnormally elevated COX-2 causes promotion of cellular proliferation, suppression of apoptosis, enhancement of angiogenesis, and invasiveness, which leads to the oncogenesis [18]. More than two decades before, anticancer properties of nonsteroidal anti-inflammatory drugs (NSAIDs) were discovered [6]. Since then various studies have indicated that long-term

use of aspirin and other NSAIDs decrease the incidence of colorectal, esophageal, breast, lung, and bladder cancers [19] via depression of prostaglandin E_2 (PGE_2) synthesis while inhibiting COX-2, which results in the suppression of proliferation [20].

1.3. NSAIDs as anticancer agents

Studies over the years have established that inflammation and cancer are closely linked with each other. Currently existing anti-inflammatory agents have displayed remarkable anticancer efficacy against various types of cancers, particularly, colon, breast, pancreatic, prostate, lung, and skin cancers. Numerous researchers all over the world are engaged in the design and discovery of NSAIDs as anticancer agents. Such NSAID derivatives (**1**–**27**) discovered as antiproliferative and antitumor agents in the recent past are discussed below.

1.3.1. Development of various NSAID derivatives as anticancer agents

Zhang *et al*. (2000) screened the anticancer potential of indomethacin against chronic myeloid leukemia cells [21]. They discovered that at 400 µmol/l concentration, indomethacin triggered the apoptosis and suppressed the growth of K562 cells and primary culture bone marrow cells obtained from six chronic myelogenous leukemia patients. Maguire and coworkers (2001) synthesized indomethacin analogs bearing both *N*-benzyl and *N*-benzoyl groups for their ability to suppress multidrug resistance-associated protein-1 (MRP-1) mediated drug efflux in a human lung carcinoma cell line, DLKP [22]. The results showed that substitution of halogen atoms, specifically *p*-halogen atom substituted *N*-benzyl and *N*-benzoyl rings yielded compounds with MRP-1 inhibitory capability. The aldo-keto reductase family 1 member C3 (AKR1C3) is an enzyme; catalyze the conversion of aldehydes and ketones to their respective alcohols by employing NADH or NADPH as cofactors. Human AKR1C3 reduces a weak androgen, androstenedione to strong androgen testosterone, and a weak

estrogen estrone to potent estrogen 17β-estradiol, employing NADPH as a coenzyme. Therefore, AKR1C3 is an appealing target for the discovery of drugs targeting hormone dependent cancers, *viz.* prostate, breast, and endometrial cancers. Intending to inhibit AKR1C3, Gobec *et al.* (2005) synthesized analogs of diclofenac and naproxen [23]. The most potent analog, 3-phenoxybenzoic acid (**1**) displayed IC_{50} of 0.68 µmol against AKR1C3. Thus, compound **1** represents a potential pharmacophore to be further developed as AKR1C3 inhibitor for treating hormonal based cancers. Aromatase or estrogen synthase is an enzyme which mediates biosynthesis of estrogens. Su *et al.* (2009) performed lead optimization of nimesulide analogs towards COX-2 to prevail over aromatase inhibitor resistance in the breast cancer cells [24]. Synthesized analogs were evaluated against long-standing estrogen deprived MCF-7aro (LTEDaro) breast cancer cell line, which is the biological model of aromatase inhibitor resistance for hormone-dependent breast cancer. Several tested compounds showed IC_{50} values close to 1 µmol against LTEDaro cells and among them **2** was found to be most efficacious with IC_{50} of 1.00 µmol, while reference drug nimesulide displayed IC_{50} of 170.30 µmol against LTEDaro breast cancer cells.

Synthesis and cytotoxicity of poly(anhydride esters) of salicylate derivatives, *viz.* halogenated salicylates, aminosalicylates, salicylsalicylic acid, and thiolsalicylic acid was reported by Schmeltzer and co-workers (2005) [25]. To assess the cytotoxic potential, authors screened the compounds against L929 fibroblast cells in serum containing medium and found that the morphology of cells remained unchanged after the treatment with most of the compounds. In the contemporary effort, Congiu *at al.* (2005) synthesized derivatives of flufenamic acid for anticancer activity [26]. Structural variations on the flufenamic acid scaffold yielded a series of (hetero)aryl esters of *N*-(2-(trifluoromethyl)-pyridin-4-yl)anthranilic acid. Among these synthesized new array of compounds, analog **3** with pyridinyl substitution displayed remarkable *in vitro* antiproliferative

efficacy with chemosensitive profile exhibiting a number of GI_{50} values at concentrations below 10^{-7} mol in the full panel of NCI-60 human tumor cell lines.

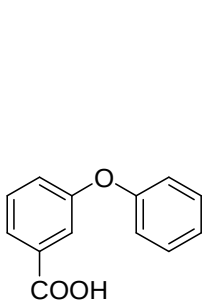

1

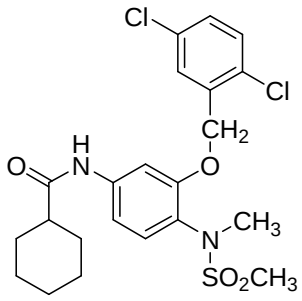

2

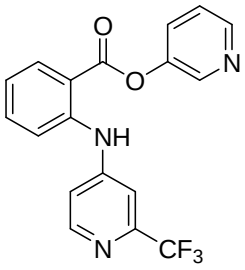

3

Riboflavin or vitamin B_2 acts as micronutrients for normal and cancer cells, though rapidly dividing cancer cells need higher amounts of nutrients than the normal cells. A covalent linking of micronutrients with the anticancer agents is one of the new strategies currently being practiced to enhance internalization of the anticancer agents into the cancerous cells. Banekovich and associates (2007) synthesized dexibuprofen derivatives covalently linked to tetraacetylated riboflavin by way of alkylene spacers of changeable length [27]. Biological evaluation studies revealed that the test compounds were significantly active against MCF-7 (breast cancer cells) and HT-29 (colon carcinoma cells) cells with IC_{50} values in the range of 8–15 µmol. Compound **4** was found to be the most cytotoxic with IC_{50} values of 7.8 and 9.3 µmol against MCF-7 and HT-29 cells, respectively. In an effort to establish NSAIDs as anticancer agents, new series of anti-tumor thiolated and nonthiolated polyaspartamide–diclofenac and –fenoprofen prodrugs were synthesized in the lab of Barbarić and colleagues (2007) [28]. Results of *in vitro* anticancer assay disclosed that compounds with polyaspartamide-type polymers, particularly thiolated polymers significantly suppressed the tumor cell proliferation and growth. The diclofenac prodrugs were found to be more active than the fenoprofen counterparts. The most potent diclofenac–PAHMA congener (**5**) showed IC_{50}s of 75, 18, 34, 61, 64, and 28

μmol against Hep-2, HeLa, MIA PaCa-2, SW-620, MCF-7, and WI-38 cell lines respectively, while against the same cell lines diclofenac exhibited IC_{50}s of 43, 26, 55, 51, 60, and 67 μmol, correspondingly.

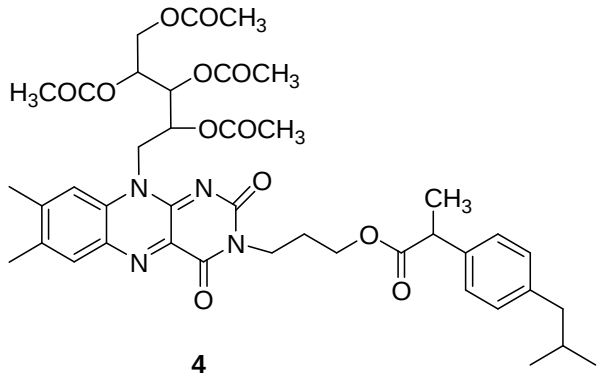

4

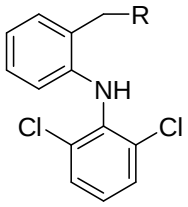

5

R=
poly[α,β-(*N*-2-aminoethyl-DL-aspartamide)]-
poly[α,β-(*N*-2-hydroxyethyl-DL-aspartamide)]-
poly[α,β-(*N*-3-mercapto-1-methoxycarbonyl-
propyl-DL-aspartamide)]

Peroxisome proliferator-activated receptor gamma (PPARγ) regulates fatty acid storage and glucose metabolism and is regarded as a novel target for the discovery of future anticancer and anti-inflammatory agents. Romeiro and teammates (2008) explained the binding of existing NSAIDs with PPARγ with the help of molecular docking analysis [29]. A docked complex of sulindac sulfide showed that it possessed the pharmacophoric prerequisites to bind with PPARγ receptor; a polar head and a hydrophobic tail that was partially buried in the pocket covered by arm II, a hydrophobic area of the receptor. Conversely, selective COX-2 inhibitors celecoxib and SC560 didn't bear the same structural requirements and were poor inhibitors of PRARγ. Bass *et al.* (2009) examined the influence of dithiolethione-modified NSAIDs on carcinogen commencement and detoxification modes in human hepatoma HepG2 and human colon LS180 cells [30]. The authors discovered that synthesized derivatives of diclofenac (**6**) and sulindac (**7**) suppressed the activity and regulation of carcinogen activating enzymes cytochromes P-450 (CYP) CYP1A1, CYP1B1, and CYP1A2 and this suppression was mediated by transcriptional regulation of the aryl hydrocarbon receptor (AhR) pathway. The NSAID derivatives lowered the carcinogen-

induced expression of CYP1A1 heterogeneous nuclear RNA, which is a measure of the transcription rate. Therefore, it can be inferred that dithiolethione-modified diclofenac (**6**) and sulindac (**7**) derivatives may act as potent chemopreventive agents by constructively harmonizing the equation of carcinogen activation and detoxification mechanisms. The phosphoramidate structure is widely known for its antiproliferative and cytotoxic characteristics. Wittine and teammates (2009) synthesized phosphoramidate compounds from 3-hydroxypropyl derivatives of NSAIDs (fenoprofen, ketoprofen, ibuprofen, indomethacin, diclofenac) [31]. Synthesized compounds were evaluated for their anticancer activity against malignant tumor cell lines (L1210, Molt4/C8, CEM, HeLa, MIA PaCa-2, SW-620, MCF-7, and H460) and normal human fibroblasts (WI-38). All the tested phosphoramidate derivatives showed noteworthy anticancer potencies with derivative **8** exhibiting highest inhibitory potential against the cervical, pancreatic, and colon carcinoma cell lines (IC_{50}s 5−7 µmol). Aspiring to develop cytotoxic agents against colon cancer, Zawidlak-Wegrzyńska *et al.* (2010) reported the synthesis and anticancer screening of ibuprofen–oligo(3-hydroxybutyrate) conjugates [32]. From the series of derivatives evaluated, **9** was found to have potential anticancer effects. It showed IC_{50}s of 37 and 31 µmol against HT-29 and HCT 116 cancer cell lines, respectively. The authors postulated that the improved antiproliferative activity of ibuprofen–oligo(3-hydroxybutyrate) conjugates may have been caused by increased cellular uptake of ester conjugates than the free drug. In a different but contemporary study, Fogli and co-workers (2010) described the synthesis of hydroxamic acid derivative of sulindac for anticancer activity against human pancreas and colon cancer cell lines [33]. Results of biological screening indicated that the hydroxamic acid derivative of sulindac and its sulfone and sulfide metabolites were potent anticancer agents that displayed IC_{50}s values in the range of 6–64 µmol. Sulfide derivative (**10**) was the most active and showed IC_{50}s of 32 and 6 µmol against MIA PaCa-2, and COLO 320 cancer cells, respectively. The mechanistic study disclosed that hydroxamic acid derivatives

induced apoptosis, augmented Bax/Bcl-2 expression ratio, which resulted in the caspase 3/7 activation.

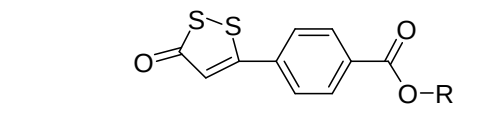

6-7

6. R=

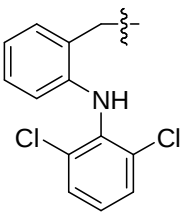

7. R=

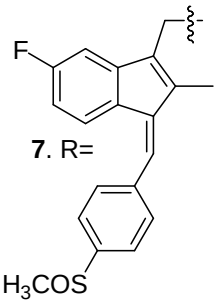

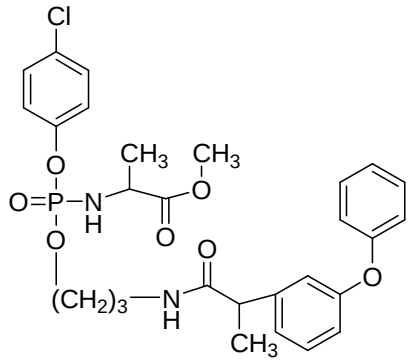

8

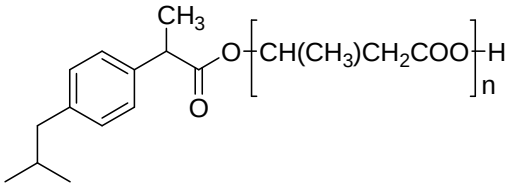

9

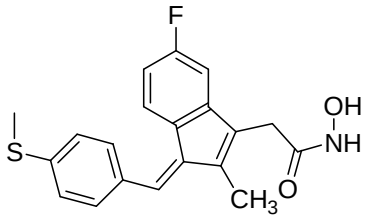

10

Chemopreventive activities of etodolac and oxyphenbutazone against mouse skin carcinogenesis were studied by Kapadia *et al.* (2010) [34]. The authors reported the inhibition of 7,12-dimethylbenz(a)anthracene (DMBA)-induced two-stage mouse skin carcinogenesis by etodolac (ETD), while peroxynitrite (PN)-induced and 12-*O*-tetradecanoylphorbol-13-acetate (TPA)-promoted skin tumors in the mouse by oxyphenbutazone (OPB). Topical administration of ETD at a very low dose of 85 nmol exhibited a remarkable reduction in both tumor incidence and burden. This effect was accompanied by a delay in the tumor latency period. The orally administered 0.0025% dose of OPB was also proved to be chemopreventive. The COX-2 selective inhibitor celecoxib is believed as more

potent antiproliferative and cytotoxic agent than nonselective COX inhibitors. In a hybrid synthesis approach, Desai and co-workers (2010) conjugated two powerful anti-inflammatory and anticancer pharmacophores with the objective to enhance the biological activity [35]. They hypothesized that sulfonamide pharmacophore and pyrazole ring of celecoxib is critical for the proapoptotic activity, while selenium is proven anticancer agent and therefore, synthesized selenocoxib (**11**) by making a substitution at the 3 position of the pyrazole ring. When evaluated against PAIII cells derived from a metastatic prostate tumor and PC-3M human metastatic prostate cancer cells, selenocoxib demonstrated IC_{50}s of around 5 µmol against both the cells, while IC_{50}s of celecoxib was found to be greater than 20 µmol against the same cell lines. Selenocoxib and celecoxib also exhibited a declined expression of COX-2 in PAIII cells. In a mechanistic study, PAIII cells treated with selenocoxib showed decreased levels of HIF-1α, p-AKT, and Bcl-2. These results proved that selenocoxib was more potent anticancer agent than celecoxib against prostate cancer.

Glyoxalase-1 is a thio-dependent methylglyoxal detoxification enzyme, considered as the potential target for antitumor drug development. Liu and colleagues (2011) studied kinetic analysis, molecular docking, and molecular dynamics simulations on indomethacin and its analogs to find out anticancer activity of these compounds, targeting human glyoxalase-I (GLO1) [36]. The study revealed that indomethacin was a prospective agent to be developed as GLO1 inhibitor, as it binds with all subsites of the active site pocket of GLO1 and stabilized the flexible loop (152–159 residues). To target both human and murine cancer cells, Su *et al.* (2011) synthesized amide derivatives of fenbufen and ethacrynic acid through a facial preparation of 1-amino-4-azidobutane followed by a coupling with large number of carboxylic acids [37]. Synthesized derivatives were tested against two human cell lines (MCF7 and A549) and two murine cell lines (C26 and TRAMP-C1). Fenbufen derivatives displayed better anticancer activity than the ethacrynic acid derivatives and cytotoxicity of

fenbufen derivatives **12** and **13** was comparable to that of cisplatin. In a recent study, Chennamaneni and associates (2012) synthesized indomethacin and sulindac derivatives as antiproliferative agents [38]. One of the synthesized indomethacin derivatives **14** exhibited IC_{50}s in the range of 0.51−17.19 µmol against variety of cancer cell lines, *viz.* SK-BR-3, H292, H522, MDA-MB-468, MCF-7, and IMR90. The mechanistic study concluded that compounds act through COX independent anticancer mechanism and compound **14** was found to be inhibitor of tubulin polymerization. Although, the parent compound indomethacin didn't show inhibitory potential against the tubulin protein. Molecular docking analysis disclosed that, 3,4,5-trimethoxyphenyl group of **14** was located in the hydrophobic pocket defined by Ala-250, Cys-241, Val-238, Tyr-202, Ile-378, and Leu-255 residues of the colchicines binding site of tubulin.

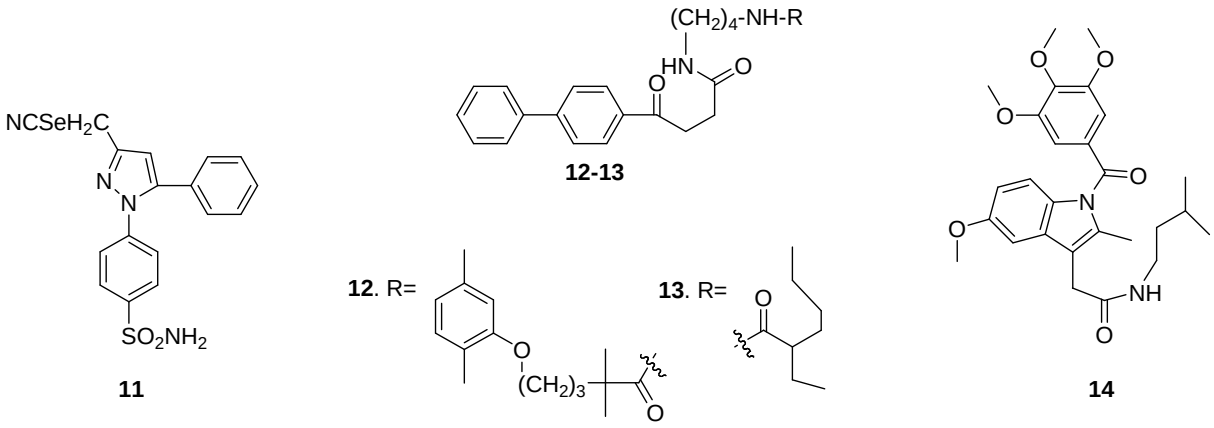

Gliomas are tumors that originate from cells of astrocytic lineage and represent brain tumors. Rosenbaum *at al.* (2005) synthesized and screened a library of indomethacin analogs in the cytotoxicity assay using the MRP-1 (multidrug resistance-associated protein-1) expressing human glioblastoma cell line T98G as a model system [39]. Nine of the 60 evaluated compounds enhanced the doxorubicin-mediated cytotoxicity at an equal or superior level than the indomethacin. Compound **15** increased the doxorubicin-induced cytotoxicity by

a 2.4-fold and emerged as the promising candidate to be developed as a potent MRP-1 inhibitor. In another study against glioma, Bernardi and fellow workers (2006) screened the chemically unrelated NSAIDs, indomethacin, acetaminophen, sulindac sulfide, and NS-398 (N-[2-cyclohexyloxy)-4-nitrophenyl]methane-sulfonamide) against C6 and U138-MG glioma cell lines [40]. The study disclosed that treatment of glioma cells with NSAIDs lead to a decline in cell numbers and pointed out caspase-3/7-independent apoptotic cell death. Indomethacin inhibited the cell cycle progression of glioma cells and decreased the cell counting mediated by c-Src and ERK signaling. In a peculiar approach to treat glioma, Lee *et al.* (2011) developed nanoprodrugs of flufenamic acid [41]. Exceedingly hydrophobic monomeric and dimeric prodrugs of flufenamic acid were synthesized via esterification method and subsequently developed into nanoprodrugs of size 120 to140 nm using the spontaneous emulsification method. The monomeric nanoprodrug (**16**) displayed IC_{50} of 20 µmol against U87-MG glioma cells (brain tumor cells), while flufenamic acid showed IC_{50} of 100 µmol, indicating that the developed nanoprodrug was more potent than the parent drug. Conversely, the dimeric nanoprodrug did not exhibit any similar effect on the proliferation and viability of U87-MG glioma cells.

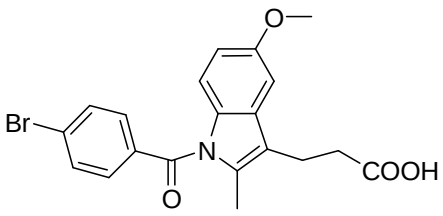

15

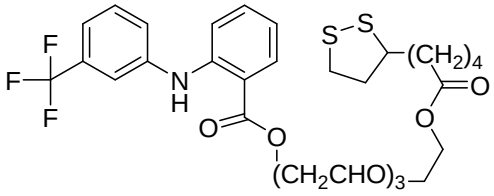

16

1.3.2. Gaseous mediator-releasing NSAID derivatives as anticancer agents

Several *in vitro* and *in vivo* studies have shown that NO-releasing NSAIDs possess anticancer activities. It is also well established that elevated levels of

NO promotes tumor cells to undergo apoptosis. Therefore, the synthesis of NO-donating NSAIDs as antitumor agents is a promising approach to fight the battle against the cancer. Yeh and associates (2004) evaluated and compared the anticancer effects of seven pairs of conventional NSAIDs (aspirin, salicylic acid, indomethacin, sulindac, ibuprofen, flurbiprofen, and piroxicam) and their corresponding NO–NSAIDs [42]. In contrast to parent NSAIDs, all NO–NSAIDs (excluding NO-piroxicam, which is a salt and not a true NO-NSAID) displayed superior inhibitory potential against the growth of HT-29 and HCT-15 colon cancer cells and showed 7−689-fold increase in IC_{50}s against HT-29 cells and 1.7−1083-fold increase in IC_{50}s against HCT-cells, when compared to the parent NSAIDs. In a subsequent study, Bézière *et al.* (2008) designed and synthesized profen–NO hybrid molecules for anti-inflammatory and anticancer activities, specifically targeting human prostatic cancer cells [43]. The authors found that apart from COX inhibition, time-dependent NO-release contributed to the anticancer activity of the compounds. A ketoprofen–NO hybrid compound (**17**) exhibited IC_{50} of 0.73 µmol against COX-2, while at 100 µmol dose, it showed 26% growth inhibition against PC-3 prostate cancer cells. The IC_{50} of ketoprofen against COX-2 was found to be 0.69 µmol and it didn't show any growth inhibition of PC-3 cells. Hypoxic tumor cells are believed to be resistant against chemotherapy. Stewart and associates (2009) studied the effects of NO-donating sulindac analog (**18**) on PC-3 prostate cancer cells maintained under hypoxic conditions [44]. The authors noticed that NO–sulindac (**18**) produced pro-apoptotic, cytotoxic, and antiproliferative effects on the PC-3 cells under normoxic and hypoxic conditions. NO–sulindac was found to be notably more cytotoxic than sulindac at every oxygen level. It was seen that both HIF-1α and Akt phosphorylation levels were lowered on treatment with NO–sulindac. The authors further stated that both the sulindac/linker and NO-donating subunits contributed to the anticancer properties of NO–sulindac. Along with NO-releasing agents, H_2S-donating agents have also been shown to possess great anticancer potential. In this approach, recently Kodela *et al.* (2012) synthesized

novel aspirin hybrids possessing both NO- and H_2S-releasing moieties and evaluated against eleven different human cancer cell lines of six different tissue origins [45]. Among the compounds tested for anticancer activity, 4-(3-thioxo-3H-1,2-dithiol-5-yl)phenyl 2-((4-(nitrooxy)-butanoyl)oxy) benzoate (**19**) was found to be most potent with an IC_{50} of 0.048 µmol against HT-29 colon cancer cells. Compound **19** was at least 100,000-times more potent than the aspirin in HT-29 cells. The compound **19** also displayed anti-inflammatory activity equipotent to aspirin, determined in carrageenan-induced rat paw edema model. In another recent study, Cheng and co-workers (2012) studied the effects of NONO-donating NSAIDs on the adhesion of melanoma cells [46]. For their efforts, they synthesized novel NONO–aspirin and NONO–naproxen compounds and evaluated against human melanoma M624 cells. The study indicated that both of the NONO–NSAIDs decreased adhesion of M624 cells on vascular cellular adhesion molecule-1 (VCAM-1) by 20–30% and on fibronectin by 25–44%. Also, NONO–naproxen (**20**) was capable of suppressing the activity (~56%) of β1 integrin that binds with α4 integrin to generate late stage antigen-4 (VLA-4), the ligand of VCAM-1. Therefore, it can be inferred that diazeniumdiolate (NO•)-releasing moiety was crucial for decreasing the adhesion between VLA-4 and its ligands.

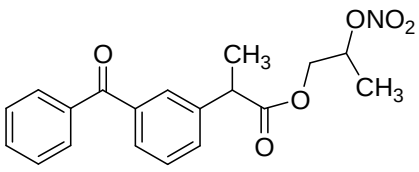

17

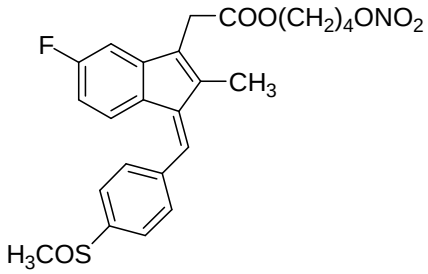

18

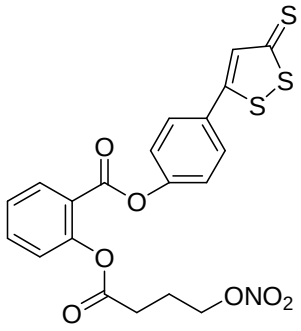

19

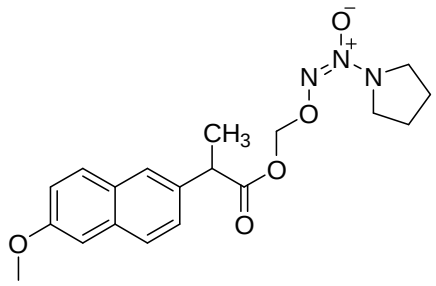

20

1.3.3. NSAID–metal complexes as anticancer agents

Cisplatin was first metal based compound to be introduced as an antitumor agent in the market. Since then, plausible efforts have been made to the design and discovery of metal based cytotoxic agents. Here, we document recently synthesized and screened NSAID–metal complexes targeting various cancers. Ott *et al.* (2005) developed cytotoxic cobalt-alkyne complexes of aspirin [47]. All the synthesized complexes were evaluated against MCF-7 and MDA-MB-231 cell lines. From the set of metal complexes tested, Co-ASS or [2-acetoxy-(2-propynyl) benzoate]hexacarbonyldicobalt (**21**) was revealed as the lead compound with IC_{50} values of 1.4 and 1.9 µmol against MCF-7 and MDA-MB-231 cell lines, respectively. Other complexes such as desacetoxy derivative Co-Benz, amide derivatives Co-ASSAM and Co-Phthal, and the structural isomer Co-3-Acetbenz were found to be less active against both the cell lines. In the subsequent study, Rubner and fellow workers (2010) synthesized transition metal complexes of aspirin and screened for growth inhibition, antiproliferative effects, and apoptosis induction in breast (MCF-7, MDA-MB-231) and colon cancer (HT-29) cell lines, and for COX-1/2 inhibitory effects in the isolated isoenzymes [48]. Aspirin derivative, Prop-ASS-Ru_3 or [(μ^3-η^2)-(prop-2-ynyl)-2-acetoxybenzoate]triruthenium nonacarbonyl (**22**) exhibited highly potent anticancer activity which was correlated with apoptosis induction. In a similar but another study, the same research team (2010) reported the synthesis and

biological screening of [cyclopentadienyl]metalcarbonyl complexes of aspirin, by employing metals; molybdenum, manganese, cobalt, thallium, and rhodium [49]. Synthesized complexes showed feeble activity against COX enzymes, whereas against breast (MCF-7, MDA-MB-231) and colon cancer (HT-29) cell lines, all the complexes displayed considerable cytotoxic effects. Aspirin–thorium complex, Et-Cp-ASS-Th (**23**) exhibited maximum cytotoxicity against MDA-MB-231 and HT-29 cells with IC_{50}s of 11.4 and 4.6 µmol, respectively, while another aspirin–thorium complex, But-Cp-ASS-Th (**24**) displayed highest activity towards MCF-7 cells with IC_{50} of 5.4 µmol. Clinically used cytotoxic agent cisplatin showed IC_{50}s of 2.0, 3.3, and 2.4 µmol against MCF-7, MDA-MB-231, and HT-29 cancer cell lines, respectively. In a recent advancement of NSAIDs based metal complexes, O'Connor *et al.* (2012), developed salicylic acid–copper(II) complexes with DNA binding and cleaving capabilities against cisplatin sensitive and resistant cancer cells for promising chemotherapeutic potential [50]. Synthesized complexes **25–27** showed cytotoxicity against cisplatin sensitive breast (MCF-7), prostate (DU-145), and colon (HT-29) cancer cell lines and cisplatin resistant ovarian cells (SK-OV-3) in micromolar doses and were found to be more potent than the cisplatin. Furthermore, these complexes also exhibited strong *in vitro* DNA binding and cleavage capabilities.

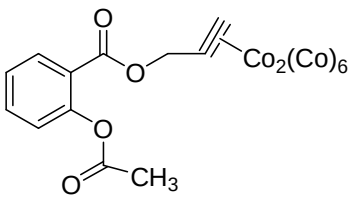

21

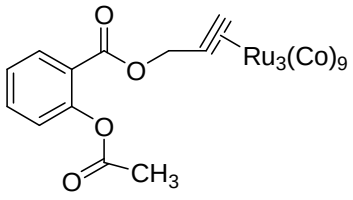

22

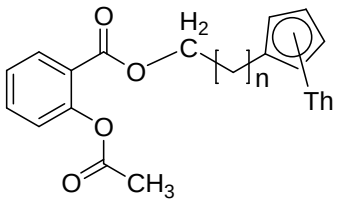

23. n= 2
24. n= 4

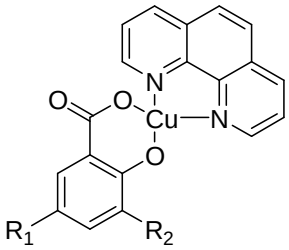

25. R_1= H, R_2= H
26. R_1= $CH(CH_3)_2$, R_2= $CH(CH_3)_2$
27. R_1= H, R_2= OCH_3

1.3.4. Present status and future of NSAID derivatives as anticancer agents

Ongoing preclinical and clinical studies of NSAIDs and their derivatives, probably to provide an answer related to their applications in the prevention and treatment of various cancers along with GI and cardiovascular safety issues [51]. Epidemiological statistics propose that the occurrence of breast, colorectal, and lung cancers is inversely associated with the use of aspirin and other NSAIDs [52,53]. Ample facts imply that COX is one of the decisive targets that regulate the anticancer effects of NSAIDs [54]. The finding of a relationship between levels of COX-2 in human lung and colon cancers and patient forecast was quoted as additional confirmation of the prospective significance of COX-2 as a target for cancer therapeutics [54–56]. Various studies have established that aspirin can lessen the immediate risk of colon adenomas in patients with a previous record of adenomas [52,57]. An additional study verified that the incidence and mortality from lung cancer in patients administering aspirin was appreciably less in the non-smokers and past smokers than those who did not take aspirin [52,58]. Another NSAID, sulindac has been reported to reduce the reappearance and polyp number in familial adenomatous polyposis (FAP) patients [52,59] and caused degeneration of existing adenomas [52,60]. Other NSAIDs, ibuprofen and piroxicam have also been found to lower the risk of developing carcinomas [51,61–62].

Presently, there are at least 98 clinical trials exploring the use of selective COX-2 inhibitor celecoxib in the prevention and treatment of cancer [52,63]. Previous clinical trials in patients suffering from FAP confirmed that celecoxib initiated considerable regression of developed adenomas [52,60] and these discoveries led to the accelerated FDA approval of celecoxib for adjuvant therapy in the treatment of FAP in 1999 [64]. Till date, celecoxib is the only NSAID approved by FDA for the therapy of FAP [65]. APPROVe (Adenomatous Polyp PRevention On Vioxx) trial was undertaken by Merck in 2001 to screen the potential of rofecoxib against adenomatous polyp [66–68]. Though, study was later terminated due to the increased risk of cardiovascular adverse effects caused by rofecoxib [68].

Numerous other NO-releasing, H_2S-releasing NSAIDs [69,70] and NSAID–metal complexes have also shown promising anticancer properties and are being investigated in several preclinical studies. Based on the results obtained in various preclinical and clinical studies of NSAIDs and their derivative, it can be concluded that the use of NSAIDs decreases the incidence of primary cancers, suppress the growth of emerging tumors, while regressing the developed cancers and thereby reduces mortality among the cancer patients [52]. Accordingly, in the near future, existing NSAIDs and NSAID derivatives may supplement the current arsenal available to fight against the cancer.

In brief, existing NSAIDs suffer from GI toxicities and cardiovascular adverse effects. Novel NO- and H_2S-releasing NSAIDs offers a ray of hope to alleviate the problems associated with current NSAIDs. Moreover, these agents have shown promising activity and safety profiles in various preclinical and clinical trials. It is now proved that inflammation plays a critical role in the initiation and propagation of cancer. The use of NSAIDs can reduce the incidence and reappearance of various cancers and thereby reduce the overall mortality rates in patients. The use of NSAIDs in conjunction with classical anticancer agents is making headway, and is likely to provide many new therapeutic strategies to

treat cancer in the coming time. The developing hybrid compounds such as NO–NSAIDs, NONO–NSAIDs, HS–NSAIDs, NSAID–metal complexes and selective COX-2 inhibitors along with existing NSAIDs may symbolize the future generation of therapeutics to treat both inflammation and cancer. Nonetheless, optimal dosage, frequency, therapy regimen, benefit-risk ratio, and the detailed mechanism by which these agents act still remained to be solved.

CHAPTER 2

RESEARCH ENVISAGED AND PRESENT WORK

Since the ages, human civilization has relied on natural resources to cater for their basic needs, not the least of which are medicines for the treatment of a broad range of diseases [71]. In the present day drug discovery approach, there are three main sources of new chemical entities; original natural products, semi-synthetically modified natural products, and combinatorial synthetic compounds [72]. Among these, the natural products show high diversity as they bear many chiral centers and specific stereochemistry [72] and are generally derived through specific biosynthetic pathways, like shikimate, polyketide or mevalonate, leading to a particular class of compounds [73,74]. Accordingly, natural products have played and continue to play a significant role in the drug discovery process, specifically in the domain of chemotherapeutics [72]. Indeed, greater than 60% of the marketed drugs are of natural origin [72]. Within the spheres of cancer therapy, over the time period from the 1940 to 2012, of the 175 approved small molecules, 131 (74.8%) are other than synthetic, with 85 (48.6%) in fact being either natural products or semi-synthetic natural products [75].

Lantana camara Linn. (Verbenaceae) is one of the noxious weed that grows in tropical and sub-tropical regions of the world. Lantadenes are pentacyclic triterpenoids present in the leaves of *Lantana camara*. Opportunely, this weed also grows abundantly in the surrounding areas of our laboratory. Previous studies carried out by our group revealed that lantadenes possess chemotherapeutic potential against various cancers [76–79]. Recently, lantadene A and B along with their few other semi-synthetic derivatives showed potent cytotoxicity against the NCI-60, a panel of 60 diverse human cancer cell lines,

screened at the National Cancer Institute, USA. These compounds were particularly more active against lung carcinoma cell lines and demonstrated cytotoxicity even superior to the Cisplatin [80]. The mechanistic study undertaken by our group indicated NF-κB modulating effects of these compounds [76–77,81].

Recent studies have confirmed that cancer and inflammation are closely related with each other [6,8,10–11,15,17]. Many inflammatory mediators, such as TNF-α, NF-κB, COX-2, PGE_2, and cyclin D1 are up-regulated in the various cancers [7–9]. Persistent inflammation stimulates generation of TNF-α, which in turn activates IKK. The IKK then phosphorylates and subsequently degrades IκBα, leading to a translocation of free NF-κB into the nucleus, where it binds with the DNA and mediates transcription of proteins (ex. cyclin D1) responsible for the cell proliferation and differentiation. Interrelationship or crosstalk between the regulations of NF-κB and COX-2 is complex and is still not well understood. Although in the COX-regulated pathway, the prostaglandins are produced and among them, particularly PGE_2 is responsible for the angiogenesis and vasculogenesis. As we know that actively growing tumor cells meet their increased blood and nutrient supply through an angiogenesis, thereby COX-2 has emerged as a promising target for cancer therapeutics.

NSAIDs exert their effects by suppressing COX that leads to a decline in PGE_2 production. Over the last two decades, extensive research has established the COX-mediated chemopreventive and anticancer potentials of NSAIDs. Currently, numerous NSAIDs, such as aspirin, ibuprofen, ketoprofen, naproxen, diclofenac, coxibs and their derivatives are being developed under various anticancer drug discovery paradigms. One of such predominant drug discovery strategies is a conjugation of NSAIDs with other potentially acting anticancer scaffolds and in the majority of cases, these anticancer scaffolds act through a mechanism different than NSAIDs, leading to an additive effect.

These observations collectively identify combination therapy of COX-2 and NF-κB inhibitors as a logical and promising therapeutic strategy against various inflammatory diseases and cancer. Moreover, a single chemical moiety simultaneously acting on two different targets not only combats cancer more vigorously but also bears the less possibility of resistance development. The conjugated or hybrid compounds may also alleviate the issues pertaining to absorption, distribution, metabolism, excretion, and toxicity, while displaying better patient compliance than the relative physical mixture.

Based on these explained factors, we decided to synthesize conjugates of NSAIDs (**Fig. 2.1**), namely aspirin (**28**), ibuprofen (**29**), ketoprofen (**30**), naproxen (**31**), and diclofenac (**32**) with the various lantadenes (**33**–**38**, **Fig. 2.2**) as novel dual acting inhibitors of the COX-2 and NF-κB. As NF-κB is activated by IκBα and IKK mediated pathway; therefore, isolated and synthesized compounds were also evaluated against IκBα and IKK. The most potent compounds were also tested against NF-κB-regulated protein cyclin D1. An inflammatory product PGE_2 is produced by an action of COX-2 and this led to the screening of compounds against both of these targets.

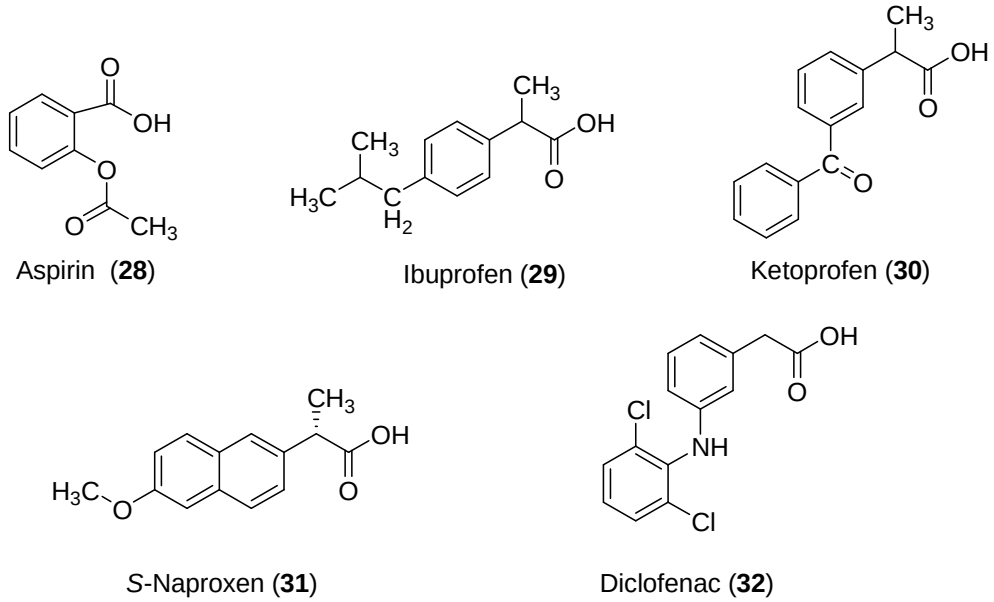

Figure 2.1. The chemical structures of NSAIDs (**28**–**32**) used for the synthesis of lantadene–NSAID ester conjugates

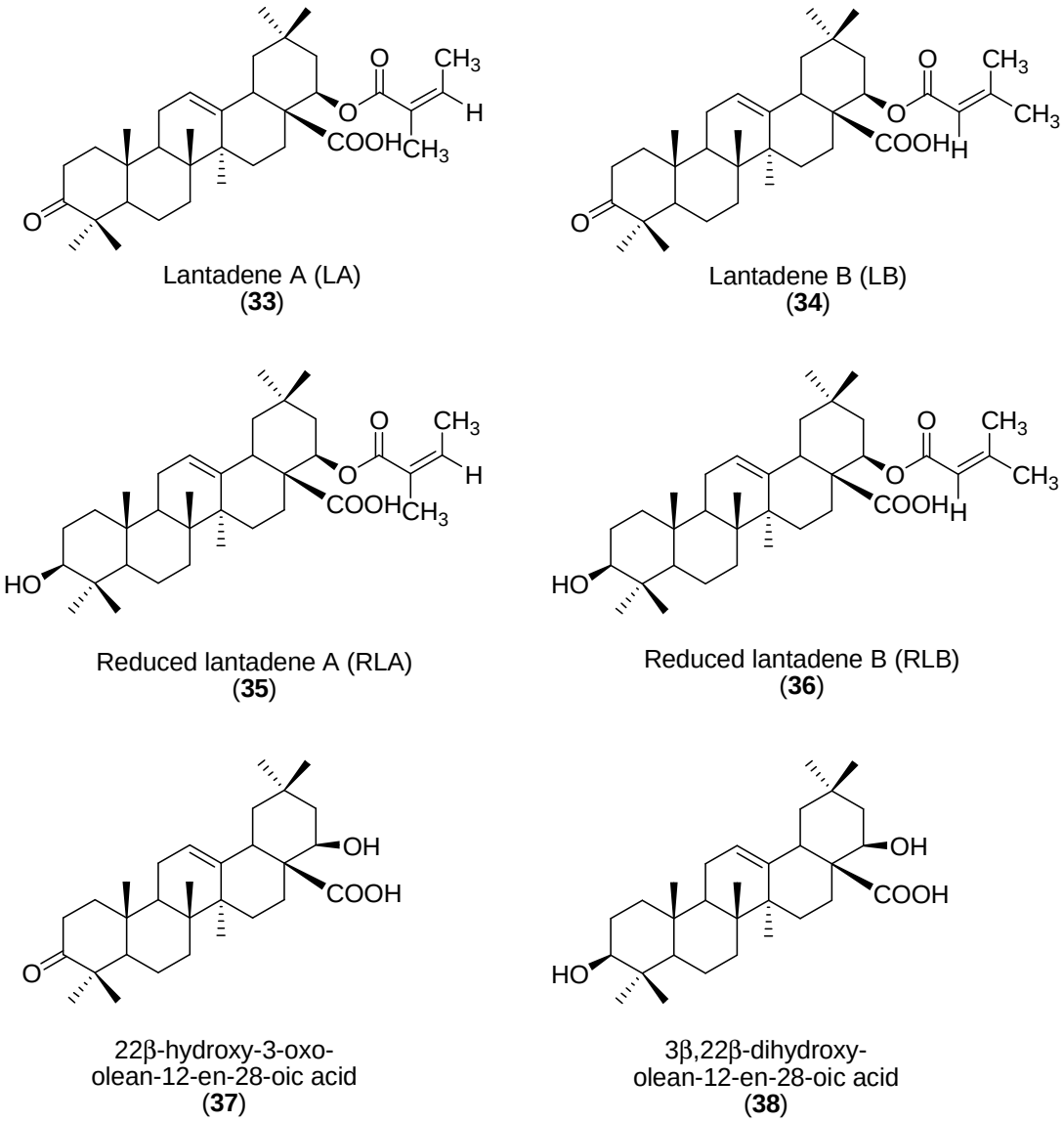

Figure 2.2. The chemical structures of parent lantadenes (**33**–**38**) used for the synthesis of lantadene–NSAID ester conjugates

CHAPTER 3

MATERIALS AND METHODS

3.1. General experimental methods

All the chemicals and solvents were purchased from Spectrochem, SD fine chemicals limited, Loba Chemie, HiMedia, Finar chemicals, Merck, and Sigma-Aldrich, India. Antibodies to IκBα, COX-2, and cyclin D1 were purchased from Santa Cruz Biotechnology (Santa Cruz, CA, USA). The anti-β-actin antibody was purchased from Sigma Chemicals (St Louis, MO, USA). Progresses of the reactions were monitored on Merck TLC plates, silica gel 60 F_{254} (Merck, Germany). For purification of compounds, glass columns of appropriate sizes were used. Melting points were determined on the digital melting point apparatus (Indosati scientific lab equipments, India) and were uncorrected. FT-IR spectra of isolated and synthesized compounds were recorded on a PerkinElmer spectrum 400 FT-IR and FT-NIR spectrophotometer using potassium bromide pellets. NMR spectra of compounds were recorded with a Bruker AVANCE II 400 NMR spectrometer using $CDCl_3$, DMSO-d_6, and a mixture of $CDCl_3$ and DMSO-d_6 as solvents, and chemical shifts were presented in parts per million (δ). Tetramethylsilane was used as an internal standard in NMR analysis. The ESI-MS spectra of compounds were recorded on a Waters Micromass Q-T of micro Mass spectrometer using electrospray ionization at 70 eV. Elemental analyses of compounds were carried out with a 2400 CHN analyzer (PerkinElmer, USA). For high-performance liquid chromatography (HPLC) analysis, a Waters HPLC system comprised of Waters 717plus autosampler, Waters 515 HPLC pumps, Waters Spherisorb ODS2 (80 Å, 5 µm, 4.6 × 250 mm) C18 column, Waters 2996 PDA detector, and empower software system 2.1 was used.

3.2. Isolation and synthesis of lantadene congeners

3.2.1 Plant materials

Leaves of weed *Lantana camara* Linn. were collected in September 2010 from Palampur (H.P.), India. The plant material was collected from private land and we confirm that the owner of the land gave their permission for us to collect the plant from his site. We further confirm that the plant collected was not an endangered or protected species. The leaves were shade-dried and powdered. The plant material was taxonomically identified and authenticated by Dr. Sunil Dutta, Scientist, National Medicinal Plant Board, Ayush, New Delhi, India. A voucher specimen (LC; 097 JUIT) have been deposited in the Herbarium of Jaypee University of Information Technology, Waknaghat, India.

3.2.2. Quantification of lantadene A and B in lantana leaves

Lantana leaves were shade-dried and finely powdered by using an electronic grinder. The five different extracts were then prepared by macerating 10 g of finely powdered lantana leaves in 100 ml each of tetrahydrofuran (THF), chloroform, ethyl acetate, ethanol, and methanol (MeOH) at room temperature for 24 h with intermittent shaking. The extracts were then filtered and the filtrates were used for the quantification of lantadene A and B by using HPLC. The standard lantadene A and B were prepared as 1 mg/10 ml in methanol. The isocratic solvent system; methanol-acetonitrile-water-acetic acid (68:20:12:0.01) was used as a mobile phase. The injection volume was 10 µl and the flow-rate was kept at 1 ml/min. The detection was made at 210 nm. Quantification was done by applying the formula: [(area of sample/area of standard) × (weight of standard/volume of standard) × (volume of sample/weight of sample)] × 100.

3.2.3. Extraction and isolation of lantadene A (33) and B (34)

1 kg of lantana leaves powder was extracted with 5 L of ethyl acetate at room temperature for 24 h with intermittent shaking. The extract was filtered and 250

g of activated charcoal was added to it for 1 h. The extract was filtered again and the filtrate was concentrated under reduced pressure in a rotary evaporator. To the concentrated extract, 100 ml of chloroform was added and partitioned with 100 ml of water. The aqueous layer was again washed with chloroform (100 ml × 2). The organic portion was finally evaporated to dryness to yield the crude mixture of lantadenes, 0.448% w/w (4.48 ± 0.216 g). Lantadene A and B were isolated from a mixture of crude lantadenes with the help of column chromatography (14 cm silica gel bed height, 110.30 g silica gel of 100–200 mesh, and 4 cm column diameter) in a mobile phase of petroleum ether (60–80 °C): ethyl acetate (4:1). ($R_{f:}$ lantadene A: 0.40, lantadene B: 0.37).

3.2.3.1. 22*β*-Angeloyloxy-3-oxo-olean-12-en-28-oic acid (33)

Mp: 285–286 °C. Anal. calcd. for $C_{35}H_{52}O_5$ (552.38): %C, 76.05; H, 9.48. Found: %C, 76.10; H, 9.49. IR (KBr, cm^{-1}): 3308.77 (O–H), 2952.45, (C–H), 1736.06 (C=O keto), 1715.85 (C=O ester), 1702.14 (C=O acid), 1649.42 (C=C). ^{1}H NMR (400 MHz, $CDCl_3$, δ ppm): 5.9759–6.0295 (1H, m, C-33-H), 5.3816 (1H, s, C-12-H), 5.0911 (1H, s, C-22-H), 3.0321–3.0734 (1H, dd, *J*= 13.76, 3.36 Hz, C-18-H), 2.5175–2.6028 (1H, m, C-2-Ha), 2.3396–2.4033 (1H, m, C-2-Hb), 1.1754 (3H, s, CH_3), 1.0920 (3H, s, CH_3), 1.0538 (6H, s, CH_3), 1.0032 (3H, s, CH_3), 0.8951 (3H, s, CH_3), 0.8271 (3H, s, CH_3). ^{13}C NMR (100 MHz, $CDCl_3$, δ ppm): 217.70 (C-3), 179.28 (C-28), 166.27 (C-31), 143.11 (C-13), 139.07 (C-33), 127.59 (C-32), 122.50 (C-12), 75.85 (C-22), 55.30 (C-5), 50.59 (C-17), 47.45 (C-9), 46.88 (C-4), 45.94 (C-19) 42.00 (C-14), 39.22 (C-8), 39.11 (C-1), 38.46 (C-18), 37.72 (C-21), 36.78 (C-10), 34.14 (C-2), 33.70 (C-29), 32.19 (C-7), 30.05 (C-20), 27.57 (C-15), 26.45 (C-23), 26.15 (C-27), 25.79 (C-30), 24.19 (C-16), 23.51 (C-11), 21.49 (C-6), 20.59 (C-35), 19.48 (C-26), 16.85 (C-24), 15.68 (C-34), 15.11 (C-25). ESI-MS (*m/z*): 553.40 (M^++1).

3.2.3.2. 22*β*-Senecioyloxy-3-oxo-olean-12-en-28-oic acid (34)

Mp: 283–284 °C. Anal. calcd. for $C_{35}H_{52}O_5$ (552.38): %C, 76.05; H, 9.48. Found: %C, 76.13; H, 9.50. IR (KBr, cm^{-1}): 3289.29 (O–H), 2950.25, 2925.42,

2864.39 (C–H), 1738.61 (C=O keto), 1712.29 (C=O ester), 1693.62 (C=O acid), 1648.72 (C=C). ^{1}H NMR (400 MHz, $CDCl_3$, δ ppm): 5.5577 (1H, s, C-32-H), 5.3785 (1H, s, C-12-H), 5.0404 (1H, s, C-22-H), 3.0072–3.0488 (1H, dd, *J*= 13.44, 3.48 Hz, C-18-H), 2.5190–2.6039 (1H, m, C-2-Ha), 2.3417–2.4022 (1H, m, C-2-Hb), 1.1754 (3H, s, CH_3), 1.0906 (3H, s, CH_3), 1.0656 (3H, s, CH_3), 1.0486 (3H, s, CH_3), 1.0027 (3H, s, CH_3), 0.8845 (3H, s, CH_3), 0.8388 (3H, s, CH_3). ^{13}C NMR (100 MHz, $CDCl_3$, δ ppm): 217.77 (C-3), 178.84 (C-28), 165.33 (C-31), 157.16 (C-33), 143.09 (C-13), 122.37 (C-12), 115.96 (C-32), 75.20 (C-22), 55.30 (C-5), 50.57 (C-17), 47.45 (C-9), 46.87 (C-4), 45.97 (C-19) 42.05 (C-14), 39.24 (C-8), 39.17 (C-1), 38.54 (C-18), 37.63 (C-21), 36.77 (C-10), 34.16 (C-2), 33.75 (C-29), 32.26 (C-7), 30.07 (C-20), 27.59 (C-15), 27.46 (C-35), 26.44 (C-23), 26.28 (C-27), 25.77 (C-30), 24.13 (C-16), 23.56 (C-11), 21.50 (C-6), 20.25 (C-34), 19.52 (C-26), 16.85 (C-24), 15.16 (C-25). ESI-MS (*m/z*): 553.50 (M^++1).

3.2.4. Synthesis of 3*β*-hydroxy-22*β*-angeloyloxy-olean-12-en-28-oic acid (35) and 3*β*-hydroxy-22*β*-senecioyloxy-olean-12-en-28-oic acid (36)

Compound **33** and **34** weighing 1000 mg (1.80 mmol) each were separately stirred with 68.09 mg (1.80 mmol) of sodium borohydride ($NaBH_4$) in a 50 ml solution of methanol (25 ml) and tetrahydrofuran (THF) (25 ml) for 7 h (**Scheme 3.1**). After completion of the reaction, dilute hydrochloric acid (HCl) solution was added to quench the $NaBH_4$. The organic solvents were evaporated in a rotary evaporator and the precipitated reduced lantadenes were extracted with dichloromethane (DCM). The solvent was removed under reduced pressure to afford **35** (902.12 mg, 89.88%) (pet. ether: ethyl acetate; 4:1, R_f; 0.31) and **36** (879.18 mg, 87.60%) (pet. ether: ethyl acetate; 4:1, R_f; 0.28), respectively.

3.2.4.1. 3*β*-Hydroxy-22*β*-angeloyloxy-olean-12-en-28-oic acid (35)

Yield: 89.88% (902.12 mg), Mp: 279–280 °C. Anal. calcd. for $C_{35}H_{54}O_5$ (554.40): %C, 75.77; H, 9.81. Found: %C, 75.84; H, 9.78. IR (KBr, cm^{-1}):

3482.87 (O–H), 2948.99, 2875.53 (C–H), 1717.87 (C=O ester), 1701.25 (C=O acid), 1650.10 (C=C). ^{1}H NMR (400 MHz, $CDCl_3$, δ ppm): 5.9627–6.0167 (1H, m, C-33-H), 5.3523 (1H, s, C-12-H), 5.0219 (1H, s, C-22-H), 3.2080–3.2430 (1H, dd, *J* = 9.64, 2.48 Hz, C-3-H), 2.9866–3.0551 (1H, dd, *J* = 22.48, 3.24 Hz, C-18-H), 1.1602 (3H, s, CH_3), 0.9910 (6H, s, CH_3), 0.9178 (3H, s, CH_3), 0.8883 (3H, s, CH_3), 0.7855 (3H, s, CH_3), 0.7694 (3H, s, CH_3). ^{13}C NMR (100 MHz, $CDCl_3$, δ ppm): 179.66 (C-28), 166.32 (C-31), 143.08 (C-13), 138.88 (C-33), 127.69 (C-32), 122.64 (C-12), 79.02 (C-3), 75.96 (C-22), 55.18 (C-5), 50.55 (C-17), 47.63 (C-9), 46.02 (C-19), 41.87 (C-14) 39.22 (C-8), 38.75 (C-4), 38.40 (C-18), 38.31 (C-1), 37.70 (C-21), 37.05 (C-10), 33.72 (C-29), 32.60 (C-7), 30.04 (C-20), 28.10 (C-2), 27.56 (C-15), 26.61 (C-23), 26.18 (C-27), 25.90 (C-30), 24.21 (C-16), 23.44 (C-11), 20.61 (C-6), 20.23 (C-35), 18.23 (C-26), 17.01 (C-24), 15.60 (C-34), 15.44 (C-25). ESI-MS (*m/z*): 555.50 (M^++1).

3.2.4.2. 3*β*-Hydroxy-22*β*-Senecioyloxy-olean-12-en-28-oic acid (36)

Yield: 87.60% (879.18 mg), Mp: 277–278 °C. Anal. calcd. for $C_{35}H_{54}O_5$ (554.40): %C, 75.77; H, 9.81. Found: %C, 75.72; H, 9.80. IR (KBr, cm^{-1}): 3480.79 (O–H), 2949.59, 2875.08 (C–H), 1717.98 (C=O ester), 1701.98 (C=O acid), 1651.68 (C=C). ^{1}H NMR (400 MHz, $CDCl_3$, δ ppm): 5.4899 (1H, s, C-32-H), 5.2901 (1H, s, C-12-H), 4.9638 (1H, s, C-22-H), 3.1349–3.1725 (1H, dd, *J* = 10.12, 2.96 Hz, C-3-H), 2.9234–2.9700 (1H, dd, *J* = 14.12, 4.72 Hz, C-18-H), 1.1862 (3H, s, CH_3), 1.0924 (3H, s, CH_3), 0.9334 (3H, s, CH_3), 0.9207 (3H, s, CH_3), 0.8511 (3H, s, CH_3), 0.8128 (3H, s, CH_3), 0.7145 (3H, s, CH_3). ^{13}C NMR (100 MHz, $CDCl_3$, δ ppm): 178.25 (C-28), 165.33 (C-31), 157.20 (C-33), 143.06 (C-13), 128.86 (C-12), 116.00 (C-32), 79.01 (C-3), 75.22 (C-22), 55.19 (C-5), 50.53 (C-17), 47.63 (C-9), 46.01 (C-19), 41.92 (C-14) 39.24 (C-8), 38.76 (C-4), 38.45 (C-18), 38.42 (C-1), 37.64 (C-21), 37.04 (C-10), 33.78 (C-29), 32.66 (C-7), 30.08 (C-20), 28.11 (C-2), 27.61 (C-15), 27.48 (C-35), 27.17 (C-23), 26.31 (C-27), 25.89 (C-30), 24.12 (C-16), 23.46 (C-11), 20.76 (C-6), 20.24 (C-34), 19.20 (C-26), 16.97 (C-24), 15.45 (C-25). ESI-MS (*m/z*): 555.40 (M^++1).

3.2.5. Synthesis of 22*β*-hydroxy-3-oxo-olean-12-en-28-oic acid (37)

To a 1 g mixture of **33** and **34**, 100 ml of 10% ethanolic potassium hydroxide (KOH) was added and the reaction mixture was refluxed for 6 h (**Scheme 3.1**). After completion of the reaction, dilute HCl solution was added to the reaction mixture to neutralize the KOH and the product precipitated out was washed with water (100 ml × 3) and purified through column chromatography to afford the compound **37** (651.17 mg, 76.47%).

3.2.5.1. 22*β*-Hydroxy-3-oxo-olean-12-en-28-oic acid (37)

Yield: 76.47%, Mp: 240–242 °C. Anal. calcd. for $C_{30}H_{46}O_4$ (470.34): %C, 76.55; H, 9.85. Found: %C, 76.62; H, 9.87. IR (KBr, cm^{-1}): 3439.83, 3261.69 (O–H), 2929.90, 2868.21 (C–H), 1730.93 (C=O keto), 1706.08 (C=O acid), 1622.39 (C=C). ^{1}H NMR (400 MHz, $CDCl_3$+DMSO-d_6 mixture, δ ppm): 5.2486–5.2637 (1H, t, *J*= 3.02 Hz, C-12-H), 3.7501–3.7670 (1H, t, *J*= 3.38 Hz, C-22-H), 3.5997 (1H, s (br), C-22-OH), 2.9251–2.9699 (1H, dd, *J*= 13.20, 4.28 Hz, C-18-H), 2.4448–2.5298 (1H, m, C-2-Ha), 2.2748–2.3405 (1H, m, C-2-Hb), 1.1238 (3H, s, CH_3), 1.0769 (3H, s, CH_3), 0.9908 (3H, s, CH_3), 0.8440 (3H, s, CH_3), 0.8330 (3H, s, CH_3), 0.7805 (3H, s, CH_3), 0.7094 (3H, s, CH_3). ^{13}C NMR (100 MHz, $CDCl_3$+DMSO-d_6 mixture, δ ppm): 216.41 (C-3), 176.33 (C-28), 144.25 (C-13), 120.77 (C-12), 77.23 (C-22), 54.56 (C-5), 51.07 (C-17), 47.10 (C-9), 46.70 (C-4), 45.96 (C-19) 41.74 (C-14), 38.79 (C-8), 38.75 (C-1), 38.52 (C-18), 38.00 (C-21), 36.22 (C-10), 33.68 (C-2), 33.59 (C-29), 31.82 (C-7), 29.77 (C-20), 27.31 (C-15), 27.02 (C-23), 26.13 (C-27), 25.25 (C-30), 23.88 (C-16), 22.97 (C-11), 21.00 (C-6), 19.11 (C-26), 16.52 (C-24), 14.67 (C-25). ESI-MS (negative-ion mode, *m/z*): 470.32 (M^-) (469.29 (M^-–1).

3.2.6. Synthesis of 3*β*,22*β*-Dihydroxy-olean-12-en-28-oic acid (38)

470.68 mg (1 mmol) of compound **37** was stirred with 37.83 mg (1 mmol) of $NaBH_4$ in a 50 ml solution of methanol (25 ml) and THF (25 ml) for 7 h (**Scheme 3.1**). After completion of the reaction, dilute HCl solution was added

to the reaction mixture to quench the $NaBH_4$. The organic solvents were removed under reduced pressure and precipitated product was extracted with DCM. The solvent was removed under reduced pressure to afford a compound **38**, which was further purified by using the column chromatography (silica gel of 100–200 mesh and a gradient mobile phase of hexane-ethyl acetate).

3.2.6.1. 3*β*,22*β*-Dihydroxy-olean-12-en-28-oic acid (38)

Yield: 87.79%, Mp: 282–284 °C. Anal. calcd. for $C_{30}H_{48}O_4$ (472.36): %C, 76.23; H, 10.24. Found: %C, 76.29; H, 10.23. IR (KBr, cm^{-1}): 3435.07 (O–H), 2948.50, 2876.33 (C–H), 1705.76 (C=O), 1648.59 (C=C). ^{1}H NMR (400 MHz, $CDCl_3$+DMSO-d_6 mixture, δ ppm): 11.4773 (1H, s (br), C-28-H (COOH)), 5.2267–5.2441 (1H, t, *J*= 3.48 Hz, C-12-H), 4.1543 (1H, s (br), C-22-OH), 3.7499–3.7654 (1H, t, *J*= 3.10 Hz, C-22-H), 3.5768 (1H, s (br), C-3-OH), 3.0544–3.0934 (1H, t, *J*= 7.80 Hz, C-3-H), 2.9195–2.9626 (1H, dd, *J*= 13.84, 3.56 Hz, C-18-H), 1.1270 (3H, s, CH_3), 1.0925 (3H, s, CH_3), 0.9397 (3H, s, CH_3), 0.8953 (3H, s, CH_3), 0.8513 (3H, s, CH_3), 0.7982 (3H, s, CH_3), 0.7250 (3H, s, CH_3). ^{13}C NMR (100 MHz, $CDCl_3$+DMSO-d_6 mixture, δ ppm): 176.23 (C-28), 143.82 (C-13), 120.96 (C-12), 77.16 (C-3), 72.70 (C-22), 54.80 (C-5), 51.00 (C-17), 47.10 (C-9), 46.06 (C-19), 41.63 (C-14), 41.11 (C-8), 38.80 (C-4), 38.30 (C-18), 38.10 (C-1), 37.93 (C-21), 36.52 (C-10), 33.71 (C-29), 32.42 (C-7), 29.79 (C-20), 27.96 (C-2), 27.32 (C-15), 27.06 (C-23), 26.80 (C-27), 25.38 (C-30), 23.89 (C-16), 22.90 (C-11), 17.90 (C-6), 16.69 (C-26), 15.63 (C-24), 15.03 (C-25). ESI-MS (negative-ion mode, *m/z*): 472.30 (M^-) 471.20 (M^-–1).

3.2.7. Synthesis of Methyl 22*β*-hydroxy-3-oxo-olean-12-en-28-ate (39)

Compound **37** (1 mmol, 470.68 mg) was refluxed with potassium carbonate (3 mmol, 414.61 mg) in acetone for 1 h. After that dimethyl sulfate (2 mmol, 189.66 µl) was added to the reaction mixture and refluxing was continued for another 11 h (**Scheme 3.1**). After completion of the reaction, acetone was removed under reduced pressure, the reaction mixture was poured into water,

and the precipitated product was extracted with DCM. Organic solvent was removed in a rotary evaporator and the crude product was chromatographed over silica gel (100–200 mesh) and eluted with a gradient mobile phase of hexane-ethyl acetate to yield the final purified product (**39**).

3.2.7.1. Methyl 22*β*-hydroxy-3-oxo-olean-12-en-28-ate (39)

Yield: 72.00%, Mp: 190-192 °C. Anal. calcd. for $C_{31}H_{48}O_4$ (484.36): %C, 76.82; H, 9.98. Found: %C, 76.83; H, 9.96. IR (KBr, cm^{-1}): 3518 (O-H), 2945 (C-H), 1729 (C=O keto), 1708 (C=O ester). ^{1}H NMR (400 MHz, $CDCl_3$, δ ppm): 5.3678–5.3843 (1H, t, *J*= 6.60 Hz, C-12-H), 3.8837–3.8989 (1H, t, *J*= 6.08 Hz, C-22-H), 3.6702 (3H, s, C-31-H), 3.0396–3.0843 (1H, dd, *J*= 13.84, 4.04 Hz, C-18-H), 2.5138–2.5995 (1H, m, C-2-Ha), 2.3312–2.3962 (1H, m, C-2-Hb), 1.1555 (3H, s, CH_3), 1.1262 (3H, s, CH_3), 1.0862 (3H, s, CH_3), 1.0628 (3H, s, CH_3), 1.0473 (3H, s, CH_3), 0.8997 (3H, s, CH_3), 0.8244 (3H, s, CH_3). ^{13}C NMR (100 MHz, $CDCl_3$, δ ppm): 217.83 (C-3), 176.14 (C-28), 143.43 (C-13), 122.19 (C-12), 74.62 (C-22), 55.33 (C-5), 52.43 (C-31), 51.58 (C-17), 47.46 (C-9), 46.87 (C-4), 45.97 (C-19), 42.11 (C-14), 41.39 (C-8), 39.27 (C-1), 39.19 (C-18), 38.26 (C-21), 36.75 (C-10), 34.18 (C-2), 33.92 (C-29), 32.21 (C-7), 30.15 (C-20), 27.79 (C-15), 27.20 (C-23), 26.41 (C-27), 25.74 (C-30), 24.49 (C-16), 23.55 (C-11), 21.50 (C-6), 19.57 (C-26), 16.72 (C-24), 15.09 (C-25). ESI-MS (*m/z*): 507.50 $(M+Na)^+$, 991.90 $(2M+Na)^+$.

3.2.8. Synthesis of Methyl 3*β*,22*β*-dihydroxy-olean-12-en-28-ate (40)

Equimolar amount of compound **39** (1 mmol, 484.71 mg) and sodium borohydride (1 mmol, 37.83 mg) was stirred in a 50 ml solution of methanol-tetrahydrofuran (25 ml MeOH+25 ml THF) for 7 h (**Scheme 3.1**). At the end of the reaction, sodium borohydride remained was quenched with a dilute HCl solution. Organic solvents were removed in a rotary evaporator and the precipitated product was extracted with DCM. The DCM was removed under reduced pressure and the crude product was further purified with the help of

column chromatography (silica gel: 100–200 mesh) using a gradient mobile phase of hexane-ethyl acetate to give the final purified product (**40**).

3.2.8.1. Methyl 3*β*,22*β*-dihydroxy-olean-12-en-28-ate (40)

Yield: 86.70%, Mp: 179-180 °C. Anal. calcd. for $C_{31}H_{50}O_4$ (486.37): %C, 76.50; H, 10.35. Found: %C, 76.47; H, 10.33. IR (KBr, cm^{-1}): 3566.56 (O-H), 3368.50 (O-H), 3270.80 (O-H of COOH), 2949.35, 2931.00, 2872.49 (C-H), 1711.48 (C=O), 1565.60 (C=C). ^{1}H NMR (400 MHz, $CDCl_3$, δ ppm): 5.3429–5.3608 (1H, t, *J*= 7.16 Hz, C-12-H), 3.8716–3.8883 (1H, t, *J*= 6.68 Hz, C-22-H), 3.6632 (3H, s, C-31-H), 3.1955–3.2352 (1H, dd, *J*= 11.36, 5.00 Hz, C-3-H), 3.0220–3.0672 (1H, dd, *J*= 13.88, 4.20 Hz, C-18-H), 1.1420 (3H, s, CH_3), 1.1216 (3H, s, CH_3), 0.9877 (3H, s, CH_3), 0.9221 (3H, s, CH_3), 0.8978 (3H, s, CH_3), 0.7835 (3H, s, CH_3), 0.7667 (3H, s, CH_3). ^{13}C NMR (100 MHz, $CDCl_3$, δ ppm): 176.21 (C-28), 143.33 (C-13), 122.44 (C-12), 78.99 (C-3), 74.70 (C-22), 55.22 (C-5), 52.44 (C-31), 51.55 (C-17), 47.62 (C-9), 46.02 (C-19), 42.00 (C-14), 41.38 (C-8), 39.29 (C-18), 38.75 (C-4), 38.48 (C-1), 38.18 (C-21), 37.02 (C-10), 33.91 (C-29), 32.69 (C-7), 30.14 (C-20), 28.09 (C-2), 27.79 (C-15), 27.21 (C-23), 27.18 (C-27), 25.85 (C-30), 24.53 (C-16), 23.46 (C-11), 18.32 (C-6), 16.80 (C-26), 15.58 (C-24), 15.38 (C-25). ESI-MS (*m/z*): 509.40 $(M+Na)^+$.

3.2.9. Synthesis of 3*β*-hydroxylimino-substituted 22*β*-Angeloyloxy/22*β*-Senecioyloxy-olean-12-en-28-oic acids (41–42)

1 mmol (552.78 mg) of lantadene (**33**, **34**) was refluxed with 10 equivalent of hydroxylamine hydrochloride (10 mmol, 694.90 mg) in pyridine at 92–95 °C for 8 h **(Scheme 3.1)**. The reaction mixture was poured into the 10% HCl solution and the product was extracted with DCM and washed for a further three times with a 10% HCl solution (100 ml × 3). The organic solvent was removed under reduced pressure till dryness and the crude product obtained was subjected to column chromatography using the silica gel (100–200 mesh) and a gradient mobile phase of hexane-ethyl acetate to yield the final purified product (**41**–**42**).

3.2.9.1. 22*β*-Angeloyloxy-3-hydroxylimino-olean-12-en-28-oic acid (41)

Yield: 59.88%, Mp: 235-236 °C. Anal. calcd. for $C_{35}H_{53}NO_5$ (567.39): %C, 74.04; H, 9.41. Found: %C, 74.00; H, 9.40. IR (KBr, cm^{-1}): 3271.11 (O-H), 2951.50 (C-H), 1718.30 (C=O), 1647.24 (C=C). ^{1}H NMR (400 MHz, $CDCl_3$+DMSO-d_6 mixture, δ ppm): 11.7341 (1H, s (br), C-28-H (COOH)), 5.9792–6.0290 (1H, m, C-33-H), 5.3471–5.3645 (1H, t, *J*= 6.96 Hz, C-12-H), 5.0170–5.0317 (1H, t, *J*= 5.88 Hz, C-22-H), 2.2019–2.2610 (1H, m, C-2-Ha), 2.0594–2.1419 (1H, m, C-2-Hb), 1.1498 (3H, s, CH_3), 1.0272 (3H, s, CH_3), 1.0189 (6H, s, 2×CH_3), 1.0096 (3H, s, CH_3), 0.8932 (3H, s, CH_3), 0.8598 (3H, s, CH_3). ^{13}C NMR (100 MHz, $CDCl_3$+DMSO-d_6 mixture, δ ppm): 175.35 (C-28), 165.77 (C-31), 164.22 (C-3), 143.11 (C-13), 137.35 (C-33), 127.57 (C-32), 121.46 (C-12), 75.60 (C-22), 55.29 (C-5), 49.65 (C-17), 46.60 (C-9), 45.53 (C-19), 41.51 (C-14), 39.50 (C-4), 38.81 (C-8), 38.12 (C-18), 37.79 (C-1), 37.39 (C-21), 36.50 (C-10), 33.31 (C-29), 31.99 (C-7), 29.55 (C-20), 27.18 (C-15), 27.06 (C-23), 25.76 (C-27), 25.27 (C-30), 23.64 (C-16), 23.10 (C-2), 22.89 (C-11), 20.07 (C-6), 18.51 (C-35), 16.42 (C-26), 16.34 (C-34), 15.14 (C-24), 14.40 (C-25). ESI-MS (negative-ion mode, *m/z*): 567.30 (M^-), 566.30 (M^-–1).

3.2.9.2. 22*β*-Senecioyloxy-3-hydroxylimino-olean-12-en-28-oic acid (42)

Yield: 59.53%, Mp: 231-232 °C. Anal. calcd. for $C_{35}H_{53}NO_5$ (567.39): %C, 74.04; H, 9.41. Found: %C, 74.10; H, 9.42. IR (KBr, cm^{-1}): 3256.38 (O-H), 2953.32, 2926.07, 2859.85 (C-H), 1738.33 (C=O), 1720.33 (C=O), 1647.17 (C=C). ^{1}H NMR (400 MHz, $CDCl_3$+DMSO-d_6 mixture, δ ppm): 11.7373 (1H, s (br), C-28-H (COOH)), 5.5564 (1H, s, C-32-H), 5.3506 (1H, s, C-12-H), 5.0073–5.0238 (1H, t, *J*= 6.60 Hz, C-22-H), 2.2105–2.2568 (1H, m, C-2-Ha), 2.0545-2.1524 (1H, m, C-2-Hb), 1.1478 (3H, s, CH_3), 1.0251 (3H, s, CH_3), 1.0167 (6H, s, 2×CH_3), 1.0086 (3H, s, CH_3), 0.8872 (3H, s, CH_3), 0.8578 (3H, s, CH_3). ^{13}C NMR (100 MHz, $CDCl_3$+DMSO-d_6 mixture, δ ppm): 181.24 (C-28), 165.73 (C-31), 164.08 (C-3), 156.41 (C-33), 143.12 (C-13), 121.49 (C-12), 116.77 (C-32), 75.59 (C-22), 55.28 (C-5), 49.52 (C-17), 46.59 (C-9), 45.55 (C-19), 41.52 (C-

14), 39.48 (C-4), 38.81 (C-8), 38.00 (C-18), 37.80 (C-1), 37.40 (C-21), 36.51 (C-10), 33.33 (C-29), 32.00 (C-7), 29.56 (C-20), 27.21 (C-15), 27.06 (C-23), 26.00 (C-35), 25.77 (C-27), 25.27 (C-30), 23.57 (C-16), 23.12 (C-2), 22.89 (C-11), 20.08 (C-6), 16.39 (C-26), 16.33 (C-34), 15.15 (C-24), 14.43 (C-25). ESI-MS (negative-ion mode, *m/z*): 568.30 (M^-+1).

3.2.10. Synthesis of 3*β*,22*β*-Diacetoyloxy-olean-12-en-28-oic acid (43)

Compound **38** (1 mmol, 472.70 mg) and acetyl chloride (3 mmol, 213.30 µl) were refluxed in pyridine in the presence of 4-dimethylaminopyridine (4-DMAP) for 10 h at 92–95 ºC (**Scheme 3.1**). At the end of the reaction, a 10% HCl solution was added to the reaction mixture and the precipitated product was extracted with DCM. The product was washed for a further three times with a 10% HCl solution (100 ml × 3) and purified by using the column chromatography (silica gel: 100–200 mesh) in a gradient mobile phase of hexane-ethyl acetate.

3.2.10.1. 3*β*,22*β*-Diacetoyloxy-olean-12-en-28-oic acid (43)

Yield: 59.25%, Mp: 301-303 °C. Anal. calcd. for $C_{34}H_{52}O_6$ (556.38): %C, 73.34; H, 9.41. Found: %C, 73.36; H, 9.40. IR (KBr, cm^{-1}): 3355.26 (O-H of COOH), 2990.34, 2950.25, 2923.26, 2876.39, 2847.49 (C-H), 1731.60 (C=O ester). ^{1}H NMR (400 MHz, $CDCl_3$, δ ppm): 5.3430–5.3599 (1H, t, *J*= 6.76 Hz, C-12-H), 5.0028–5.0172 (1H, t, *J*= 5.76 Hz, C-22-H), 4.4800–4.5196 (1H, t, *J*= 15.84 Hz, C-3-H), 2.9854–3.0298 (1H, dd, *J*= 13.76, 4.00 Hz, C-18-H), 2.0498 (3H, s, C-2′-H), 1.9411 (3H, s, C-2′′-H), 1.1530 (3H, s, CH_3), 1.0225 (3H, s, CH_3), 0.9472 (3H, s, CH_3), 0.8944 (3H, s, CH_3), 0.8693 (3H, s, CH_3), 0.8606 (3H, s, CH_3), 0.7650 (3H, s, CH_3). ^{13}C NMR (100 MHz, $CDCl_3$, δ ppm): 180.23 (C-28), 171.08 (C-1′), 169.70 (C-1′′), 142.86 (C-13), 122.71 (C-12), 80.85 (C-3), 76.14 (C-22), 55.25 (C-5), 50.56 (C-17), 47.52 (C-9), 45.76 (C-19), 41.80 (C-14), 39.24 (C-8), 38.14 (C-18), 38.10 (C-1), 37.68 (C-4), 37.68 (C-21), 36.94 (C-10), 33.69 (C-29), 32.56 (C-7), 30.01 (C-20), 28.02 (C-15), 27.56 (C-23), 26.29 (C-27), 25.86

(C-30), 23.91 (C-16), 23.50 (C-11), 23.44 (C-2), 21.31 (C-2′), 21.10 (C-4′), 18.09 (C-6), 17.05 (C-26), 16.67 (C-24), 15.49 (C-25). ESI-MS (negative-ion mode, *m/z*): 556.20 (M^-), 555.20 (M^-–1).

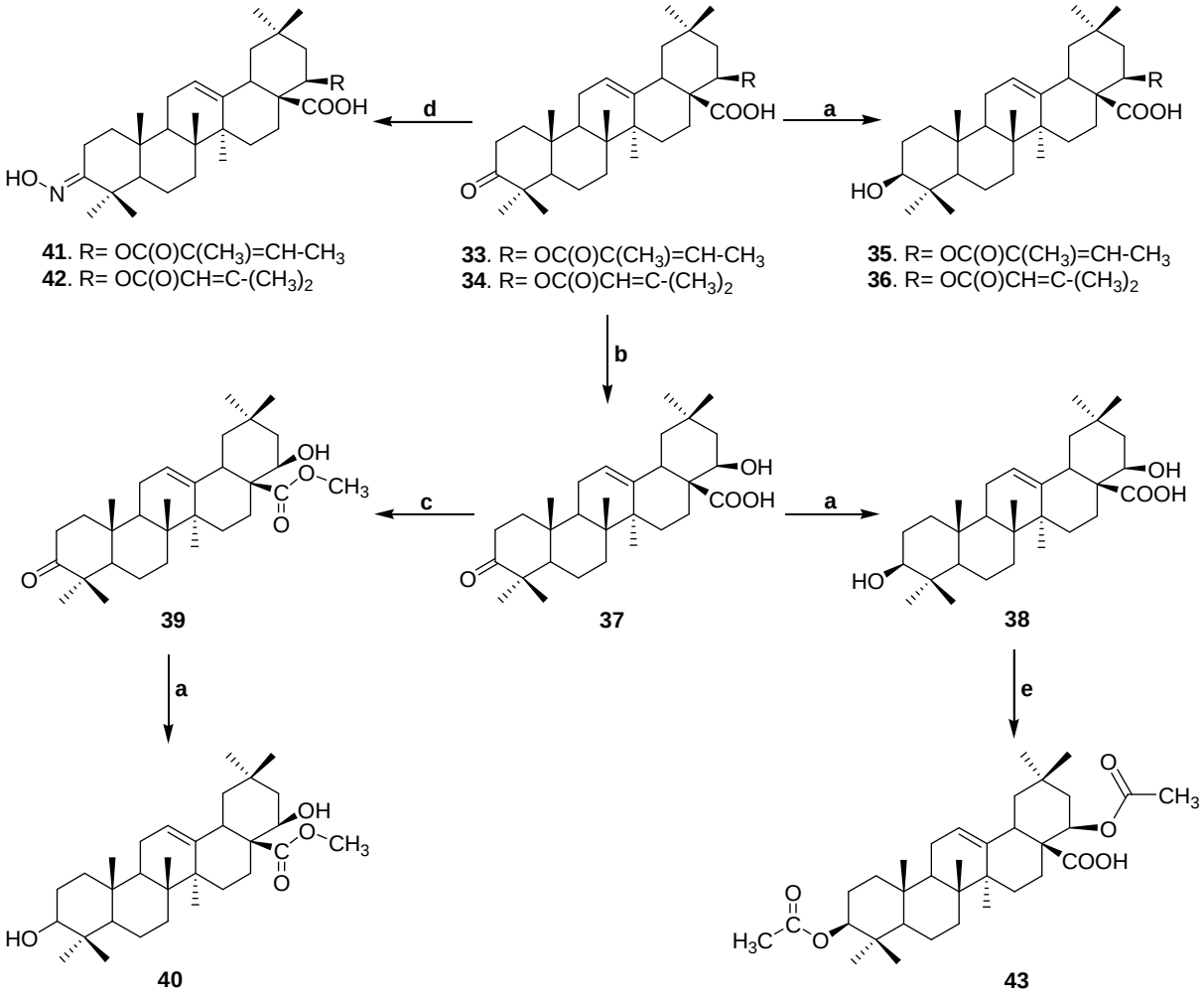

Scheme 3.1. Synthesis of lantadene congeners **35**–**43**. Reagents and conditions: (a) $NaBH_4$, MeOH-THF, stir 7 h; (b) 10% Ethanolic KOH, reflux 6 h; (c) K_2CO_3, $(CH_3O)_2SO_2$, acetone, reflux, 12 h; (d) $NH_4OH.HCl$, pyridine, reflux 92–95 °C, 8 h; (e) CH_3-CO-Cl, 4-DMAP, pyridine, reflux 92–95 °C, 10 h.

3.2.11. Synthesis of 3*β*-substituted and 22*β*-substituted olean-12-en-28-oic acids (44–54)

Compounds **44**–**47**, **52** were synthesized through a single step process, while compounds **48**–**51** and **53**–**54** were synthesized via a two step process. In the first step of the synthesis of compounds **48**–**51** and **53**–**54**, the acid function was converted into the anhydride function. The acid and acetyl chloride in the presence of pyridine were refluxed in DCM for 4–5 h (**Scheme 3.2**). The reaction mixture was concentrated and washed with chloroform (100 ml × 3) under reduced pressure at 60–65 °C to afford solid to semisolid anhydride products of the respective acids, which were used in the next step without further purification.

In the synthesis of 3*β*-substituted (**44**–**51)** and 22*β*-substituted (**52**–**54)** olean-12-en-28-oic acids step, compounds **35**, **36**, and **37** with appropriate carbonyl chlorides/anhydrides were refluxed in pyridine in the presence of 4-DMAP for 10–14 h at 92–95 ºC (**Scheme 3.3**). The reaction mixture was poured into 10% HCl solution and the precipitated product was extracted with DCM and washed for a further three times with a 10% HCl solution (100 ml × 3). The organic layer was evaporated to dryness and the crude product obtained was chromatographed over silica gel (100–200 mesh) and eluted with varying ratios of hexane-ethyl acetate to give the final purified products (**44**–**54**).

3.2.11.1. 3*β*-Acetoyloxy-22*β*-angeloyloxy-olean-12-en-28-oic acid (44)

Yield: 84.10%, Mp: 178-180 °C. Anal. calcd. for $C_{37}H_{56}O_6$ (596.41): %C, 74.46; H, 9.46. Found: %C, 74.50; H, 9.45. IR (KBr, cm^{-1}): 2950.19, 2877.28 (C-H), 1736.33 (C=O ester), 1719.91 (C=O acid), 1649.60 (C=C). ^{1}H NMR (400 MHz, $CDCl_3$, δ ppm): 5.8822–5.9399 (1H, m, C-33-H), 5.2740–5.2889 (1H, t, *J*= 5.96 Hz, C-12-H), 4.9972–5.0118 (1H, t, *J*= 5.84 Hz, C-22-H), 4.4116–4.4512 (1H, t, *J*= 15.84 Hz, C-3-H), 2.9424–2.9862 (1H, dd, *J*= 13.92, 3.96 Hz, C-18-H), 1.9830 (3H, s, C-2′-H), 1.0885 (3H, s, CH_3), 0.9247 (3H, s, CH_3), 0.8730 (3H, s, CH_3), 0.8227 (3H, s, CH_3), 0.8015 (3H, s, CH_3), 0.7957 (3H, s, CH_3), 0.6959

(3H, s, CH_3). ^{13}C NMR (100 MHz, $CDCl_3$, δ ppm): 179.56 (C-28), 171.12 (C-1′), 166.34 (C-31), 143.08 (C-13), 138.79 (C-33), 127.69 (C-32), 122.62 (C-12), 80.88 (C-3), 75.96 (C-22), 55.26 (C-5), 50.54 (C-17), 47.55 (C-9), 45.97 (C-19), 41.83 (C-14) 39.22 (C-8), 38.35 (C-18), 38.28 (C-4), 38.07 (C-1), 37.70 (C-21), 36.95 (C-10), 33.70 (C-29), 32.55 (C-7), 30.04 (C-20), 28.04 (C-15), 27.55(C-23), 26.15 (C-27), 25.85 (C-30), 24.20 (C-16), 23.51 (C-11), 23.43 (C-2), 21.35 (C-2′), 20.56 (C-6), 18.11 (C-35), 17.01 (C-26), 16.70 (C-24), 15.65 (C-34), 15.51 (C-25). ESI-MS (negative-ion mode, *m/z*): 596.30 (M^-), 595.30 (M^-–1).

3.2.11.2. 3*β*-Acetoyloxy-22*β*-senecioyloxy-olean-12-en-28-oic acid (45)

Yield: 82.09%, Mp: 172-174 °C. Anal. calcd. for $C_{37}H_{56}O_6$ (596.41): %C, 74.46; H, 9.46. Found: %C, 74.49; H, 9.47. IR (KBr, cm^{-1}): 2949.03 (C-H), 1720.98 (C=O acid), 1653.63 (C=C). ^1H NMR (400 MHz, $CDCl_3$, δ ppm): 5.4733–5.4789 (1H, t, *J*= 2.24 Hz, C-32-H), 5.2685–5.2841 (1H, t, *J*= 6.24 Hz, C-12-H), 4.9927–5.0069 (1H, t, *J*= 5.68 Hz, C-22-H), 4.4113–4.4508 (1H, t, *J*= 15.80 Hz, C-3-H), 2.9395–2.9834 (1H, dd, *J*= 13.92, 3.92 Hz, C-3-H), 1.9825 (3H, s, C-2′-H), 1.0870 (3H, s, CH_3), 0.9227 (3H, s, CH_3), 0.8722 (3H, s, CH_3), 0.8213 (3H, s, CH_3), 0.8007 (3H, s, CH_3), 0.7959 (3H, s, CH_3), 0.6922 (3H, s, CH_3). ^{13}C NMR (100 MHz, $CDCl_3$, δ ppm): 180.09 (C-28), 171.14 (C-1′), 166.33 (C-31), 157.16 (C-33), 143.09 (C-13), 122.59 (C-12), 115.95 (C-32), 80.88 (C-3), 75.96 (C-22), 55.25 (C-5), 50.55 (C-17), 47.55 (C-9), 45.97 (C-19), 41.81 (C-14) 39.21 (C-8), 38.29 (C-18), 38.24 (C-4), 38.06 (C-1), 37.69 (C-21), 36.95 (C-10), 33.70 (C-29), 32.53 (C-7), 30.04 (C-20), 28.04 (C-15), 27.53 (C-23), 27.49 (C-35), 26.15 (C-27), 25.85 (C-30), 24.20 (C-16), 23.50 (C-11), 23.43 (C-2), 21.34 (C-2′), 20.56 (C-6), 18.39 (C-34), 17.02 (C-26), 16.69 (C-24), 15.50 (C-25). ESI-MS (negative-ion mode, *m/z*): 596.30 (M^-), 595.30 (M^-–1).

3.2.11.3. 3*β*-Benzoyloxy-22*β*-angeloyloxy-olean-12-en-28-oic acid (46)

Yield: 90.00%, Mp: 117-119 °C. Anal. calcd. for $C_{42}H_{58}O_6$ (658.42): %C, 76.56; H, 8.87. Found: %C, 76.55; H, 8.88. IR (KBr, cm^{-1}): 3064.72, 2950.36, 2876.88 (C-H), 1716.97 (C=O), 1650.27 (C=C). ^1H NMR (400 MHz, $CDCl_3$, δ ppm):

8.0325–8.0887 (2H, m, C-3′ & C-7′-Ar-H), 7.5310–7.6216 (1H, m, C-5′-Ar-H), 7.4215–7.4646 (2H, m, C-4′ & C-6′-Ar-H), 5.9550–6.0677 (1H, m, C-33-H), 5.3776–5.3950 (1H, t, *J*= 6.96 Hz, C-12-H), 5.0955–5.1105 (1H, t, *J*= 6.00 Hz, C-22-H), 4.7317–4.7724 (1H, m, C-3-H), 3.0441–3.0865 (1H, dd, *J*= 13.64, 4.40 Hz, C-18-H), 1.1947 (3H, s, CH_3), 1.0267 (3H, s, CH_3), 1.0142 (3H, s, CH_3), 1.0058 (3H, s, CH_3), 0.9493 (3H, s, CH_3), 0.9077 (3H, s, CH_3), 0.8131 (3H, s, CH_3). ^{13}C NMR (100 MHz, $CDCl_3$, δ ppm): 181.10 (C-28), 166.52 (C-31), 166.31 (C-1′), 142.30 (C-13), 139.84 (C-33), 132.74 (C-5′), 130.44 (C-2′), 129.54 (C-3′ & C-7′), 128.71 (C-32), 128.33 (C-4′ & C-6′), 123.35 (C-12), 81.58 (C-3), 75.97 (C-22), 55.45 (C-5), 50.61 (C-17), 47.66 (C-9), 45.90 (C-19), 42.13 (C-14), 39.53 (C-8), 39.30 (C-18), 38.77 (C-4), 38.12 (C-1), 37.99 (C-21), 37.01 (C-10), 33.71 (C-29), 32.62 (C-7), 30.06 (C-20), 28.21 (C-15), 27.63 (C-23), 26.18 (C-27), 25.88 (C-30), 25.75 (C-16), 23.59 (C-11), 23.47 (C-2), 20.45 (C-6), 18.21 (C-35), 16.98 (C-26), 16.73 (C-24), 15.63 (C-34), 15.52 (C-25). ESI-MS (negative-ion mode, *m/z*): 658.00 (M^-), 657.20 (M^-–1).

3.2.11.4. 3*β*-Benzoyloxy-22*β*-senecioyloxy-olean-12-en-28-oic acid (47)

Yield: 88.17%, Mp: 115-116 °C. Anal. calcd. for $C_{42}H_{58}O_6$ (658.42): %C, 76.56; H, 8.87. Found: %C, 76.60; H, 8.85. IR (KBr, cm^{-1}): 2950.46, 2877.90, 2665.64 (C-H), 1716.35 (C=O), 1649.60 (C=C). ^{1}H NMR (400 MHz, $CDCl_3$, δ ppm): 8.0327–8.0921 (2H, m, C-3′ & C-7′-Ar-H), 7.5285–7.6294 (1H, m, C-5′-Ar-H), 7.4187–7.4861 (2H, m, C-4′ & C-6′-Ar-H), 5.5628–5.5689 (1H, t, *J*= 2.44 Hz, C-32-H), 5.3730–5.3896 (1H, t, *J*= 6.64 Hz, C-12-H), 5.0464–5.0615 (1H, t, *J*= 6.04 Hz, C-22-H), 4.7309–4.7716 (1H, m, C-3-H), 3.0210–3.0653 (1H, dd, *J*= 13.72, 4.04 Hz, C-18-H), 1.1943 (3H, s, CH_3), 1.0264 (3H, s, CH_3), 1.0167 (3H, s, CH_3), 1.0062 (3H, s, CH_3), 0.9499 (3H, s, CH_3), 0.8970 (3H, s, CH_3), 0.8201 (3H, s, CH_3). ^{13}C NMR (100 MHz, $CDCl_3$, δ ppm): 179.16 (C-28), 166.31 (C-31), 165.34 (C-1′), 157.12 (C-33), 143.06 (C-13), 132.74 (C-5′), 130.95 (C-2′), 129.54 (C-3′ & C-7′), 128.33 (C-4′ & C-6′), 122.57 (C-12), 115.99 (C-32), 81.52 (C-3), 75.28 (C-22), 55.38 (C-5), 50.63 (C-17), 47.59 (C-9), 46.01 (C-19), 41.96

(C-14), 39.31 (C-8), 38.47 (C-18), 38.19 (C-4), 38.11 (C-1), 37.68 (C-21), 37.01 (C-10), 33.79 (C-29), 32.64 (C-7), 30.09 (C-20), 28.22 (C-15), 27.63 (C-23), 27.42 (C-35), 26.31 (C-27), 25.88 (C-30), 24.14 (C-16), 23.59 (C-11), 23.51 (C-2), 20.22 (C-6), 18.20 (C-34), 16.98 (C-26), 16.96 (C-24), 15.54 (C-25). ESI-MS (negative-ion mode, *m/z*): 658.30 (M^-), 657.00 (M^-–1).

3.2.11.5. 3*β*-(2-Chlorobenzoyloxy)-22*β*-angeloyloxy-olean-12-en-28-oic acid (48)

Yield: 85.53%, Mp: 176-178 °C. Anal. calcd. for $C_{42}H_{57}ClO_6$ (692.38): %C, 72.76; H, 8.29. Found: %C, 72.82; H, 8.31. IR (KBr, cm^{-1}): 2948.62, 2877.90 (C-H), 1720.58 (C=O), 1548.70 (C=C). ^{1}H NMR (400 MHz, $CDCl_3$, δ ppm): 7.7959–7.8191 (1H, m, C-7′-Ar-H), 7.3828–7.4741 (2H, m, C-4′ & C-5′-Ar-H), 7.2916–7.3325 (1H, m, C-6′-Ar-H), 5.9508–6.0081 (1H, m, C-33-H), 5.3552–5.3709 (1H, t, *J*= 6.28 Hz, C-12-H), 5.0753–5.0892 (1H, t, *J*= 5.56 Hz, C-22-H), 4.7682–4.8085 (1H, m, C-3-H), 3.0253–3.0687 (1H, dd, *J*= 13.68, 3.72 Hz, C-18-H), 1.1884 (3H, s, CH_3), 0.9928 (3H, s, CH_3), 0.9828 (3H, s, CH_3), 0.9761 (3H, s, CH_3), 0.9450 (3H, s, CH_3), 0.9006 (3H, s, CH_3), 0.7889 (3H, s, CH_3). ^{13}C NMR (100 MHz, $CDCl_3$, δ ppm): 181.40 (C-28), 166.35 (C-1′), 165.71 (C-31), 143.11 (C-13), 138.78 (C-33), 133.48 (C-5′), 132.30 (C-3′), 131.26 (C-7′), 131.05 (C-4′), 130.93 (C-2′), 127.67 (C-32), 126.56 (C-6′), 122.59 (C-12), 82.63 (C-3), 75.99 (C-22), 55.38 (C-5), 50.59 (C-17), 47.57 (C-9), 45.98 (C-19), 41.87 (C-14), 39.22 (C-8), 38.25 (C-18), 38.17 (C-4), 37.96 (C-1), 37.69 (C-21), 36.99 (C-10), 33.70 (C-29), 32.55 (C-7), 30.07 (C-20), 28.21 (C-15), 27.55 (C-23), 26.15 (C-27), 25.91 (C-30), 24.22 (C-16), 23.50 (C-11), 23.46 (C-2), 20.56 (C-6), 18.13 (C-35), 17.02 (C-26), 16.70 (C-24), 15.65 (C-34), 15.53 (C-25). ESI-MS (negative-ion mode, *m/z*): 691.60 (M^-).

3.2.11.6. 3*β*-(2-Chlorobenzoyloxy)-22*β*-senecioyloxy-olean-12-en-28-oic acid (49)

Yield: 84.52%, Mp: 170-172 °C. Anal. calcd. for $C_{42}H_{57}ClO_6$ (692.38): %C, 72.76; H, 8.29. Found: %C, 72.79; H, 8.30. IR (KBr, cm^{-1}): 2949, 2877 (C-H),

1717 (C=O), 1651 (C=C). ^{1}H NMR (400 MHz, $CDCl_3$, δ ppm): 7.7950–7.8183 (1H, m, C-7′-Ar-H), 7.3818–7.4814 (2H, m, C-4′ & C-5′-Ar-H), 7.2909–7.3319 (1H, m, C-6′-Ar-H), 5.5659–5.5721 (1H, t, *J*= 2.48 Hz, C-32-H), 5.3732–5.3897 (1H, t, *J*= 6.60 Hz, C-12-H), 5.0436–5.0578 (1H, t, *J*= 5.68 Hz, C-22-H), 4.7666–4.8069 (1H, m, C-3-H), 3.0136–3.0580 (1H, dd, *J*= 13.56, 4.44 Hz, C-18-H), 1.1922 (3H, s, CH_3), 1.0137 (3H, s, CH_3), 0.9908 (6H, s, 2×CH_3), 0.9799 (3H, s, CH_3), 0.8939 (3H, s, CH_3), 0.8124 (3H, s, CH_3). ^{13}C NMR (100 MHz, $CDCl_3$, δ ppm): 178.49 (C-28), 165.41 (C-1′), 164.66 (C-31), 156.13 (C-33), 142.02 (C-13), 132.46 (C-5′), 131.34 (C-3′), 130.21 (C-7′), 130.01 (C-4′), 129.94 (C-2′), 125.52 (C-6′), 121.49 (C-12), 114.92 (C-32), 81.61 (C-3), 74.22 (C-22), 54.37 (C-5), 49.57 (C-17), 46.54 (C-9), 44.95 (C-19), 40.89 (C-14), 38.25 (C-8), 37.37 (C-18), 37.17 (C-4), 36.93 (C-1), 36.66 (C-21), 35.96 (C-10), 32.72 (C-29), 31.56 (C-7), 29.04 (C-20), 27.17 (C-15), 26.56 (C-23), 26.42 (C-35), 25.27 (C-27), 25.11 (C-30), 24.85 (C-16), 23.17 (C-11), 23.11 (C-2), 19.20 (C-6), 17.13 (C-34), 15.98 (C-26), 15.94 (C-24), 14.49 (C-25). ESI-MS (negative-ion mode, *m/z*): 691.60 (M^-).

3.2.11.7. 3*β*-Cinnamoyloxy-22*β*-angeloyloxy-olean-12-en-28-oic acid (50)

Yield: 89.50%, Mp: 174-176 °C. Anal. calcd. for $C_{44}H_{60}O_6$ (684.44): %C, 77.16; H, 8.83. Found: %C, 77.13; H, 8.85. IR (KBr, cm^{-1}): 3266 (O-H of COOH), 2950, 2877 (C-H), 1719 (C=O), 1649 (C=C). ^{1}H NMR (400 MHz, $CDCl_3$, δ ppm): 7.6478–7.6878 (1H, d, *J*= 16 Hz, C-3′-Ar-H), 7.5207–7.5446 (2H, m, C-5′ & C-9′-Ar-H), 7.3725–7.3890 (3H, m, C-6′, C-8′ & C-7′-Ar-H), 6.4243–6.4643 (1H, d, *J*= 16 Hz, C-2′-H), 5.9749–6.0328 (1H, m, C-33-H), 5.3658–5.3833 (1H, t, *J*= 7.00 Hz, C-12-H), 5.0882–5.1019 (1H, t, *J*= 5.48 Hz, C-22-H), 4.6313–4.6713 (1H, t, *J*= 16 Hz, C-3-H), 3.0294–3.0740 (1H, dd, *J*= 13.96, 3.92 Hz, C-18-H), 1.1817 (3H, s, CH_3), 1.0093 (3H, s, CH_3), 0.9796 (3H, s, CH_3), 0.9532 (3H, s, CH_3), 0.9234 (3H, s, CH_3), 0.9029 (3H, s, CH_3), 0.7933 (3H, s, CH_3). ^{13}C NMR (100 MHz, $CDCl_3$, δ ppm): 179.30 (C-28), 165.85 (C-31), 165.28 (C-1′), 143.35 (C-3′), 142.06 (C-13), 137.75 (C-33), 133.47 (C-4′), 129.15 (C-7′),

127.83 (C-6′ & C-8′), 127.02 (C-5′ & C-9′), 126.63 (C-32), 121.57 (C-12), 116.30 (C-2′), 79.89 (C-3), 74.94 (C-22), 54.27 (C-5), 49.54 (C-17), 46.53 (C-9), 44.95 (C-19), 40.80 (C-14), 38.21 (C-8), 37.20 (C-18), 37.07 (C-4), 36.92 (C-1), 36.66 (C-21), 35.95 (C-10), 32.66 (C-29), 31.51 (C-7), 29.01 (C-20), 27.08 (C-15), 26.51 (C-23), 25.11 (C-27), 24.85 (C-30), 23.19 (C-16), 22.58 (C-11), 22.41 (C-2), 19.52 (C-6), 17.09 (C-35), 16.02 (C-26), 15.84 (C-24), 14.61 (C-34), 14.47 (C-25). ESI-MS (negative-ion mode, *m/z*): 683.70 (M^-).

3.2.11.8. 3*β*-Cinnamoyloxy-22*β*-senecioyloxy-olean-12-en-28-oic acid (51)

Yield: 85.99%, Mp: 165-166 °C. Anal. calcd. for $C_{44}H_{60}O_6$ (684.44): %C, 77.16; H, 8.83. Found: %C, 77.23; H, 8.84. IR (KBr, cm^{-1}): 3240 (O-H of COOH), 2947, 2875 (C-H), 1745 (C=O ester), 1715 (C=O acid), 1635 (C=C). ^{1}H NMR (400 MHz, $CDCl_3$, δ ppm): 7.6488–7.6887 (1H, d, *J*= 15.96 Hz, C-3′-Ar-H), 7.5206–7.5445 (2H, m, C-5′ & C-9′-Ar-H), 7.3722–7.3885 (3H, m, C-6′, C-8′ & C-7′-Ar-H), 6.4254–6.4654 (1H, d, *J*= 16 Hz, C-2′-H), 5.5490–5.5552 (1H, t, *J*= 2.48 Hz, C-32-H), 5.3506–5.3683 (1H, t, *J*= 7.08 Hz, C-12-H), 5.0753–5.0874 (1H, t, *J*= 4.84 Hz, C-22-H), 4.6323–4.6722 (1H, t, *J*= 15.96 Hz, C-3-H), 3.0231–3.0646 (1H, dd, *J*= 13.92, 3.52 Hz, C-18-H), 1.1778 (3H, s, CH_3), 1.0006 (3H, s, CH_3), 0.9776 (3H, s, CH_3), 0.9539 (3H, s, CH_3), 0.9230 (3H, s, CH_3), 0.8987 (3H, s, CH_3), 0.7826 (3H, s, CH_3). ^{13}C NMR (100 MHz, $CDCl_3$, δ ppm): 180.12 (C-28), 166.83 (C-31), 166.27 (C-1′), 157.13 (C-33), 144.33 (C-3′), 143.04 (C-13), 134.45 (C-4′), 130.14 (C-7′), 128.82 (C-6′ & C-8′), 128.00 (C-5′ & C-9′), 122.57 (C-12), 118.71 (C-2′), 115.89 (C-32), 80.87 (C-3), 75.91 (C-22), 55.25 (C-5), 50.51 (C-17), 47.51 (C-9), 45.92 (C-19), 41.78 (C-14), 39.18 (C-8), 38.20 (C-18), 38.05 (C-4), 37.90 (C-1), 37.64 (C-21), 36.93 (C-10), 33.65 (C-29), 32.50 (C-7), 29.99 (C-20), 28.06 (C-15), 27.99 (C-23), 27.49 (C-35), 26.10 (C-27), 25.83 (C-30), 24.17 (C-16), 23.57 (C-11), 23.40 (C-2), 20.52 (C-6), 18.06 (C-34), 16.99 (C-26), 16.82 (C-24), 15.48 (C-25). ESI-MS (negative-ion mode, *m/z*): 683.70 (M^-).

3.2.11.9. 22*β*-Benzoyloxy-3-oxo-olean-12-en-28-oic acid (52)

Yield: 55.15%, Mp: 123-124 °C. Anal. calcd. for $C_{37}H_{50}O_5$ (574.37): %C, 77.31; H, 8.77. Found: %C, 77.25; H, 8.75. IR (KBr, cm^{-1}): 2949.41 (C-H), 1720.54 (C=O), 1603.96 (C=C). ^{1}H NMR (400 MHz, $CDCl_3$, δ ppm): 7.7746–7.7974 (2H, m, C-3′ & C-7′-Ar-H), 7.3507–7.3908 (1H, m, C-5′-Ar-H), 7.2097–7.2294 (2H, m, C-4′ & C-6′-Ar-H), 5.3667–5.3839 (1H, t, *J*= 6.88 Hz, C-12-H), 5.1223–5.1373 (1H, t, *J*= 6.00 Hz, C-22-H), 3.0982–3.1430 (1H, dd, *J*= 13.80, 4.12 Hz, C-18-H), 2.4412–2.5270 (1H, m, C-2-Ha), 2.2664–2.3317 (1H, m, C-2-Hb), 1.1857 (3H, s, CH_3), 1.1249 (3H, s, CH_3), 1.0218 (3H, s, CH_3), 0.9854 (3H, s, CH_3), 0.8841 (3H, s, CH_3), 0.8210 (3H, s, CH_3), 0.7370 (3H, s, CH_3). ^{13}C NMR (100 MHz, $CDCl_3$, δ ppm): 217.68 (C-3), 178.11 (C-28), 165.12 (C-1′), 143.09 (C-13), 132.90 (C-5′), 130.06 (C-2′), 129.47 (C-3′ & C-7′), 128.28 (C-4′ & C-6′), 122.63 (C-12), 76.82 (C-22), 55.32 (C-5), 50.69 (C-17), 47.44 (C-9), 46.87 (C-4), 45.96 (C-19), 42.09 (C-14), 39.23 (C-8), 39.11 (C-18), 38.52 (C-1), 37.60 (C-21), 36.78 (C-10), 34.12 (C-2), 33.66 (C-29), 32.19 (C-7), 29.98 (C-20), 27.61 (C-15), 26.46 (C-23), 26.26 (C-27), 25.80 (C-30), 24.01 (C-16), 23.53 (C-11), 21.49 (C-6), 19.54 (C-26), 16.81 (C-24), 15.11 (C-25). ESI-MS (negative-ion mode, *m/z*): 574.30 (M^-), 573.30 (M^-–1).

3.2.11.10. 22*β*-(2-Chlorobenzoyloxy)-3-oxo-olean-12-en-28-oic acid (53)

Yield: 49.57%, Mp: 193-195 °C. Anal. calcd. for $C_{37}H_{49}ClO_5$ (608.33): %C, 72.94; H, 8.11. Found: %C, 72.93; H, 8.13. IR (KBr, cm^{-1}): 2955.55, 2927.40, 2874.30 (C-H), 1735.52 (C=O keto), 1703.58 (C=O), 1591.67 (C=C). ^{1}H NMR (400 MHz, $CDCl_3$, δ ppm): 7.8866–7.9101 (1H, m, C-7′-Ar-H), 7.3686–7.4244 (2H, m, C-4′ & C-5′-Ar-H), 7.2473–7.2884 (1H, m, C-6′-Ar-H), 5.3250–5.3424 (1H, t, *J*= 6.96 Hz, C-12-H), 5.2060–5.2206 (1H, t, *J*= 5.84 Hz, C-22-H), 3.0374–3.0820 (1H, dd, *J*= 13.76, 4.24 Hz, C-18-H), 2.4468–2.5326 (1H, m, C-2-Ha), 2.2759–2.3412 (1H, m, C-2-Hb), 1.1811 (3H, s, CH_3), 1.1258 (3H, s, CH_3), 1.0210 (3H, s, CH_3), 0.9776 (3H, s, CH_3), 0.8789 (3H, s, CH_3), 0.8395 (3H, s, CH_3), 0.7925 (3H, s, CH_3). ^{13}C NMR (100 MHz, $CDCl_3$, δ ppm): 217.99

(C-3), 180.46 (C-28), 170.27 (C-1′), 142.91 (C-13), 133.34 (C-5′), 132.37 (C-3′), 131.41 (C-7′), 130.96 (C-4′), 129.28 (C-2′), 126.62 (C-6′), 122.61 (C-12), 77.37 (C-22), 55.22 (C-5), 50.67 (C-17), 47.41 (C-9), 46.83 (C-4), 45.80 (C-19), 41.95 (C-14), 39.21 (C-8), 39.04 (C-18), 38.27 (C-1), 37.57 (C-21), 36.73 (C-10), 34.09 (C-2), 33.62 (C-29), 32.05 (C-7), 30.02 (C-20), 27.56 (C-15), 26.41 (C-23), 26.32 (C-27), 25.81 (C-30), 24.04 (C-16), 23.48 (C-11), 21.43 (C-6), 19.47 (C-26), 16.78 (C-24), 15.06 (C-25). ESI-MS (negative-ion mode, *m/z*): 609.50 (M^-+1), 607.50 (M^-–1).

3.2.11.11. 22*β*-Cinnamoyloxy-3-oxo-olean-12-en-28-oic acid (54)

Yield: 56.59%, Mp: 281-283 °C. Anal. calcd. for $C_{39}H_{52}O_5$ (600.38): %C, 77.96; H, 8.72. Found: %C, 77.99; H, 8.73. IR (KBr, cm^{-1}): 3210 (O-H of COOH), 2950, 2872 (C-H), 1738 (C=O keto), 1699 (C=O), 1632 (C=C). ^{1}H NMR (400 MHz, $CDCl_3$, δ ppm): 7.4707–7.5108 (1H, d, *J*= 16.04 Hz, C-3′-Ar-H), 7.3828–7.4063 (2H, m, C-5′ & C-9′-Ar-H), 7.3229–7.3530 (3H, m, C-6′, C-8′ & C-7′-Ar-H), 6.1513–6.1914 (1H, d, *J*= 16.04 Hz, C-2′-Ar-H), 5.4020–5.4190 (1H, t, *J*= 6.80 Hz, C-12-H), 5.0958–5.1106 (1H, t, *J*= 5.92 Hz, C-22-H), 3.1014–3.1460 (1H, dd, *J*= 13.84, 4.20 Hz, C-18-H), 2.5140–2.5996 (1H, m, C-2-Ha), 2.3373–2.4024 (1H, m, C-2-Hb), 1.1825 (3H, s, CH_3), 1.0890 (3H, s, CH_3), 1.0422 (3H, s, CH_3), 1.0372 (3H, s, CH_3), 1.0086 (3H, s, CH_3), 0.8936 (3H, s, CH_3), 0.8448 (3H, s, CH_3). ^{13}C NMR (100 MHz, $CDCl_3$, δ ppm): 218.03 (C-3), 180.44 (C-28), 165.56 (C-1′), 144.94 (C-3′), 143.05 (C-13), 134.33 (C-4′), 130.74 (C-7′), 128.94 (C-6′ & C-8′), 128.36 (C-5′ & C-9′), 122.57 (C-12), 118.10 (C-2′), 76.52 (C-22), 55.32 (C-5), 50.82 (C-17), 47.47 (C-9), 46.90 (C-4), 45.94 (C-19), 42.08 (C-14), 39.28 (C-8), 39.16 (C-18), 38.46 (C-1), 37.73 (C-21), 36.77 (C-10), 34.16 (C-2), 33.69 (C-29), 32.18 (C-7), 30.10 (C-20), 27.64 (C-15), 26.45 (C-23), 26.34 (C-27), 25.79 (C-30), 24.01 (C-16), 23.57 (C-11), 21.10 (C-6), 19.54 (C-26), 16.69 (C-24), 15.12 (C-25). ESI-MS (negative-ion mode, *m/z*): 599.60 (M^-).

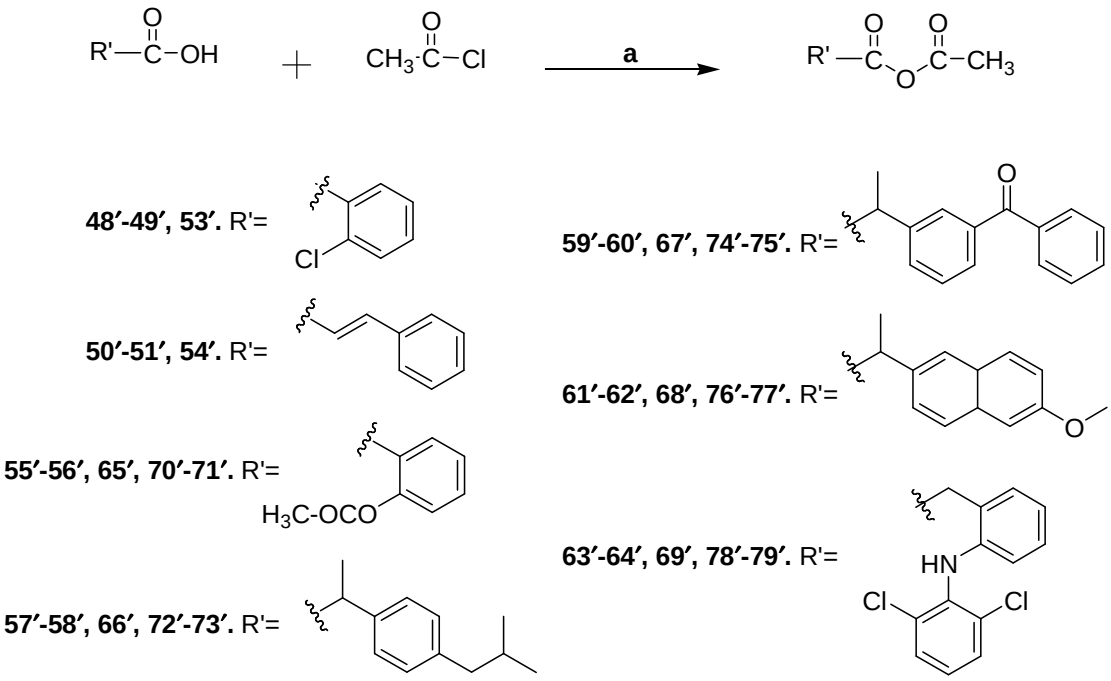

Scheme 3.2. Synthesis of anhydride derivatives of aromatic acids (**48′**–**51′** and **53′**–**54′**) and NSAIDs (**55′**–**79′**) for the esterification step. Reagents and conditions: (a) Pyridine, DCM/THF, reflux 4–5 h.

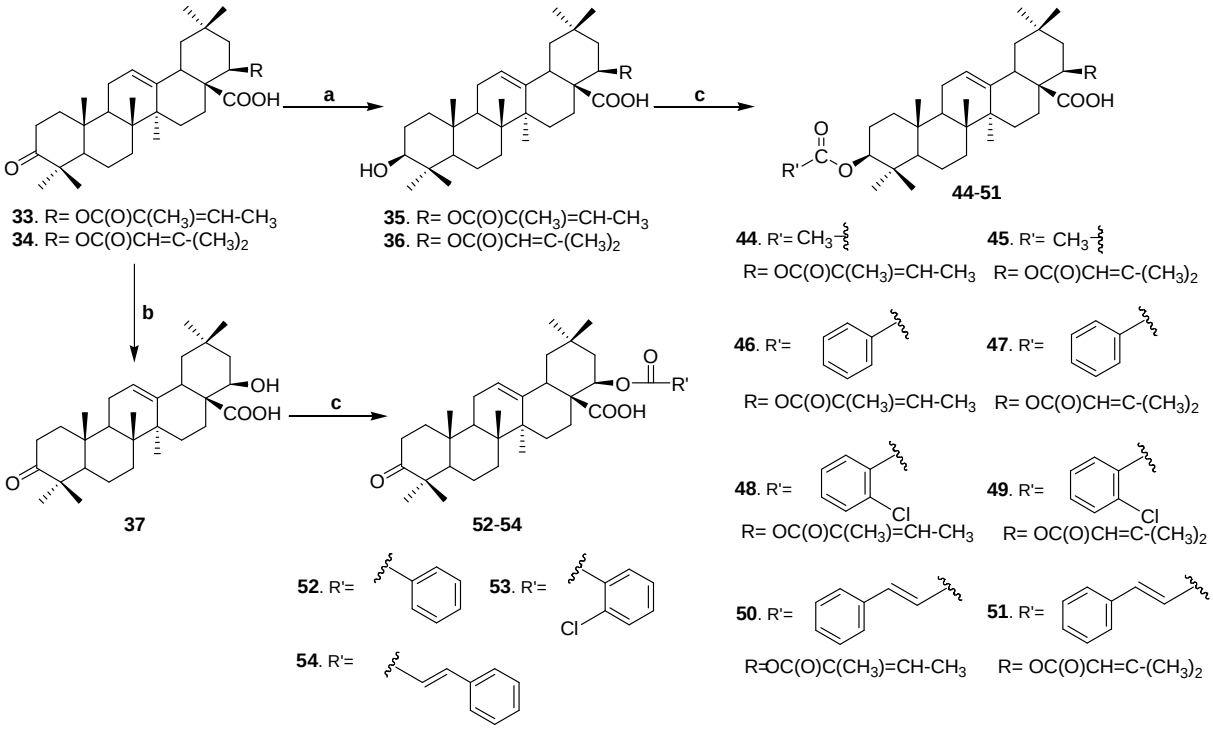

Scheme 3.3. Synthesis of lantadene esters congeners **44**–**54**. Reagents and conditions: (a) $NaBH_4$, MeOH-THF, stir 7 h; (b) 10% Ethanolic KOH, reflux 6 h; (c)) R′-CO-Cl/R′-CO-O-CO-CH_3, 4-DMAP, pyridine, reflux 92–95 °C, 10–14 h.

3.2.12. Synthesis of 3*β*-substituted and 22*β*-substituted olean-12-en-28-oic acids (55–69)

Compounds **55–69** were synthesized in two steps. In step 1, the acidic group of NSAIDs was converted into the anhydride group (**Scheme 3.2**). An equimolar quantity of NSAID and acetyl chloride in the presence of pyridine was refluxed in dichloromethane (ibuprofen, ketoprofen, and naproxen)/tetrahydrofuran (aspirin and diclofenac) for 4–5 h. The reaction mixture was concentrated and washed with chloroform (100 ml × 3) under reduced pressure at 60–65 °C to afford solid to semisolid anhydride products of the respective NSAIDs, which were used in the next step without further purification.

In step 2, an equimolar amount of compound **35**/**36**/**37** and appropriate anhydride product of NSAID was refluxed in pyridine in the presence of 4-DMAP for 10–14 h at 92–95 ºC (**Scheme 3.4**). The reaction mixture was poured into the 10% HCl solution and the precipitated product was extracted with DCM and washed for a further three times with a 10% HCl solution (100 ml × 3). The organic layer was evaporated to dryness and the reaction mixture obtained was chromatographed over silica gel (100–200 mesh) and eluted with varying ratios of hexane-ethyl acetate to give the final purified products (**55**–**69**).

3.2.12.1. (3*β*)-(2-Acetoxybenzoyloxy)-22*β*-angeloyloxy-olean-12-en-28-oic acid (55)

Yield: 24.93% (201.10 mg), Mp: 99–101 °C. Anal. calcd. for $C_{44}H_{60}O_8$ (716.43): %C, 73.71; H, 8.44. Found: %C, 73.75; H, 8.45. IR (KBr, cm^{-1}): 2951.38, 2876.85 (C–H), 1721.72 (C=O ester), 1608.06 (C=C). ^{1}H NMR (400 MHz, $CDCl_3$, δ ppm): 7.8953–7.9189 (1H, dd, *J* = 7.76, 1.76 Hz, C-7′-Ar-H), 7.5766–7.6203 (1H, dt, C-5′-Ar-H), 7.4435–7.4662 (1H, dd, *J* = 8.24, 0.8 Hz, C-4′-Ar-H), 7.3390–7.3793 (1H, dt, C-6′-Ar-H), 5.9316–5.9533 (1H, m, C-33-H), 5.3206–5.3256 (1H, t, *J* = 1.00 Hz, C-12-H), 5.0374–5.0500 (1H, t, *J* = 2.52 Hz, C-22-H), 4.4089–4.4486 (1H, t, *J* = 7.94 Hz, C-3-H), 2.9835–2.9888 (1H, t, *J* = 1.06 Hz, C-18-H), 2.2883 (3H, s, C-9′-H), 1.1845 (3H, s, CH_3), 1.1096 (3H, s,

CH_3), 0.9493 (3H, s, CH_3), 0.9092 (3H, s, CH_3), 0.8624 (3H, s, CH_3), 0.7905 (3H, s, CH_3), 0.7394 (3H, s, CH_3). ^{13}C NMR (100 MHz, $CDCl_3$, δ ppm): 180.24 (C-28), 174.57 (C-1′), 170.33 (C-8′), 168.08 (C-31), 148.56 (C-3′), 143.16 (C-13), 138.90 (C-33), 133.36 (C-5′), 131.79 (C-7′), 127.35 (C-32), 126.22 (C-6′), 123.87 (C-4′), 123.84 (C-2′), 122.54 (C-12), 80.67 (C-3), 75.49 (C-22), 55.23 (C-5), 50.59 (C-17), 47.26 (C-9), 45.32 (C-19), 41.61 (C-14), 39.30 (C-8), 38.47 (C-18), 38.26 (C-4), 38.08 (C-1), 37.10 (C-21), 36.53 (C-10), 33.00 (C-29), 32.82 (C-7), 29.76 (C-20), 27.59 (C-15), 27.04 (C-23), 26.20 (C-27), 25.65 (C-30), 25.39 (C-16), 23.48 (C-2), 23.16 (C-11), 21.64 (C-9′), 20.72 (C-6), 20.35 (C-35), 19.68 (C-26), 17.57 (C-24), 16.21 (C-34), 15.51 (C-25). ESI-MS (negative-ion mode, *m/z*): 716.40 (M^-), 715.40 (M^-–1).

3.2.12.2. (3*β*)-(2-Acetoxybenzoyloxy)-22*β*-senecioyloxy-olean-12-en-28-oic acid (56)

Yield: 22.63% (182.56 mg), Mp: 91–93 °C. Anal. calcd. for $C_{44}H_{60}O_8$ (716.43): %C, 73.71; H, 8.44. Found: %C, 73.77; H, 8.46. IR (KBr, cm^{-1}): 2950.58, 2877.29 (C–H), 1718.34 (C=O ester), 1606.84 (C=C). ^{1}H NMR (400 MHz, $CDCl_3$, δ ppm): 7.8259–7.8501 (1H, dd, *J* = 7.96, 1.72 Hz, C-7′-Ar-H), 7.5672–7.6106 (1H, dt, C-5′-Ar-H), 7.3293–7.3511 (1H, dd, *J* = 7.68, 1.04 Hz, C-4′-Ar-H), 7.2082–7.2492 (1H, dt, C-6′-Ar-H), 5.4975–5.5036 (1H, t, *J* = 1.22 Hz, C-32-H), 5.2459–5.2614 (1H, t, *J* = 3.10 Hz, C-12-H), 5.0435–5.0591 (1H, t, *J* = 3.12 Hz, C-22-H), 4.3937–4.4327 (1H, t, *J* = 7.80 Hz, C-3-H), 2.9874–3.0324 (1H, dd, *J* = 14.04, 4.60 Hz, C-18-H), 2.2827 (3H, s, C-9′-H), 1.1844 (3H, s, CH_3), 1.1139 (3H, s, CH_3), 0.9562 (3H, s, CH_3), 0.9024 (3H, s, CH_3), 0.8600 (3H, s, CH_3), 0.8425 (3H, s, CH_3), 0.7457 (3H, s, CH_3). ^{13}C NMR (100 MHz, $CDCl_3$, δ ppm): 180.29 (C-28), 174.30 (C-1′), 169.73 (C-8′), 166.46 (C-31), 162.18 (C-33), 150.76 (C-3′), 142.97 (C-13), 133.57 (C-5′), 130.89 (C-7′), 125.94 (C-6′), 123.81 (C-4′), 123.76 (C-2′), 122.74 (C-12), 117.76 (C-32), 81.60 (C-3), 76.05 (C-22), 55.42 (C-5), 50.79 (C-17), 47.60 (C-9), 45.96 (C-19), 41.92 (C-14), 39.48 (C-8), 39.31 (C-18), 38.46 (C-4), 38.18 (C-1), 38.04 (C-21), 36.98

(C-10), 33.69 (C-29), 32.61 (C-7), 30.06 (C-20), 27.65 (C-15), 27.61 (C-35), 26.30 (C-23), 26.19 (C-27), 25.82 (C-30), 24.19 (C-16), 23.53 (C-11), 23.47 (C-2), 21.31 (C-9′), 21.14 (C-6), 20.47 (C-34), 18.17 (C-26), 16.95 (C-24), 15.33 (C-25). ESI-MS (negative-ion mode, *m/z*): 716.50 (M^-), 715.50 (M^-–1), 713.50 (M^-–3).

3.2.12.3. (3*β*)-((*RS*)-2-(4-Isobutylphenyl)propanoyloxy)-22*β*-angeloyloxy-olean-12-en-28-oic acid (57)

Yield: 69.99% (523.61 mg), Mp: 132–133 °C. Anal. calcd. for $C_{48}H_{70}O_6$ (742.52): %C, 77.59; H, 9.50. Found: %C, 77.55; H, 9.48. IR (KBr, cm^{-1}): 3306.74 (O–H), 2951.65, 2874.48 (C–H), 1726.03 (C=O ester), 1650.61 (C=C). ^{1}H NMR (400 MHz, $CDCl_3$, δ ppm): 7.1887–7.2087 (2H, d, *J* = 8.00 Hz, C-5′ & C-9′-Ar-H), 7.0614–7.1026 (2H, m, C-6′ & C-8′-Ar-H), 5.9331–5.9909 (1H, m, C-33-H), 5.3251–5.3435 (1H, t, *J* = 3.68 Hz, C-12-H), 5.0603–5.0744 (1H, t, *J* = 2.82 Hz, C-22-H), 4.4066–4.4463 (1H, t, *J* = 7.94 Hz, C-3-H), 3.6538–3.7056 (1H, m, C-2′-H), 2.9992–3.0437 (1H, dd, *J* = 13.68, 4.28 Hz, C-18-H), 2.4305–2.4485 (2H, d, *J* = 7.20 Hz, C-10′-H), 1.1374 (3H, s, CH_3), 0.9896 (3H, s, CH_3), 0.9093 (3H, s, CH_3), 0.8865–0.8905 (6H, d, CH_3), 0.8772 (3H, s, CH_3), 0.7779 (3H, s, CH_3), 0.6969 (3H, s, CH_3), 0.5506 (3H, s, CH_3). ^{13}C NMR (100 MHz, $CDCl_3$, δ ppm): 179.60 (C-28), 174.36 (C-1′), 166.34 (C-31), 143.02 (C-13), 140.37 (C-7′), 138.64 (C-33), 138.17 (C-4′), 129.19 (C-5′ & C-9′), 127.72 (C-32), 127.28 (C-6′ & C-8′), 122.64 (C-12), 80.84 (C-3), 75.96 (C-22), 55.24 (C-5), 50.59 (C-17), 47.52 (C-9), 45.97 (C-19), 45.66 (C-2′), 45.01 (C-10′), 41.87 (C-14), 39.23 (C-8), 38.37 (C-18), 38.05 (C-4), 37.89 (C-1), 37.77 (C-21), 36.90 (C-10), 33.68 (C-29), 32.56 (C-7), 30.22 (C-11′), 30.03 (C-20), 27.57 (C-15), 27.43 (C-23), 26.15 (C-27), 25.83 (C-30), 24.20 (C-16), 23.51 (C-11), 23.42 (C-2), 22.88 (C-12′ & C-13′), 20.51 (C-6), 18.16 (C-3′), 17.89 (C-35), 16.92 (C-26), 16.46 (C-24), 15.61 (C-34), 15.42 (C-25). ESI-MS (negative-ion mode, *m/z*): 742.60 (M^-), 741.60 (M^-–1).

3.2.12.4. (3*β*)-((*RS*)-2-(4-Isobutylphenyl)propanoyloxy)-22*β*-senecioyloxy-olean-12-en-28-oic acid (58)

Yield: 67.10% (502.00 mg), Mp: 127–128 °C. Anal. calcd. for $C_{48}H_{70}O_6$ (742.52): %C, 77.59; H, 9.50. Found: %C, 77.67; H, 9.54. IR (KBr, cm^{-1}): 3295.21 (O–H), 2952.25, 2874.24 (C–H), 1725.87 (C=O ester), 1650.19 (C=C). ^{1}H NMR (400 MHz, $CDCl_3$, δ ppm): 7.1889–7.2090 (2H, d, *J* = 8.04 Hz, C-5′ & C-9′-Ar-H), 7.0616–7.0881 (2H, m, C-6′ & C-8′-Ar-H), 5.5370–5.5431 (1H, t, *J* = 1.22 Hz, C-32-H), 5.3244–5.3417 (1H, t, *J* = 3.46 Hz, C-12-H), 5.0602–5.0745 (1H, t, *J* = 2.86 Hz, C-22-H), 4.4072–4.4469 (1H, t, *J* = 7.94 Hz, C-3-H), 3.6540–3.7055 (1H, m, C-2′-H), 2.9984–3.0421 (1H, dd, *J* = 13.60, 3.96 Hz, C-18-H), 2.4311–2.4489 (2H, d, *J* = 7.12 Hz, C-10′-H), 1.1375 (3H, s, CH_3), 0.9898 (3H, s, CH_3), 0.9032 (3H, s, CH_3), 0.8844–0.8906 (6H, d, CH_3), 0.8769 (3H, s, CH_3), 0.7715 (3H, s, CH_3), 0.6970 (3H, s, CH_3), 0.5512 (3H, s, CH_3). ^{13}C NMR (100 MHz, $CDCl_3$, δ ppm): 179.70 (C-28), 174.36 (C-1′), 166.28 (C-31), 158.39 (C-33), 143.05 (C-13), 140.37 (C-7′), 138.17 (C-4′), 129.14 (C-5′ & C-9′), 127.21 (C-6′ & C-8′), 122.63 (C-12), 117.01 (C-32), 80.88 (C-3), 75.92 (C-22), 55.23 (C-5), 50.58 (C-17), 47.52 (C-9), 45.98 (C-19), 45.66 (C-2′), 45.03 (C-10′), 41.85 (C-14), 39.22 (C-8), 38.33 (C-18), 38.06 (C-4), 37.88 (C-1), 37.77 (C-21), 36.93 (C-10), 33.68 (C-29), 32.54 (C-7), 30.22 (C-11′), 30.02 (C-20), 27.94 (C-35), 27.57 (C-15), 27.55 (C-23), 26.16 (C-27), 25.84 (C-30), 24.22 (C-16), 23.50 (C-11), 23.43 (C-2), 22.88 (C-12′ & C-13′), 20.55 (C-6), 18.17 (C-3′), 17.89 (C-34), 16.97 (C-26), 16.45 (C-24), 15.63 (C-25). ESI-MS (negative-ion mode, *m/z*): 742.60 (M^-), 741.60 (M^-–1).

3.2.12.5. (3*β*)-((*RS*)-2-(3-Benzoylphenyl)propanoyloxy)-22*β*-angeloyloxy-olean-12-en-28-oic acid (59)

Yield: 68.05% (454.16 mg), Mp: 140–141 °C. Anal. calcd. for $C_{51}H_{66}O_7$ (790.48): %C, 77.43; H, 8.41. Found: %C, 77.49; H, 8.43. IR (KBr, cm^{-1}): 3308.75 (O–H), 2948.49, 2876.83 (C–H), 1721.54 (C=O ester), 1662.79 (C=O keto), 1598.38 (C=C). ^{1}H NMR (400 MHz, $CDCl_3$, δ ppm): 7.7531–7.8027 (3H,

m, C-12′, C-16′, & C-5′-Ar-H), 7.6574–7.6891 (1H, m, C-7′-Ar-H), 7.5435–7.6144 (2H, m, C-14′ & C-9′-Ar-H), 7.4166–7.4997 (3H, m, C-13′, C-15′, & C-8′-Ar-H), 5.9663–6.0242 (1H, m, C-33-H), 5.3389–5.3518 (1H, t, *J* = 2.58 Hz, C-12-H), 5.0720–5.0864 (1H, t, *J* = 2.88 Hz, C-22-H), 4.4618–4.5025 (1H, t, *J* = 8.14 Hz, C-3-H), 3.7744–3.8317 (1H, m, C-2′-H), 3.0043–3.0483 (1H, dd, *J* = 13.84, 4.04 Hz, C-18-H), 1.1520 (3H, s, CH_3), 0.9946 (3H, s, CH_3), 0.8976 (3H, s, CH_3), 0.8884 (3H, s, CH_3), 0.7491 (3H, s, CH_3), 0.7149 (3H, s, CH_3), 0.6187 (3H, s, CH_3). ^{13}C NMR (100 MHz, $CDCl_3$, δ ppm): 196.65 (C-10′), 179.02 (C-28), 173.82 (C-1′), 166.30 (C-31), 143.06 (C-13), 140.94 (C-6′), 139.02 (C-33), 137.79 (C-4′), 137.56 (C-11′), 132.50 (C-9′), 131.62 (C-14′), 130.07 (C-12′ & C-16′), 129.28 (C-5′), 128.91 (C-8′), 128.44 (C-7′), 128.32 (C-13′ & C-15′), 127.61 (C-32), 122.62 (C-12), 81.30 (C-3), 75.88 (C-22), 54.23 (C-5), 50.55 (C-17), 47.51 (C-9), 45.96 (C-19), 45.79 (C-2′), 41.87 (C-14), 39.20 (C-8), 38.35 (C-18), 37.97 (C-4), 37.87 (C-1), 37.76 (C-21), 36.92 (C-10), 33.71 (C-29), 32.54 (C-7), 30.04 (C-20), 27.75 (C-15), 27.53 (C-23), 26.15 (C-27), 25.85 (C-30), 24.20 (C-16), 23.46 (C-11), 23.41 (C-2), 21.61 (C-6), 20.59 (C-35), 18.32 (C-3′), 17.99 (C-26), 16.93 (C-24), 15.68 (C-25), 15.44 (C-34). ESI-MS (negative-ion mode, *m/z*): 790.40 (M^-), 789.40 (M^-–1).

3.2.12.6. (3*β*)-((*RS*)-2-(3-Benzoylphenyl)propanoyloxy)-22*β*-senecioyloxy-olean-12-en-28-oic acid (60)

Yield: 65.44% (436.79 mg), Mp: 133–134 °C. Anal. calcd. for $C_{51}H_{66}O_7$ (790.48): %C, 77.43; H, 8.41. Found: %C, 77.40; H, 8.42. IR (KBr, cm^{-1}): 3307.72 (O–H), 2947.97, 2876.73 (C–H), 1722.04 (C=O ester), 1662.40 (C=O keto), 1598.45 (C=C). ^{1}H NMR (400 MHz, $CDCl_3$, δ ppm): 7.7519–7.7965 (3H, m, C-12′, C-16′, & C-5′-Ar-H), 7.6531–7.6849 (1H, m, C-7′-Ar-H), 7.5384–7.6079 (2H, m, C-14′ & C-9′-Ar-H), 7.4108–7.4930 (3H, m, C-13′, C-15′, & C-8′-Ar-H), 5.5404–5.5465 (1H, t, *J* = 1.22 Hz, C-32-H), 5.3301–5.3439 (1H, t, *J* = 2.76 Hz, C-12-H), 5.0631–5.0777 (1H, t, *J* = 2.92 Hz, C-22-H), 4.4429–4.4825 (1H, t, *J* = 7.92 Hz, C-3-H), 3.7539–3.8109 (1H, m, C-2′-H), 3.0016–3.0448

(1H, dd, *J* = 13.40, 3.96 Hz, C-18-H), 1.1438 (3H, s, CH_3), 0.9913 (3H, s, CH_3), 0.9062 (3H, s, CH_3), 0.8867 (3H, s, CH_3), 0.7439 (3H, s, CH_3), 0.7168 (3H, s, CH_3), 0.6232 (3H, s, CH_3). ^{13}C NMR (100 MHz, $CDCl_3$, δ ppm): 196.57 (C-10′), 179.59 (C-28), 173.61 (C-1′), 166.32 (C-31), 157.09 (C-33), 143.05 (C-13), 141.22 (C-6′), 137.89 (C-4′), 137.58 (C-11′), 132.46 (C-9′), 131.59 (C-14′), 130.02 (C-12′ & C-16′), 129.26 (C-5′), 128.87 (C-8′), 128.47 (C-7′), 128.30 (C-13′ & C-15′), 122.58 (C-12), 115.97 (C-32), 81.31 (C-3), 75.93 (C-22), 55.22 (C-5), 50.57 (C-17), 47.53 (C-9), 45.98 (C-19), 45.79 (C-2′), 41.87 (C-14), 39.23 (C-8), 38.34 (C-18), 38.02 (C-4), 37.87 (C-1), 37.77 (C-21), 36.91 (C-10), 33.68 (C-29), 32.58 (C-7), 30.02 (C-20), 27.76 (C-15), 27.54 (C-23), 27.44 (C-35), 26.15 (C-27), 25.84 (C-30), 24.21 (C-16), 23.47 (C-11), 23.42(C-2), 23.22 (C-6), 20.53 (C-34), 18.28 (C-3′), 18.07 (C-26), 16.95 (C-24), 15.62 (C-25). ESI-MS (negative-ion mode, *m/z*): 789.50 (M^-–1).

3.2.12.7. (3*β*)-((+)-(*S*)-2-(6-Methoxynaphthalen-2-yl)propanoyloxy)-22*β*-angeloyloxy-olean-12-en-28-oic acid (61)

Yield: 68.56% (482.79 mg), Mp: 159–160 °C. Anal. calcd. for $C_{49}H_{66}O_7$ (766.48): %C, 76.73; H, 8.67. Found: %C, 76.80; H, 8.65. IR (KBr, cm^{-1}): 3304.63 (O–H), 2949.46, 2876.89 (C–H), 1725.59 (C=O ester), 1633.21 (C=C). ^{1}H NMR (400 MHz, $CDCl_3$, δ ppm): 7.6035–7.6285 (3H, d, *J* = 10.00, C-7′, C-12′, & C-5′-Ar-H), 7.3282–7.3536 (1H, dd, *J* = 8.44, 1.76 Hz, C-13′-Ar-H), 7.0287–7.0722 (2H, m, C-8′ & C-10′-Ar-H), 5.8689–5.9256 (1H, m, C-33-H), 5.2488–5.2629 (1H, t, *J* = 2.82 Hz, C-12-H), 4.9843–4.9975 (1H, t, *J* = 2.64 Hz, C-22-H), 4.3784–4.4183 (1H, t, *J* = 7.98 Hz, C-3-H), 3.8347 (3H, s, C-14′-H), 3.7382–3.7911 (1H, m, C-2′-H), 2.9202–2.9636 (1H, dd, *J* = 13.60, 3.88 Hz, C-18-H), 1.0583 (3H, s, CH_3), 0.9142 (3H, s, CH_3), 0.8231 (3H, s, CH_3), 0.8094 (3H, s, CH_3), 0.6533 (3H, s, CH_3), 0.6339 (3H, s, CH_3), 0.5019 (3H, s, CH_3). ^{13}C NMR (100 MHz, $CDCl_3$, δ ppm): 179.67 (C-28), 174.29 (C-1′), 166.29 (C-31), 157.55 (C-9′), 143.04 (C-13), 138.79 (C-33), 136.02 (C-4′), 133.63 (C-11′), 129.25 (C-7′), 128.93 (C-6′), 127.68 (C-32), 126.97 (C-12′), 126.40 (C-5′),

126.02 (C-13′), 122.60 (C-12), 118.87 (C-8′), 105.60 (C-10′), 81.03 (C-3), 75.92 (C-22), 55.28 (C-14′), 55.22 (C-5), 50.56 (C-17), 47.51 (C-9), 46.00 (C-19), 45.98 (C-2′), 41.85 (C-14), 39.21 (C-8), 38.34 (C-18), 38.04 (C-4), 37.87 (C-1), 37.72 (C-21), 36.90 (C-10), 33.68 (C-29), 32.54 (C-7), 30.02 (C-20), 27.71 (C-15), 27.52 (C-23), 26.15 (C-27), 25.83 (C-30), 24.22 (C-16), 23.51 (C-11), 23.42 (C-2), 20.55 (C-6), 18.19 (C-3′), 17.95 (C-35), 16.95 (C-26), 16.56 (C-24), 15.63 (C-25), 15.42 (C-34). ESI-MS (negative-ion mode, *m/z*): 766.40 (M^-), 765.40 (M^-–1).

3.2.12.8. (3*β*)-((+)-(*S*)-2-(6-Methoxynaphthalen-2-yl)propanoyloxy)-22*β*-senecioyloxy-olean-12-en-28-oic acid (62)

Yield: 68.61% (483.16 mg), Mp: 154–155 °C. Anal. calcd. for $C_{49}H_{66}O_7$ (766.48): %C, 76.73; H, 8.67. Found: %C, 76.83; H, 8.70. IR (KBr, cm^{-1}): 3306.93 (O–H), 2948.06, 2876.91 (C–H), 1725.76 (C=O ester), 1633.95 (C=C). ^{1}H NMR (400 MHz, $CDCl_3$, δ ppm): 7.6027–7.6386 (3H, m, C-7′, C-12′, & C-5′-Ar-H), 7.3332–7.3585 (1H, dd, *J* = 8.48, 1.64 Hz, C-13′-Ar-H), 7.0330–7.0782 (2H, m, C-8′ & C-10′-Ar-H), 5.4707–5.4759 (1H, t, *J* = 1.04 Hz, C-32-H), 5.2570–5.2707 (1H, t, *J* = 2.74 Hz, C-12-H), 4.9435–4.9554 (1H, t, *J* = 2.38 Hz, C-22-H), 4.3800–4.4200 (1H, t, *J* = 8.00 Hz, C-3-H), 3.8417 (3H, s, C-14′-H), 3.7416–3.7944 (1H, m, C-2′-H), 2.8995–2.9435 (1H, dd, *J* = 13.36, 4.28 Hz, C-18-H), 1.0610 (3H, s, CH_3), 0.9182 (3H, s, CH_3), 0.8242 (3H, s, CH_3), 0.8017 (3H, s, CH_3), 0.6691 (3H, s, CH_3), 0.6346 (3H, s, CH_3), 0.4967 (3H, s, CH_3). ^{13}C NMR (100 MHz, $CDCl_3$, δ ppm): 178.59 (C-28), 174.45 (C-1′), 165.31 (C-31), 157.53 (C-9′), 157.20 (C-33), 143.01 (C-13), 135.82 (C-4′), 133.61 (C-11′), 129.27 (C-7′), 128.91 (C-6′), 126.98 (C-12′), 126.41 (C-5′), 125.92 (C-13′), 122.51 (C-12), 118.89 (C-8′), 115.96 (C-32), 105.55 (C-10′), 81.05 (C-3), 75.19 (C-22), 55.30 (C-14′), 55.23 (C-5), 50.52 (C-17), 47.49 (C-9), 45.96 (C-19), 45.86 (C-2′), 41.89 (C-14), 39.20 (C-8), 38.39 (C-18), 38.01 (C-4), 37.87 (C-1), 37.76 (C-21), 36.89 (C-10), 33.69 (C-29), 32.53 (C-7), 30.03 (C-20), 27.70 (C-15), 27.54 (C-23), 27.47 (C-35), 26.29 (C-27), 25.84 (C-30), 24.12 (C-16),

23.50 (C-11), 23.43 (C-2), 20.23 (C-6), 18.43 (C-34), 18.20 (C-3′), 16.93 (C-26), 16.71 (C-24), 15.64 (C-25). ESI-MS (negative-ion mode, *m/z*): 765.50 (M^-–1).

3.2.12.9. (3*β*)-(2-(2-(2,6-Dichlorophenylamino)phenyl)acetoyloxy)-22*β*-angeloyloxy-olean-12-en-28-oic acid (63)

Yield: 20.64% (127.09 mg), Mp: 165–167 °C. Anal. calcd. for $C_{49}H_{63}Cl_2NO_6$ (831.40): %C, 70.66; H, 7.62. Found: %C, 70.62; H, 7.61. IR (KBr, cm^{-1}): 3386.89 (N–H), 3259.33 (O–H), 3078.83, 2951.21, 2877.39 (C–H), 1721.17 (C=O ester). ^{1}H NMR (400 MHz, $CDCl_3$+DMSO-d_6 mixture, δ ppm): 9.4642 (1H, s, N-9′-H), 7.3048–7.3249 (2H, d, *J* = 8.04 Hz, C-12′ & C-14′-Ar-H), 7.1383–7.1564 (1H, d, *J* = 7.24 Hz, C-8′-Ar-H), 6.9102–6.9751 (2H, m, C-13′ & C-6′-Ar-H), 6.7328–6.7693 (1H, t, *J* = 7.30 Hz, C-7′-Ar-H), 6.3527–6.3724 (1H, d, *J* = 7.88 Hz, C-5′-Ar-H), 5.9558–6.0067 (1H, m, C-33-H), 5.3090–5.3265 (1H, t, *J* = 3.50 Hz, C-12-H), 5.0084–5.0221 (1H, t, *J* = 2.74 Hz, C-22-H), 4.4191–4.4579 (1H, t, *J* = 7.76 Hz, C-3-H), 3.5934 (2H, s, C-2′-H), 3.0285–3.0658 (1H, dd, *J* = 12.92, 2.52 Hz, C-18-H), 1.1653 (3H, s, CH_3), 1.0040 (3H, s, CH_3), 0.9336 (3H, s, CH_3), 0.8922 (3H, s, CH_3), 0.8559 (3H, s, CH_3), 0.8481 (3H, s, CH_3), 0.8239 (3H, s, CH_3). ^{13}C NMR (100 MHz, $CDCl_3$+DMSO-d_6 mixture, δ ppm): 177.12 (C-28), 175.71 (C-1′), 165.80 (C-31), 143.46 (C-13), 143.04 (C-4′), 138.09 (C-10′), 137.23 (C-33), 129.23 (C-8′), 129.06 (C-11′ & C-15′), 128.37 (C-12′ & C-14′), 127.78 (C-6′), 127.67 (C-32), 125.52 (C-3′), 122.88 (C13′), 121.20 (C-5′), 121.11 (C-12), 119.74 (C-7′), 80.17 (C-3), 75.75 (C-22), 54.79 (C-5), 49.66 (C-17), 47.05 (C-9), 45.70 (C-19), 43.51 (C-2′), 41.47 (C-14), 38.77 (C-8), 38.20 (C-18), 37.61 (C-4), 37.47 (C-1), 37.14 (C-21), 36.43 (C-10), 33.40 (C-29), 32.20 (C-7), 29.60 (C-20), 27.62 (C-15), 27.12 (C-23), 26.71 (C-27), 25.87 (C-30), 25.39 (C-16), 23.74 (C-11), 23.67 (C-2), 20.82 (C-6), 20.15 (C-35), 18.88 (C-26), 17.69 (C-24), 16.27 (C-25), 15.18 (C-34). ESI-MS (negative-ion mode, *m/z*): 833.30 (M^-+2).

3.2.12.10. (3*β*)-(2-(2-(2,6-Dichlorophenylamino)phenyl)acetoyloxy)-22*β*-senecioyloyloxy-olean-12-en-28-oic acid (64)

Yield: 16.36% (100.76 mg), Mp: 162–163 °C. Anal. calcd. for $C_{49}H_{63}Cl_2NO_6$ (831.40): %C, 70.66; H, 7.62. Found: %C, 70.73; H, 7.66. IR (KBr, cm^{-1}): 3384.71 (N–H), 3260.51 (O–H), 2950.89, 2877.41 (C–H), 1724.02 (C=O ester), 1648.65 (C=C). ^{1}H NMR (400 MHz, $CDCl_3$+DMSO-d_6 mixture, δ ppm): 9.6548 (1H, s, N-9′-H), 7.3255–7.3455 (2H, d, *J* = 8.00 Hz, C-12′ & C-14′-Ar-H), 7.1101–7.1282 (1H, d, *J* = 7.24 Hz, C-8′-Ar-H), 6.9574–6.9974 (1H, t, *J* = 8.00 Hz, C-13′-Ar-H), 6.9011–6.9388 (1H, t, *J* = 7.54 Hz, C-6′-Ar-H), 6.7224–6.7589 (1H, t, *J* = 7.30 Hz, C-7′-Ar-H), 6.3222–6.3420 (1H, d, *J* = 7.92 Hz, C-5′-Ar-H), 5.5490 (1H, s, C-32-H), 5.2727–5.2932 (1H, t, *J* = 4.10 Hz, C-12-H), 4.9772–4.9935 (1H, t, *J* = 3.26 Hz, C-22-H), 4.3989–4.4388 (1H, t, *J* = 7.98 Hz, C-3-H), 3.5479 (2H, s, C-2′-H), 3.0039–3.0501 (1H, dd, *J* = 14.20, 4.48 Hz, C-18-H), 1.1609 (3H, s, CH_3), 0.9923 (3H, s, CH_3), 0.9278 (3H, s, CH_3), 0.8857 (3H, s, CH_3), 0.8465 (3H, s, CH_3), 0.8390 (3H, s, CH_3), 0.8144 (3H, s, CH_3). ^{13}C NMR (100 MHz, $CDCl_3$+DMSO-d_6 mixture, δ ppm): 176.62 (C-28), 175.56 (C-1′), 165.69 (C-31), 155.75 (C-33), 143.58 (C-13), 143.13 (C-4′), 138.13 (C-10′), 129.93 (C-8′), 129.02 (C-11′ & C-15′), 128.51 (C-12′ & C-14′), 127.98 (C-6′), 125.24 (C-3′), 123.08 (C13′), 121.08 (C-5′), 121.05 (C-12), 119.73 (C-7′), 115.81 (C-32), 80.05 (C-3), 75.81 (C-22), 54.78 (C-5), 49.63 (C-17), 47.04 (C-9), 45.78 (C-19), 43.75 (C-2′), 41.52 (C-14), 38.80 (C-8), 38.30 (C-18), 37.65 (C-4), 37.48 (C-1), 37.16 (C-21), 36.46 (C-10), 33.47 (C-29), 32.26 (C-7), 29.65 (C-20), 27.68 (C-15), 27.15 (C-23), 26.88 (C-35), 26.16 (C-27), 25.98 (C-30), 25.44 (C-16), 23.78 (C-11), 23.72 (C-2), 20.85 (C-6), 20.20 (C-34), 17.74 (C-26), 16.38 (C-24), 15.24 (C-25). ESI-MS (negative-ion mode, *m/z*): 833.20 (M^-+2).

3.2.12.11. 22*β*-(2-Acetoxybenzoyloxy)-3-oxo-olean-12-en-28-oic acid (65)

Yield: 21.19% (150.89 mg), Mp: 128–130 °C. Anal. calcd. for $C_{39}H_{52}O_7$ (632.37): %C, 74.02; H, 8.28. Found: %C, 73.94; H, 8.27. IR (KBr, cm^{-1}):

2953.35, 2928.89, 2874.09 (C–H), 1745.18 (C=O keto), 1709.00 (C=O ester), 1612.10 (C=C). ^{1}H NMR (400 MHz, $CDCl_3$, δ ppm): 7.7487–7.7729 (1H, dd, *J* = 8.00, 1.68 Hz, C-7′-Ar-H), 7.3583–7.4016 (1H, dt, C-5′-Ar-H), 6.8983–6.9214 (1H, dd, *J* = 8.44, 0.88 Hz, C-4′-Ar-H), 6.7885–6.8289 (1H, dt, C-6′-Ar-H), 5.3117–5.3287 (1H, t, *J* = 3.40 Hz, C-12-H), 4.9546–4.9691 (1H, t, *J* = 2.90 Hz, C-22-H), 2.9400–2.9906 (1H, dd, *J* = 15.00, 6.44 Hz, C-18-H), 2.4459–2.5220 (1H, m, C-2-Ha), 2.2573–2.3355 (1H, m, C-2-Hb), 2.2894 (3H, s, C-9′-H), 1.1862 (3H, s, CH_3), 1.0242 (3H, s, CH_3), 0.9561 (3H, s, CH_3), 0.8818 (3H, s, CH_3), 0.8365 (3H, s, CH_3), 0.8278 (3H, s, CH_3), 0.7465 (3H, s, CH_3). ^{13}C NMR (100 MHz, $CDCl_3$, δ ppm): 217.78 (C-3), 176.42 (C-28), 173.15 (C-1′), 170.13 (C-8′), 149.20 (C-3′), 144.66 (C-13), 134.76 (C-5′), 132.05 (C-7′), 126.71 (C-6′), 123.75 (C-4′), 123.09 (C-2′), 122.64 (C-12), 77.47 (C-22), 55.30 (C-5), 50.04 (C-17), 47.60 (C-9), 46.09 (C-4), 45.18 (C-19), 42.09 (C-14), 39.28 (C-8), 39.04 (C-18), 38.34 (C-1), 37.96 (C-21), 36.52 (C-10), 34.16 (C-2), 33.70 (C-29), 32.45 (C-7), 30.76 (C-20), 27.78 (C-15), 26.53 (C-23), 26.29 (C-27), 25.36 (C-30), 24.37 (C-16), 23.61 (C-11), 21.48 (C-6), 21.15 (C-9′), 18.79 (C-26), 16.09 (C-24), 15.45 (C-25). ESI-MS (negative-ion mode, *m/z*): 633.40 (M^-+1), 631.40 (M^-–1).

3.2.12.12. 22*β*-((*RS*)-2-(4-Isobutylphenyl)-propanoyloxy)-3-oxo-olean-12-en-28-oic acid (66)

Yield: 54.31% (360.29 mg), Mp: 144–146 °C. Anal. calcd. for $C_{43}H_{62}O_5$ (658.46): %C, 78.38; H, 9.48. Found: %C, 78.46; H, 9.51. IR (KBr, cm^{-1}): 2953.19, 2926.65, 2868.87 (C–H), 1736.37 (C=O keto), 1707.25 (C=O ester), 1614.97 (C=C). ^{1}H NMR (400 MHz, $CDCl_3$, δ ppm): 7.1395–7.1590 (2H, d, *J* = 7.80 Hz, C-5′ & C-9′-Ar-H), 6.9667–7.0317 (2H, m, C-6′ & C-8′-Ar-H), 5.2692–5.2848 (1H, t, *J* = 3.12 Hz, C-12-H), 4.9407–4.9554 (1H, t, *J* = 2.94 Hz, C-22-H), 3.6164–3.6701 (1H, m, C-2′-H), 2.8530–2.8942 (1H, dd, *J* = 16.20, 2.28 Hz, C-18-H), 2.4403–2.5076 (1H, m, C-2-Ha), 2.3415–2.3582 (2H, d, *J* = 6.68 Hz, C-10′-H), 2.2627–2.3283 (1H, m, C-2-Hb), 1.1846 (3H, s, CH_3), 1.0721 (3H, s,

CH_3), 1.0121 (3H, s, CH_3), 0.9737 (3H, s, CH_3), 0.8130–0.8188 (6H, d, C-12′ & C-13′-CH_3),-H), 0.7965 (3H, s, CH_3), 0.7313 (3H, s, CH_3), 0.6937 (3H, s, CH_3). ^{13}C NMR (100 MHz, $CDCl_3$, δ ppm): 217.15 (C-3), 180.24 (C-28), 173.33 (C-1′), 143.03 (C-13), 140.83 (C-7′), 137.07 (C-4′), 129.39 (C-5′ & C-9′), 127.25 (C-6′ & C-8′), 122.44 (C-12), 77.22 (C-22), 55.34 (C-5), 50.38 (C-17), 47.45 (C-9), 46.88 (C-4), 45.91 (C-19), 45.25 (C-2′), 45.05 (C-10′), 42.01 (C-14), 39.23 (C-8), 39.18 (C-18), 38.45 (C-1), 37.73 (C-21), 36.77 (C-10), 34.14 (C-2), 33.52 (C-29), 32.22 (C-7), 30.20 (C-11′), 30.16 (C-20), 27.60 (C-15), 26.45 (C-23), 25.94 (C-27), 25.71 (C-30), 24.11 (C-16), 23.53 (C-11), 22.38 (C-12′ & C-13′), 21.48 (C-6), 19.55 (C-26), 18.18 (C-3′), 16.68 (C-24), 15.11 (C-25). ESI-MS (negative-ion mode, *m/z*): 658.40 (M^-), 657.50 (M^-–1).

3.2.12.13. 22*β*-((*RS*)-2-(3-Benzoylphenyl)-propanoyloxy)-3-oxo-olean-12-en-28-oic acid (67)

Yield: 48.06% (286.67 mg), Mp: 155–157 °C. Anal. calcd. for $C_{46}H_{58}O_6$ (706.42): %C, 78.15; H, 8.27. Found: %C, 78.22; H, 8.25. IR (KBr, cm^{-1}): 3292.69 (O–H), 2949.09, 2873.05 (C–H), 1735.38 (C=O 3-keto), 1704.95 (C=O ester), 1661.01 (C=O 10′-keto), 1598.96 (C=C). ^{1}H NMR (400 MHz, $CDCl_3$, δ ppm): 7.8205–7.9107 (3H, m, C-12′, C-16′, & C-5′-Ar-H), 7.6025–7.6271 (1H, m, C-7′-Ar-H), 7.4482–7.5089 (2H, m, C-14′ & C-9′-Ar-H), 7.3575–7.4171 (3H, m, C-13′, C-15′, & C-8′-Ar-H), 5.3372–5.3547 (1H, t, *J* = 3.50 Hz, C-12-H), 5.0242–5.0388 (1H, t, *J* = 2.92 Hz, C-22-H), 3.7479–3.8009 (1H, m, C-2′-H), 2.9975–3.0430 (1H, dd, *J* = 13.92, 4.40 Hz, C-18-H), 2.4986–2.5836 (1H, m, C-2-Ha), 2.3204–2.3860 (1H, m, C-2-Hb), 1.1645 (3H, s, CH_3), 1.0867 (3H, s, CH_3), 1.0448 (3H, s, CH_3), 1.0378 (3H, s, CH_3), 1.0007 (3H, s, CH_3), 0.8987 (3H, s, CH_3), 0.8847 (3H, s, CH_3). ^{13}C NMR (100 MHz, $CDCl_3$, δ ppm): 217.80 (C-3), 199.09 (C-10′), 174.65 (C-28), 172.86 (C-1′), 143.18 (C-13), 141.45 (C-6′), 137.61 (C-4′), 136.66 (C-11′), 133.36 (C-9′), 131.43 (C-14′), 130.84 (C-12′ & C-16′), 130.64 (C-5′), 129.19 (C-8′), 128.38 (C-13′ & C-15′), 128.26 (C-7′), 122.30 (C-12), 77.71 (C-22), 55.42 (C-5), 49.99 (C-17), 47.48 (C-9), 46.94 (C-

4), 46.02 (C-19), 45.32 (C-2′), 42.13 (C-14), 39.26 (C-8), 39.22 (C-18), 38.48 (C-1), 37.84 (C-21), 36.79 (C-10), 34.18 (C-2), 33.71 (C-29), 32.25 (C-7), 30.11 (C-20), 27.60 (C-15), 26.44 (C-23), 26.12 (C-27), 25.66 (C-30), 24.05 (C-16), 23.54 (C-11), 21.50 (C-6), 19.62 (C-26), 17.55 (C-3′), 17.00 (C-24), 15.07 (C-25). ESI-MS (negative-ion mode, *m/z*): 706.40 (M^-), 705.40 (M^-–1).

3.2.12.14. 22*β*-((+)-(*S*)-2-(6-Methoxynaphthalen-2-yl)-propanoyloxy)-3-oxo-olean-12-en-28-oic acid (68)

Yield: 51.05% (320.11 mg), Mp: 170–171 °C. Anal. calcd. for $C_{44}H_{58}O_6$ (682.42): %C, 77.38; H, 8.56. Found: %C, 77.31; H, 8.58. IR (KBr, cm^{-1}): 3305.93 (O–H), 2957.61, 2926.69, 2855.52 (C–H), 1734.14 (C=O 3-keto), 1706.10 (C=O ester), 1633.58, 1606.82 (C=C). ^{1}H NMR (400 MHz, $CDCl_3$, δ ppm): 7.5994–7.6327 (3H, m, C-7′, C-12′, & C-5′-Ar-H), 7.2663–7.2919 (1H, dd, *J* = 8.44, 1.76 Hz, C-13′-Ar-H), 7.0027–7.0627 (2H, m, C-8′ & C-10′-Ar-H), 5.2959–5.3128 (1H, t, *J* = 3.38, C-12-H), 4.9015–4.9171 (1H, t, *J* = 3.12 Hz, C-22-H), 3.8295 (3H, s, C-14′-H), 3.7094–3.7648 (1H, m, C-2′-H), 2.9137–2.9578 (1H, dd, *J* = 13.76, 4.16 Hz, C-18-H), 2.4318–2.5170 (1H, m, C-2-Ha), 2.2534–2.3187 (1H, m, C-2-Hb), 1.1856 (3H, s, CH_3), 1.0643 (3H, s, CH_3), 1.0028 (3H, s, CH_3), 0.9601 (3H, s, CH_3), 0.7617 (3H, s, CH_3), 0.7318 (3H, s, CH_3), 0.7066 (3H, s, CH_3). ^{13}C NMR (100 MHz, $CDCl_3$, δ ppm): 216.64 (C-3), 176.05 (C-28), 172.33 (C-1′), 156.54 (C-9′) 141.93 (C-13), 133.88 (C-4′), 132.62 (C-11′), 128.35 (C-7′), 127.78 (C-6′), 125.86 (C-12′), 125.54 (C-5′), 124.94 (C-13′), 121.48 (C-12), 117.85 (C-8′), 104.53 (C-10′), 76.75 (C-22), 54.31 (C-5), 54.24 (C-14′), 49.31 (C-17), 46.41 (C-9), 45.83 (C-4), 44.90 (C-19), 44.68 (C-2′), 41.00 (C-14), 38.17 (C-8), 38.14 (C-18), 37.49 (C-1), 36.76 (C-21), 35.73 (C-10), 33.11 (C-2), 32.51 (C-29), 31.20 (C-7), 29.89 (C-20), 26.46 (C-15), 25.39 (C-23), 24.94 (C-27), 24.61 (C-30), 23.10 (C-16), 22.48 (C-11), 21.66 (C-6), 20.45 (C-26), 18.49 (C-3′), 16.64 (C-24), 15.67 (C-25). ESI-MS (negative-ion mode, *m/z*): 682.40 (M^-), 681.40 (M^-–1).

3.2.12.15. 22*β*-(2-(2-(2,6-dichlorophenylamino)phenyl)acetoyloxy)-3-oxo-olean-12-en-28-oic acid (69)

Yield: 14.58% (80.74 mg), Mp: 178–179 °C. Anal. calcd. for $C_{44}H_{55}Cl_2NO_5$ (747.35): %C, 70.57; H, 7.40. Found: %C, 70.65; H, 7.41. IR (KBr, cm^{-1}): 3387.05 (N–H), 3258.29 (O–H), 3078.97, 3035.75, 2952.71 (C–H), 1721.13 (C=O keto), 1706.35 (C=O ester). ^{1}H NMR (400 MHz, DMSO-d_6, δ ppm): 10.0846 (1H, s, N-9′-H), 7.4399–7.4599 (2H, d, *J* = 8.00 Hz, C-12′ & C-14′-Ar-H), 7.0473–7.0865 (2H, m, C-8′ & C-13′-Ar-H), 6.9097–6.9475 (1H, t, *J* = 7.56 Hz, C-6′-Ar-H), 6.7213–6.7578 (1H, t, *J* = 7.30 Hz, C-7′-Ar-H), 6.2324–6.2521 (1H, d, *J* = 7.88 Hz, C-5′-Ar-H), 5.2404–5.2550 (1H, t, *J* = 2.92, C-12-H), 4.9104–4.9232 (1H, t, *J* = 2.56 Hz, C-22-H), 3.4080 (2H, s, C-2′-H), 2.9498–2.9917 (1H, dd, *J* = 13.72, 3.36 Hz, C-18-H), 2.4737–2.5577 (1H, m, C-2-Ha), 2.2731–2.3363 (1H, m, C-2-Hb), 1.1498 (3H, s, CH_3), 1.0041 (3H, s, CH_3), 0.9881 (3H, s, CH_3), 0.9605 (3H, s, CH_3), 0.9576 (3H, s, CH_3), 0.8673 (3H, s, CH_3), 0.8183 (3H, s, CH_3). ^{13}C NMR (100 MHz, DMSO-d_6, δ ppm): 216.20 (C-3), 175.06 (C-28), 173.77 (C-1′), 143.62 (C-13), 143.28 (C-4′), 138.11 (C-10′), 130.04 (C-8′), 129.01 (C-11′ & C-15′), 128.89 (C-12′ & C-14′), 128.24 (C-6′), 125.66 (C-3′), 123.80 (C13′), 121.15 (C-5′), 121.12 (C-12), 119.76 (C-7′), 77.39 (C-22), 54.27 (C-5), 49.63 (C-17), 46.61 (C-9), 46.15 (C-4), 45.66 (C-19), 44.15 (C-2′), 41.72 (C-14), 38.76 (C-8), 38.49 (C-18), 38.44 (C-1), 37.27 (C-21), 36.24 (C-10), 33.63 (C-2), 33.35 (C-29), 31.87 (C-7), 29.74 (C-20), 27.17 (C-15), 26.24 (C-23), 26.08 (C-27), 25.27 (C-30), 23.68 (C-16), 22.99 (C-11), 21.07 (C-6), 19.11 (C-26), 16.53 (C-24), 14.74 (C-25). ESI-MS (negative-ion mode, *m/z*): 749.26 (M^-+2), 748.21 (M^-+1).

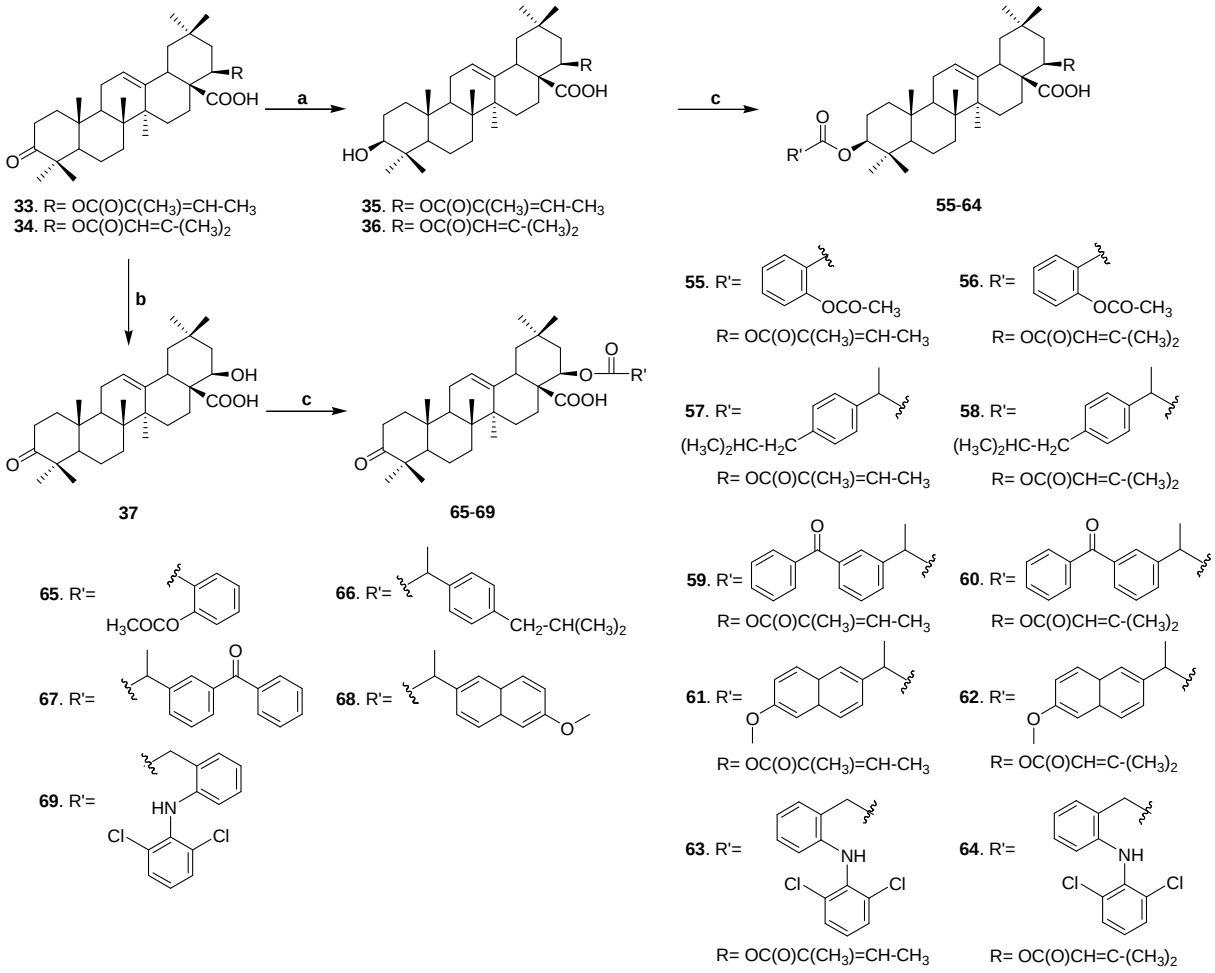

Scheme 3.4. Synthesis of lantadene–NSAID ester conjugates **55**–**69**. Reagents and conditions: (a) $NaBH_4$, MeOH-THF, stir 7 h; (b) 10% Ethanolic KOH, reflux 6 h; (c) R′-CO-O-CO-CH_3, 4-DMAP, pyridine, reflux 92–95 °C, 10–14 h.

3.2.13. Synthesis of 3*β*-substituted and 3*β*,22*β*-disubstituted olean-12-en-28-oic acids (70–79)

The synthesis of 3*β*-substituted (**70**, **72**, **74**, **76**, and **78**) and 3*β*,22*β*-disubstituted (**71**, **73**, **75**, **77**, and **79**) olean-12-en-28-oic acid prodrugs was carried out in two steps. In step 1, the carboxylic function of NSAIDs was converted into the anhydride function by the base catalyzed reaction of acid and acyl halide (**Scheme 3.2**). NSAIDs with an equimolar amount of acetyl chloride, in the presence of pyridine, were refluxed in dichloromethane (ibuprofen, ketoprofen, and naproxen)/tetrahydrofuran (aspirin and diclofenac) for 4–5 h. The organic solvent was removed in a rotary evaporator and the reaction mixture was washed with chloroform (100 ml × 3) under reduced pressure at 60–65 °C to yield solid to semisolid anhydride products of the respective NSAIDs, which were used in the subsequent step without additional purification.

In step 2, 3*β*,22*β*-dihydroxy substituted compound **38** and the anhydride derivatives of the respective NSAIDs, in the presence of 4-DMAP, were refluxed in pyridine for 10–14 h (**Scheme 3.5**). At the end of the reaction, the reaction mixture was transferred to the 10% HCl solution and precipitated product was extracted with dichloromethane and washed for a further three times with a 10% HCl solution (100 ml × 3). The organic layer was removed under reduced pressure and the crude product obtained was chromatographed over silica gel (100–200 mesh) and eluted with varying ratios of hexane-ethyl acetate to yield the final purified products (**70**–**79**).

3.2.13.1. 3*β*-(2-Acetoxybenzoyloxy)-22*β*-hydroxy-olean-12-en-28-oic acid (70)

Yield: 23.47%, Mp: 181–182 °C. Anal. calcd. for $C_{39}H_{54}O_7$ (634.39): %C, 73.78; H, 8.57. Found: %C, 73.82; H, 8.56. IR (KBr, cm^{-1}): 3429, 3355 (O–H), 2990, 2950, 2924, 2876, 2847 (C–H), 1731 (C=O), 1614, 1584 (C=C). ^{1}H NMR (400 MHz, $CDCl_3$, δ ppm): 7.8194–7.8435 (1H, dd, *J*= 8.00, 1.68 Hz, C-7′-Ar-H), 7.4308–7.4740 (1H, dt, C-5′-Ar-H), 6.9693–6.9923 (1H, dd, *J*= 8.40, 0.8 Hz, C-4′-Ar-H), 6.8604–6.9007 (1H, dt, C-6′-Ar-H), 5.3443–5.3612 (1H, t, *J*= 3.38 Hz,

C-12-H), 4.4800–4.5196 (1H, t, *J*= 7.92 Hz, C-3-H), 3.9033–3.9180 (1H, t, *J*= 2.94 Hz, C-22-H), 2.9863–3.0309 (1H, dd, *J*= 13.76, 4.12 Hz, C-18-H), 2.3532 (3H, s, C-9′-H), 1.1535 (3H, s, CH_3), 1.0226 (3H, s, CH_3), 0.9473 (3H, s, CH_3), 0.8944 (3H, s, CH_3), 0.8696 (3H, s, CH_3), 0.8609 (3H, s, CH_3), 0.7678 (3H, s, CH_3). ^{13}C NMR (100 MHz, $CDCl_3$, δ ppm): 180.05 (C-28), 171.09 (C-1′), 169.72 (C-8′), 149.63 (C-3′), 142.88 (C-13), 135.51 (C-5′), 129.74 (C-7′), 125.61 (C-6′), 123.92 (C-4′), 123.85 (C-2′), 122.67 (C-12), 80.86 (C-3), 76.15 (C-22), 55.25 (C-5), 50.54 (C-17), 47.52 (C-9), 45.77 (C-19), 41.81 (C-14), 39.24 (C-8), 38.15 (C-18), 38.09 (C-1), 37.68 (C-4), 37.68 (C-21), 36.93 (C-10), 33.69 (C-29), 32.56 (C-7), 30.01 (C-20), 28.02 (C-15), 27.56 (C-23), 26.29 (C-27), 25.86 (C-30), 23.91 (C-16), 23.50 (C-2), 23.44 (C-11), 21.11 (C-9′), 18.10 (C-6), 17.04 (C-26), 16.67 (C-24), 15.49 (C-25). ESI-MS (negative-ion mode, *m/z*): 634.50 (M^-), 633.50 (M^-–1).

3.2.13.2. 3*β*,22*β*-Di(2-acetoxybenzoyloxy)-olean-12-en-28-oic acid (71)

Yield: 17.19%, Mp: 172–173 °C. Anal. calcd. for $C_{48}H_{60}O_{10}$ (796.42): %C, 72.34; H, 7.59. Found: %C, 72.31; H, 7.57. IR (KBr, cm^{-1}): 3358.44 (O–H), 2949.33, 2926.35, 2877.47 (C–H), 1730.16 (C=O), 1614.61 (C=C). ^{1}H NMR (400 MHz, $CDCl_3$, δ ppm): 7.7515–7.8444 (2H, m, C-7′ & C-7′′-Ar-H), 7.4317–7.5244 (2H, m, C-5′ & C-5′′-Ar-H), 6.8631–7.0952 (4H, m, C-4′, C-6′ & C-4′′, C-6′′-Ar-H), 5.3489–5.3655 (1H, t, *J*= 3.32 Hz, C-12-H), 5.0076–5.0219 (1H, t, *J*= 2.86 Hz, C-22-H), 4.4802–4.5198 (1H, t, *J*= 7.92 Hz, C-3-H), 2.9877–3.0321 (1H, dd, *J*= 13.76, 4.28 Hz, C-18-H), 2.3557 (3H, s, C-9′-H), 2.2111 (3H, s, C-9′′-H), 1.1553 (3H, s, CH_3), 1.0241 (3H, s, CH_3), 0.9487 (3H, s, CH_3), 0.8958 (3H, s, CH_3), 0.8702 (3H, s, CH_3), 0.8616 (3H, s, CH_3), 0.7706 (3H, s, CH_3). ESI-MS (negative-ion mode, *m/z*): 795.60 (M^-).

3.2.13.3. 3*β*-((*RS*)-2-(4-Isobutylphenyl)propanoyloxy)-22*β*-hydroxy-olean-12-en-28-oic acid (72)

Yield: 39.49%, Mp: 109–111 °C. Anal. calcd. for $C_{43}H_{64}O_5$ (660.48): %C, 78.14; H, 9.76. Found: %C, 78.18; H, 9.74. IR (KBr, cm^{-1}): 2953, 2870 (C–H), 1733,

1713 (C=O). ^{1}H NMR (400 MHz, $CDCl_3$, δ ppm): 7.0775–7.1396 (2H, m, C-5′and C-9′-Ar-H), 6.9831–7.0163 (2H, m, C-6′ and C-8′-Ar-H), 5.2531–5.2674 (1H, t, *J*= 2.86 Hz, C-12-H), 4.3275–4.3674 (1H, m, C-3-H), 3.8523–3.8652 (1H, t, *J*= 2.58 Hz, C-22-H), 3.5256–3.6157 (1H, m, C-2′-H), 2.8519–2.8953 (1H, dd, *J*= 13.64, 3.72 Hz, C-18-H), 2.3450–2.3739 (2H, m, C-10′-H), 1.1839 (3H, s, CH_3), 1.0373 (3H, s, CH_3), 0.8129 (3H, s, CH_3), 0.8029 (6H, s, 2×CH_3), 0.7870 (3H, s, CH_3), 0.6678 (3H, s, CH_3), 0.6165 (3H, s, CH_3), 0.4648 (3H, s, CH_3). ^{13}C NMR (100 MHz, $CDCl_3$, δ ppm): 176.11 (C-28), 172.35 (C-1′), 141.90 (C-13), 139.44 (C-7′), 137.11 (C-4′), 128.06 (C-5′ & C-9′), 126.43 (C-6′ & C-8′), 121.53 (C-12), 79.84 (C-3), 75.56 (C-22), 54.19 (C-5), 49.23 (C-17), 46.44 (C-9), 44.60 (C-19), 44.42 (C-2′), 43.97 (C-10′), 40.83 (C-14), 38.14 (C-8), 37.33 (C-18), 37.02 (C-4), 36.84 (C-1), 36.72 (C-21), 35.84 (C-10), 32.49 (C-29), 31.54 (C-7), 29.18 (C-11′), 28.84 (C-20), 26.51 (C-15), 26.44 (C-23), 24.95 (C-27), 24.65 (C-30), 23.09 (C-16), 22.46 (C-11), 22.37 (C-2), 21.30 (C-12′ & C-13′), 16.83 (C-6), 16.25 (C-3′), 15.81 (C-26), 15.41 (C-24), 14.37 (C-25). ESI-MS (negative-ion mode, *m/z*): 659.60 (M^-).

3.2.13.4. 3*β*,22*β*-Di((*RS*)-2-(4-isobutylphenyl)propanoyloxy)-olean-12-en-28-oic acid (73)

Yield: 30.85%, Mp: 99–100 °C. Anal. calcd. for $C_{56}H_{80}O_6$ (848.60): %C, 79.20; H, 9.50. Found: %C, 79.23; H, 9.51. IR (KBr, cm^{-1}): 2952.20, 2876.35 (C–H), 1738.17 (C=O), 1613.56, 1585.61 (C=C). ^{1}H NMR (400 MHz, $CDCl_3$, δ ppm): 7.0370–7.2092 (8H, m, C-5′, C-9′, C-6′, C-8′, & C-5′′, C-9′′, C-6′′, C-8′′-Ar-H), 5.3193–5.3351 (1H, t, *J*= 3.16 Hz, C-12-H), 5.0102–5.0228 (1H, t, *J*= 2.52 Hz, C-22-H), 4.3978–4.4376 (1H, m, C-3-H), 3.5834–3.7208 (2H, m, C-2′-H & C-2′′-H), 2.9231–2.9658 (1H, dd, *J*= 13.64, 4.12 Hz, C-18-H), 2.4094–2.4491 (4H, m, C-10′-H & C-10′′-H), 1.113 (3H, s, CH_3), 0.9105 (3H, s, CH_3), 0.8850 (3H, s, CH_3), 0.8767 (3H, s, CH_3), 0.8734 (3H, s, CH_3), 0.8688 (3H, s, CH_3), 0.8578 (3H, s, CH_3), 0.8237 (3H, s, CH_3), 0.7491 (3H, s, CH_3), 0.6838 (3H, s, CH_3),

0.5348 (3H, s, CH_3). ESI-MS (negative-ion mode, *m/z*): 848.80 (M^-), 847.70 (M^-–1).

3.2.13.5. 3*β*-((*RS*)-2-(3-Benzoylphenyl)propanoyloxy)-22*β*-hydroxy-olean-12-en-28-oic acid (74) Yield: 31.03%, Mp: 110–112 °C. Anal. calcd. for $C_{46}H_{60}O_6$ (708.44): %C, 77.93; H, 8.53. Found: %C, 77.91; H, 8.54. IR (KBr, cm^{-1}): 3479.44 (O–H), 3061.34, 2945.16, 2876.26 (C–H), 1732.10 (C=O), 1658.12 (C=O keto), 1597.28, 1580.34 (C=C). ^{1}H NMR (400 MHz, $CDCl_3$, δ ppm): 7.7831–7.8430 (3H, m, C-12′, C-16′, & C-5′-Ar-H), 7.6742–7.6924 (1H, m, C-7′-Ar-H), 7.5525–7.6148 (2H, m, C-14′ & C-9′-Ar-H), 7.4233–7.5013 (3H, m, C-13′, C-15′, & C-8′-Ar-H), 5.3003–5.3166 (1H, t, *J*= 3.26 Hz, C-12-H), 4.4546–4.4949 (1H, t, *J*= 8.06 Hz, C-3-H), 3.9593–3.9743 (1H, t, *J*= 3.00 Hz, C-22-H), 3.7924–3.8463 (1H, m, C-2′-H), 2.9541–2.9986 (1H, dd, *J*= 13.72, 4.32 Hz, C-18-H), 1.1433 (3H, s, CH_3), 0.9773 (3H, s, CH_3), 0.9403 (3H, s, CH_3), 0.8879 (3H, s, CH_3), 0.8802 (3H, s, CH_3), 0.7824 (3H, s, CH_3), 0.7707 (3H, s, CH_3). ^{13}C NMR (100 MHz, $CDCl_3$, δ ppm): 196.43 (C-10′), 179.12 (C-28), 172.81 (C-1′), 142.99 (C-13), 140.23 (C-6′), 137.91 (C-4′), 137.41 (C-11′), 132.54 (C-9′), 131.62 (C-14′), 130.09 (C-12′ & C-16′), 129.33 (C-5′), 129.24 (C-8′), 128.57 (C-7′), 128.31 (C-13′ & C-15′), 122.54 (C-12), 79.10 (C-3), 77.55 (C-22), 55.23 (C-5), 50.05 (C-17), 47.64 (C-9), 45.41 (C-19), 45.13 (C-2′), 41.94 (C-14), 39.23 (C-8), 38.73 (C-18), 38.46 (C-4), 38.32 (C-1), 37.78 (C-21), 37.02 (C-10), 33.68 (C-29), 32.74 (C-7), 30.05 (C-20), 28.07 (C-15), 27.56 (C-23), 26.12 (C-27), 25.77 (C-30), 24.06 (C-16), 23.47 (C-11), 23.42 (C-2), 18..31 (C-6), 18.17 (C-3′), 17.48 (C-26), 16.90 (C-24), 15.57 (C-25). ESI-MS (negative-ion mode, *m/z*): 708.30 (M^-), 707.30 (M^-–1).

3.2.13.6. 3*β*,22*β*-Di((*RS*)-2-(3-benzoylphenyl)propanoyloxy)-olean-12-en-28-oic acid (75)

Yield: 24.86%, Mp: 107–108 °C. Anal. calcd. for $C_{62}H_{72}O_8$ (944.52): %C, 78.78; H, 7.68. Found: %C, 78.83; H, 7.70. IR (KBr, cm^{-1}): 3445.45 (O–H), 3061.38, 2946.13, 2875.25 (C–H), 1732.70 (C=O ester), 1660.13 (C=O keto), 1597.31,

1580.37 (C=C). ^{1}H NMR (400 MHz, $CDCl_3$, δ ppm): 7.7484–7.8598 (6H, m, C-12′, C-16′, C-5′, & C-12′′, C-16′′, C-5′′-Ar-H), 7.3511–7.6882 (12H, m, C-7′, C-14′, C-9′, C-13′, C-15′, C-8′, & C-7′′, C-14′′, C-9′′, C-13′′, C-15′′, C-8′′-Ar-H), 5.3634–5.3789 (1H, t, *J*= 3.10 Hz, C-12-H), 5.0105–5.0224 (1H, t, *J*= 2.38 Hz, C-22-H), 4.4591–4.4931 (1H, t, *J*=6.80 Hz, C-3-H), 3.6814–3.8447 (2H, m, C-2′-H & C-2′′-H), 2.9635–3.0053 (1H, dd, *J*= 13.84, 3.44 Hz, C-18-H), 1.1472 (3H, s, CH_3), 0.9622 (3H, s, CH_3), 0.8864 (3H, s, CH_3), 0.8673 (3H, s, CH_3), 0.7957 (3H, s, CH_3), 0.7059 (3H, s, CH_3), 0.6153 (3H, s, CH_3). ESI-MS (negative-ion mode, *m/z*): 944.40 (M^-–1), 943.50 (M^-–2).

3.2.13.7. 3*β*-((+)-(*S*)-2-(6-Methoxynaphthalen-2-yl)propanoyloxy)-22*β*-hydroxy-olean-12-en-28-oic acid (76)

Yield: 41.61%, Mp: 169–170 °C. Anal. calcd. for $C_{44}H_{60}O_6$ (684.44): %C, 77.16; H, 8.83. Found: %C, 77.21; H, 8.84. IR (KBr, cm^{-1}): 3422 (O–H), 2947, 2874 (C–H), 1733 (C=O), 1634, 1606 (C=C). ^{1}H NMR (400 MHz, $CDCl_3$, δ ppm): 7.6512–7.7046 (3H, m, C-7′, C-12′, & C-5′-Ar-H), 7.3991–7.4244 (1H, dd, *J*= 8.52, 1.72 Hz, C-13′-Ar-H), 7.0672–7.1400 (2H, m, C-8′ & C-10′-Ar-H), 5.3086–5.3255 (1H, t, *J*= 3.38 Hz, C-12-H), 4.4377–4.4774 (1H, t, *J*= 7.94 Hz, C-3-H), 3.8963 (3H, s, C-14′-H), 3.8062–3.8817 (2H, m, C-22-H & C-2′-H), 2.9334–2.9790 (1H, dd, *J*= 13.96, 4.52 Hz, C-18-H), 1.0966 (3H, s, CH_3), 0.8880 (3H, s, CH_3), 0.8302 (3H, s, CH_3), 0.7568 (3H, s, CH_3), 0.7262 (3H, s, CH_3), 0.6955 (3H, s, CH_3), 0.5516 (3H, s, CH_3). ^{13}C NMR (100 MHz, $CDCl_3$, δ ppm): 179.94 (C-28), 174.30 (C-1′), 157.68 (C-9′), 142.91 (C-13), 136.00 (C-4′), 133.80 (C-11′), 129.28 (C-7′), 128.28 (C-6′), 127.23 (C-12′), 126.39 (C-5′), 126.11 (C-13′), 122.57 (C-12), 119.05 (C-8′), 105.55 (C-10′), 81.01 (C-3), 76.51 (C-22), 55.28 (C-14′), 55.26 (C-5), 50.60 (C-17), 47.45 (C-9), 45.56 (C-19), 45.16 (C-2′), 41.83 (C-14), 39.19 (C-8), 38.22 (C-18), 38.05 (C-4), 37.84 (C-1), 37.67 (C-21), 36.85 (C-10), 33.49 (C-29), 32.51 (C-7), 29.78 (C-20), 28.07 (C-15), 27.65 (C-23), 27.52 (C-27), 25.75 (C-30), 24.10 (C-16), 23.49 (C-2), 23.40

(C-11), 18.27 (C-6), 18.13 (C-3′), 16.71 (C-26), 16.54 (C-24), 15.40 (C-25). ESI-MS (negative-ion mode, *m/z*): 684.50 (M^-), 683.50 (M^-–1).

3.2.13.8. 3*β*,22*β*-Di((+)-(*S*)-2-(6-methoxynaphthalen-2-yl)propanoyloxy)-olean-12-en-28-oic acid (77)

Yield: 32.21%, Mp: 135–136 °C. Anal. calcd. for $C_{58}H_{72}O_8$ (896.52): %C, 77.64; H, 8.09. Found: %C, 77.58; H, 8.07. IR (KBr, cm^{-1}): 3437.54 (O–H), 3058.48, 2944.32 (C–H), 1725.29, 1709.28 (C=O), 1633.46, 1606.36 (C=C). ^{1}H NMR (400 MHz, $CDCl_3$, δ ppm): 7.5485–7.6984 (6H, m, C-7′, C-12′, C-5′, & C-7′′, C-12′′, C-5′′-Ar-H), 7.2909–7.4193 (2H, m, C-13′ & C-13′′-Ar-H), 7.0763–7.1412 (4H, m, C-8′, C-10′ & C-8′′, C-10′′-Ar-H), 5.2679–5.2839 (1H, t, *J*= 3.20 Hz, C-12-H), 4.9809–4.9928 (1H, t, *J*= 2.38, C-22-H), 4.4419–4.4817 (1H, t, *J*= 7.96 Hz, C-3-H), 3.9067 & 3.8953 (6H (3H+3H), singlet each, C-14′-H & C-14′′-H), 3.7697–3.8579 & 3.6307-3.6829 (2H (1H+1H), multiplet each, C-2′-H & C-2′′-H), 2.7949–2.8386 (1H, dd, *J*= 13.64, 4.00 Hz, C-18-H), 1.1279 (3H, s, CH_3), 0.9308 (3H, s, CH_3), 0.8027 (3H, s, CH_3), 0.7406 (3H, s, CH_3), 0.7243 (3H, s, CH_3), 0.6906 (3H, s, CH_3), 0.5512 (3H, s, CH_3). ESI-MS (negative-ion mode, *m/z*): 895.60 (M^-–1).

3.2.13.9. 3*β*-(2-(2-(2,6-Dichlorophenylamino)phenyl)acetoyloxy)-22*β*-hydroxy-olean-12-en-28-oic acid (78)

Yield: 19.58%, Mp: 153–154 °C. Anal. calcd. for $C_{44}H_{57}Cl_2NO_5$ (749.36): %C, 70.38; H, 7.65. Found: %C, 70.33; H, 7.66. IR (KBr, cm^{-1}): 3387.23, 3259.24 (N–H & O–H), 3079.34, 2949.29, 2877.39 (C–H), 1704.37 (C=O), 1574.12 (C=C). ^{1}H NMR (400 MHz, $CDCl_3$+DMSO-d_6 mixture, δ ppm): 9.7204 (1H, s, N-9′-H), 7.3506–7.3707 (2H, d, *J*= 8.04 Hz, C-12′ & C-14′-Ar-H), 7.0962–7.1179 (1H, d, *J*= 8.68 Hz, C-8′-Ar-H), 6.9822–7.0223 (1H, t, *J*= 8.02 Hz, C-13′-Ar-H), 6.9033–6.9452 (1H, t, *J*= 8.38 Hz, C-6′-Ar-H), 6.7264–6.7656 (1H, t, *J*= 7.84 Hz, C-7′-Ar-H), 6.3043–6.3257 (1H, d, *J*= 8.56 Hz, C-5′-Ar-H), 5.2517–5.2678 (1H, t, *J*= 3.22 Hz, C-12-H), 4.3893–4.4293 (1H, m, C-3-H), 3.8711–3.8849 (1H, t, *J*= 2.76 Hz, C-22-H), 3.8088 (1H, s (br), C-22-OH), 3.5164 (2H,

s, C-2′-H), 2.9384–2.9824 (1H, dd, *J*= 13.80, 3.84 Hz, C-18-H), 1.1504 (3H, s, CH_3), 0.9998 (3H, s, CH_3), 0.9317 (3H, s, CH_3), 0.8768 (3H, s, CH_3), 0.8414 (3H, s, CH_3), 0.8369 (3H, s, CH_3), 0.7983 (3H, s, CH_3). ^{13}C NMR (100 MHz, $CDCl_3$+DMSO-d_6 mixture, δ ppm): 175.97 (C-28), 169.81 (C-1′), 143.39 (C-13), 143.14 (C-4′), 138.11 (C-10′), 129.23 (C-8′), 128.98 (C-11′ & C-15′), 128.60 (C-12′ & C-14′), 127.97 (C-6′), 125.57 (C-3′), 123.23 (C13′), 121.12 (C-12), 119.75 (C-5′), 115.75 (C-7′), 79.97 (C-3), 75.87 (C-22), 54.72 (C-5), 49.51 (C-17), 46.98 (C-9), 45.63 (C-19), 43.71 (C-2′), 41.52 (C-14), 38.79 (C-8), 38.11 (C-18), 37.64 (C-4), 37.39 (C-1), 37.16 (C-21), 36.45 (C-10), 33.42 (C-29), 32.26 (C-7), 29.63 (C-20), 27.69 (C-15), 27.11 (C-23), 26.09 (C-27), 25.41 (C-30), 23.55 (C-16), 23.09 (C-11), 22.92 (C-2), 17.73 (C-6), 16.60 (C-26), 16.42 (C-24), 15.06 (C-25). ESI-MS (negative-ion mode, *m/z*): 749.20 (M^-).

3.2.13.10. 3*β*,22*β*-Di(2-(2-(2,6-dichlorophenylamino)phenyl)acetoyloxy)-olean-12-en-28-oic acid (79)

Yield: 13.60%, Mp: 143–144 °C. Anal. calcd. for $C_{58}H_{66}Cl_4N_2O_6$ (1026.37): %C, 67.70; H, 6.47. Found: %C, 67.64; H, 6.49. IR (KBr, cm^{-1}): 3355.18 (N–H/O–H), 2990.30, 2950.24, 2925.26, 2877.35 (C–H), 1729.11 (C=O), 1604.43 (C=C). ^{1}H NMR (400 MHz, $CDCl_3$+DMSO-d_6 mixture, δ ppm): 7.3071–7.3502 (4H, m, C-12′, C-14′ & C-12′′, C-14′′-Ar-H), 7.1127–7.1714 (2H, m, C-8′ & C-8′′-Ar-H), 6.8799–7.0435 (4H, m, C-13′, C-6′ & C-13′′, C-6′′-Ar-H), 6.7122–6.7910 (2H, m, C-7′ & C-7′′-Ar-H), 6.3331–6.3684 (2H, m, C-5′ & C-5′′-Ar-H), 5.2733–5.2895 (1H, t, *J*= 3.24 Hz, C-12-H), 4.9055–4.9194 (1H, t, *J*= 2.78 Hz, C-22-H), 4.4020–4.4420 (1H, t, *J*= 8.00 Hz, C-3-H), 3.5648 & 3.5120 (4H (2H+2H), singlet each, C-2′-H & C-2′′-H), 2.9627–3.0070 (1H, dd, *J*= 13.80, 3.96 Hz, C-18-H), 1.1536 (3H, s, CH_3), 1.0109 (3H, s, CH_3), 0.9339 (3H, s, CH_3), 0.8821 (3H, s, CH_3), 0.8491 (3H, s, CH_3), 0.8424 (3H, s, CH_3), 0.8126 (3H, s, CH_3). ^{13}C NMR (100 MHz, $CDCl_3$+DMSO-d_6 mixture, δ ppm): 176.70, 172.82, 171.94, 143.07, 142.70, 142.32, 138.10, 137.04, 130.92, 130.52, 129.33, 129.02, 128.75, 128.58, 127.83, 127.50, 124.53, 124.34, 123.89, 123.51, 122.61, 121.20, 119.76,

117.00, 115.87, 80.11, 75.93, 54.77, 49.59, 47.02, 45.86, 45.60, 43.58, 41.49, 38.78, 38.07, 37.42, 37.41, 37.15, 36.43, 33.41, 32.22, 29.60, 27.65, 27.12, 26.02, 25.40, 23.53, 23.04, 22.89, 17.71, 16.53, 16.33, 15.03. ESI-MS (*m*/*z*): 1025.21 (M^-–1).

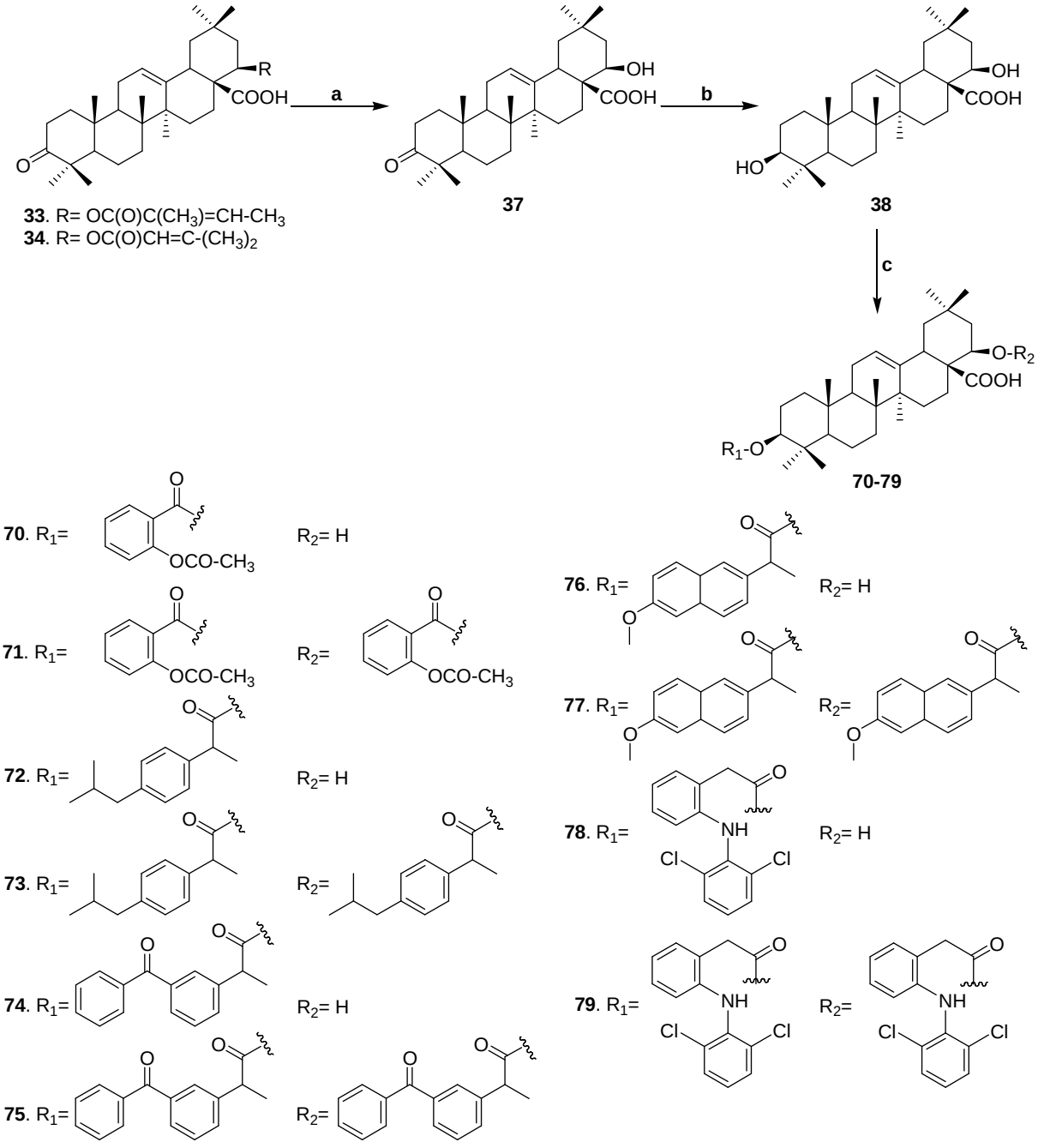

Scheme 3.5. Synthesis of lantadene–NSAID ester conjugates **70**–**79**. Reagents and conditions: (a) 10% Ethanolic KOH, reflux 6 h; (b) $NaBH_4$, MeOH–THF, stir 7 h; (c) R′-CO-O-CO-CH_3, 4-DMAP, pyridine, reflux 92–95 °C, 10–14 h.

3.3. Biological evaluations

3.3.1. *In vitro* cytotoxicity assay [81]

The A549 lung cancer cell line was procured from the American Type Culture Collection (ATCC, USA) and was grown in RPMI medium supplemented with 5% fetal bovine serum and 1% penicillin-streptomycin (Gibco, Invitrogen, USA). The A549 cells (4000 cells/well) were seeded into 96-well plates and incubated overnight for cell attachment. For treatment, the compounds were added at concentrations ranging from 0.01 to 100 µmol and incubated for 48 h. At the end of incubation, 20 µl/well of 5 mg/ml 3-(4,5-dimethythiazol-2-yl)-2,5-diphenyltetrazolium bromide (MTT) (Amresco, USA) was added and the cells were further incubated for 4 h. The supernatant was discarded and the purple formazan complex formed was dissolved using 100 µl of DMSO (Fisher Scientific, UK). The absorbance was read at 570 nm using a Spectra Max M4 microplate reader (Molecular Devices Inc., USA).

3.3.2. The *in vitro* inhibition of TNF-α-induced NF-κB activation in A549 lung cancer cells [82]

The A549 cells were cultured in 12-well plates and transiently co-transfected with 0.2 µg of a pNF-κB-Luc vector (Stratagene, La Jolla, CA) and 0.2 µg of the pSV-β-galactosidase dissolved in 3 µl lipofectamine^{TM} or lipofectamine^{TM} 2000 (Invitrogen, Carlsbad, CA) as the internal control. The plasmids were transfected according to the manufacturer's instructions. After 6 h, the medium was changed and the cells were cultured for an additional 6 h. The cells were then treated with TNF-α (15 ng/ml) and the test compounds simultaneously for 8 h. The A549 cells treated with TNF-α alone served as positive controls, while the cells without TNF-α treatment served as negative controls. The luciferase activities from these cells were then measured by using the Bright-Glo Luciferase Assay kit from Promega (Madison, WI), following the manufacturer's protocol. The relative NF-κB activities of the cells treated with the test

compounds were obtained as the ratio of its luciferase activity to that from the positive controls, both of which had been corrected with background (signals from negative controls) and cell viability. In these experimental conditions, none of the test compounds induced significant toxicity to the A549 cells (<5% reduction of cell viability). The IC_{50} of each fraction was determined by fitting the relative NF-κB activity to the drug concentration by using a sigmoidal dose-response model of varied slope in GraphPad Prism 6.0. The IC_{50} reported herein is the average of at least three replicates.

3.3.3. *In vitro* phosphorylation assay (*In vitro* IKK*β* inhibition assay) [83]

The cDNA encoding human IKK*β* was isolated by PCR with primers containing sequences encoding a FLAG tag in the carboxy-terminal region and subcloned into an insect cell expression vector, pFastBac1 (Invitrogen, U.S.A.). The Sf21 cells were infected with the IKK*β* recombinant baculovirus and cultured at 28 °C for 72 h. The cells were lysed and FLAG-tagged IKK*β* protein was purified by the affinity chromatography using an anti-FLAG M2 affinity gel (Sigma, U.S.A.). The kinase reaction of the purified human IKK*β* was performed at room temperature for 1 h in kinase reaction buffer (25 mmol/l HEPES, pH 7.5, 10 mmol/l magnesium acetate, 1mmol dithiothreitol, 0.01% bovine serum albumin, 0.01% Tween20) containing 500 nmol ATP, and bacterially expressed GST-IκBα, and then terminated by adding the same volume of Kinase-Glo™ reagent (Promega, U.S.A.). After incubating at room temperature for 10 min, the luminescent signal correlated with the amount of ATP remaining in a solution following the reaction, was measured by Wallac Arvo HTS multilabel counter (Perkin Elmer, U.S.A.).

3.3.4. The *in vitro* evaluation of COX-2 activity by the quantitation of PGE_2 [84]

The effect of test compounds on COX activity was determined by measuring PGE_2 production as described previously [84]. Briefly, the reaction mixtures

were prepared in 100 mmol Tris–HCl buffer (pH 8.0) containing 1 µmol heme, 500 µmol phenol, 300 µmol epinephrine, sufficient amount of COX-2 to generate 150 ng of PGE_2/ml and various concentrations of test compounds. The reaction was initiated by the addition of arachidonic acid (final concentration, 10 µmol) and incubated for 10 min at room temperature (final volume, 200 µl). The reaction was then terminated by adding 20 µl of the reaction mixture to 180 µl of 27.8 µmol indomethacin, and PGE_2 was quantitated by an ELISA method. The samples were diluted to the desired concentration with 100 mmol potassium phosphate buffer (pH 7.4) containing 2.34% NaCl, 0.1% bovine serum albumin, 0.01% sodium azide and 0.9 mmol Na_4EDTA. Following transfer to a 96-well plate (Nunc-Immuno Plate Maxisorp, Fisher Scientific, Pittsburgh, PA) coated with a goat anti-mouse IgG (Jackson Immuno Research Laboratories, West Grove, PA), the tracer (PGE_2-acetylcholinesterase, Cayman Chemical, Ann Arbor, MI) and primary antibody (mouse anti-PGE_2, Monsanto, St. Louis, MO) were added. Plates were then incubated at room temperature overnight, the reaction mixtures were removed, and the wells were washed with a solution of 10 mmol potassium phosphate buffer (pH 7.4) containing 0.01% sodium azide and 0.05% Tween 20. Ellman's reagent (200 µl) was added to each well and the plate was incubated at 37 °C for 3–5 h, until the control wells yielded an optical density of 0.5–1.0 at 412 nm. A standard curve with PGE_2 (Cayman Chemical, Ann Arbor, MI) was generated on the same plate, which was used to quantify the PGE_2 levels produced in the presence of test samples. The results were expressed as a percentage, relative to control (solvent-treated) samples, and dose–response curves were constructed for the determination of IC_{50} values. The IC_{50} values were generated from the results of four serial dilutions of test compounds and are the mean of three different experiments.

3.3.5. The inhibition of TNF-α-induced PGE_2 secretion [85]

The effect of compound **79** on the PGE_2 secretion was studied. The murine macrophage cell line RAW 264.7 was procured from the American Type Culture

Collection (ATCC, USA). The cells were cultured in Dulbecco's modified Eagle's medium (DMEM; GIBCO, Inc., NY, USA) supplemented with 100 U/ml of penicillin, 100 µg/ml of streptomycin and 10% fetal bovine serum (FBS; GIBCO, Inc., NY, USA). The cells were incubated in an atmosphere of 5% CO_2 at 37°C and were subcultured every 3 days. One million murine macrophage cells were seeded into a six-well plate, pretreated with the different concentrations of compound **79** for 4 h, then stimulated with 1 nmol TNF-α for 12 h. The culture media were collected and the concentration of PGE_2 was determined using a PGE_2 ELISA kit purchased from R&D Systems (Minneapolis, MN, USA).

3.3.6. The Western blot analysis of IκBα, cyclin D1, and COX-2 [86–87]

The cytoplasmic protein (30–35 mg) or whole-cell extract was prepared as described previously and resolved by employing SDS-polyacrylamide gel electrophoresis (PAGE). Then, the proteins were electrotransferred to a nitrocellulose membrane, blocked with 5% nonfat dry milk and probed with primary antibodies against IκBα, cyclin D1, and COX-2 for 2 h at 40 °C. The blotting membrane was washed, exposed to horse radish peroxidase-conjugated secondary antibodies for 1 h and the blots were finally detected by chemiluminescence.

3.4. Hydrolysis studies (HPLC studies)

The reversed-phase HPLC was used for the analysis of chemical and metabolic stability, and the chromatographic purity of compounds. The isocratic solvent systems comprising of methanol-acetonitrile-water-acetic acid (68:20:12:0.01) and methanol-acetonitrile-water-acetic acid (68:22:10:0.01) were used as a mobile phase. The mobile phase constitutes for HPLC analysis were mixed (v/v) and filtered through a 0.22 µm Millipore membrane filter. The injection volume

was 10 µl and the flow-rate was kept at 1 ml/min. The peak areas showed a good reproducibility with a relative standard deviation of 0.5%.

3.4.1. The *in vitro* chemical stability of the lead lantadene congeners in simulated gastric fluid [88,89]

The chemical stability of the lead lantadene congeners **50–51**, **63–64**, and **79** was determined in the HCl buffer of pH 2 at 37 °C. The reaction was initiated by adding 200 µl stock solution of compound (5 mg/ml in THF) to 1.80 ml of the HCl buffer of pH 2 in a screw-capped glass vial. The reaction mixture was kept in a water bath at constant temperature, and samples (200 µl) were withdrawn at an appropriate time intervals, diluted with 800 µl ACN, and analyzed by using HPLC. The level of prodrug that remained unhydrolyzed was calculated as: % remaining = (peak area at the respective time (min)/peak area at 0 min) × 100.

3.4.2. The *in vitro* metabolic stability of the lead lantadene congeners in human blood plasma [88,89]

The enzymatic hydrolysis of the lead lantadene congeners **50–51**, **63–64**, and **79** was studied in 80% human plasma diluted with an isotonic phosphate buffer of pH 7.4. The reaction was initiated by adding a 50 µl stock solution of prodrug (5 mg/ml in THF) to 450 µl of diluted plasma. The solution was incubated in a water bath at 37 °C. The samples (50 µl) were withdrawn at an appropriate time intervals and added to 1950 µl of ACN. The sample mixture was then centrifuged for 5 min at 7000 rpm and the supernatant appeared was used for the HPLC analysis. The extent of the prodrug that remained unhydrolyzed was calculated as: % remaining = (peak area at the respective time (min)/peak area at 0 min) × 100.

3.5. Molecular docking studies

3.5.1. Predicting binding mode of lantadene congeners to IKK*β*

The 3D crystal structure of IKK*β* was obtained from Protein Data Bank (PDB ID: 3QA8) [14]. The PDB structures of the ligands were prepared in CS ChemDraw Ultra 8.0. AutoDock tools 1.5.4 were used for the virtual screening studies. The receptor was initially prepared by adding polar hydrogen atoms at pH 7.4 followed by assigning the Gasteiger charges. Nonpolar hydrogens were merged and partial charges to their parent carbon atoms were added. The search space was defined as a cubic box with dimensions 40 Å × 40 Å × 40 Å and center x = −20, y = −15, z = 30. The Lamarckian genetic algorithm (LGA) was used to search the conformers of the lowest binding energies. The results of virtual screening studies were obtained as the estimated free energy of binding in kcal/mol (docking score).

3.6. Statistical analysis

Results are expressed as the mean of atleast three values and were analyzed by one way ANOVA followed by Tukey's multiple comparisons test using GraphPad Prism 6.0. The statistical significance was set at $P < 0.05$ level.

CHAPTER 4

RESULTS AND DISCUSSION

4.1. Extraction and isolation of lantadene A and B

In order to find out the optimal solvent for the extraction of lantadene A and B from the leaves of *Lantana camara* L., shade-dried powder of lantana leaves was subjected to maceration for 24 h with various solvents, namely tetrahydrofuran, chloroform, ethyl acetate, ethanol, and methanol, followed by quantification of the obtained extract for the estimation of lantadene A and B by using HPLC. The results of HPLC analysis showed that lantadene A and B were highest extracted with the ethyl acetate followed by extraction with chloroform, ethanol, tetrahydrofuran, and methanol. It was noticed that polar solvents, *viz*. methanol and ethanol were less suitable for the extraction of lantadenes, while solvents with comparatively medium polarity, such as ethyl acetate and chloroform displayed the increased extraction of lantadenes. Nevertheless, an extraction with further non-polar solvent THF yielded radically declined yield of lantadenes. It is the fact that lantadene A and B are relatively non-polar structures and therefore, solvents of relatively medium polarity, such as ethyl acetate and chloroform were the most suitable for the extraction of lantadenes, with ethyl acetate being the slightly more polar than chloroform was found to be the most optimal solvent. Amount of lantadene A and B extracted with various solvents is presented in **Table 4.1**.

Table 4.1. Quantification of lantadene A and B in lantana leaves by using various solvents

Solvent	% Lantadene A (w/w)	% Lantadene B (w/w)
Tetrahydrofuran	0.164±0.0130	0.090±0.0087
Chloroform	0.211±0.0103	0.115±0.0076
Ethyl acetate	**0.248±0.0028**	**0.131±0.0036**
Ethanol	0.170±0.0041	0.100±0.0057
Methanol	0.080±0.0028	0.047±0.0045

Followed by the optimization of the solvent for the extraction of lantadene A and B, 1 kg of lantana leaves powder was extracted with ethyl acetate. The extract was filtered and activated charcoal was added to remove the chlorophyll and other impurities. The partially colorless extract was then filtered and concentrated under the reduced pressure, followed by the chloroform–water partitioning of the extract to remove the poly-phenolic and polar impurities with water. Although, ethyl acetate–water partitioning may also be used, still chloroform being the relatively non-polar than ethyl acetate holds the edge and is more suitable for the removal of polar impurities. Chloroform layer was repeatedly washed with water and evaporated in a rotary evaporator to yield the partially purified mixture of lantadenes, which were isolated as the pure lantadene A and B with the help of column chromatography while using a mobile phase consisting of petroleum ether and ethyl acetate. The scheme of the extraction and isolation of lantadene A and B is shown in **Fig. 4.1**.

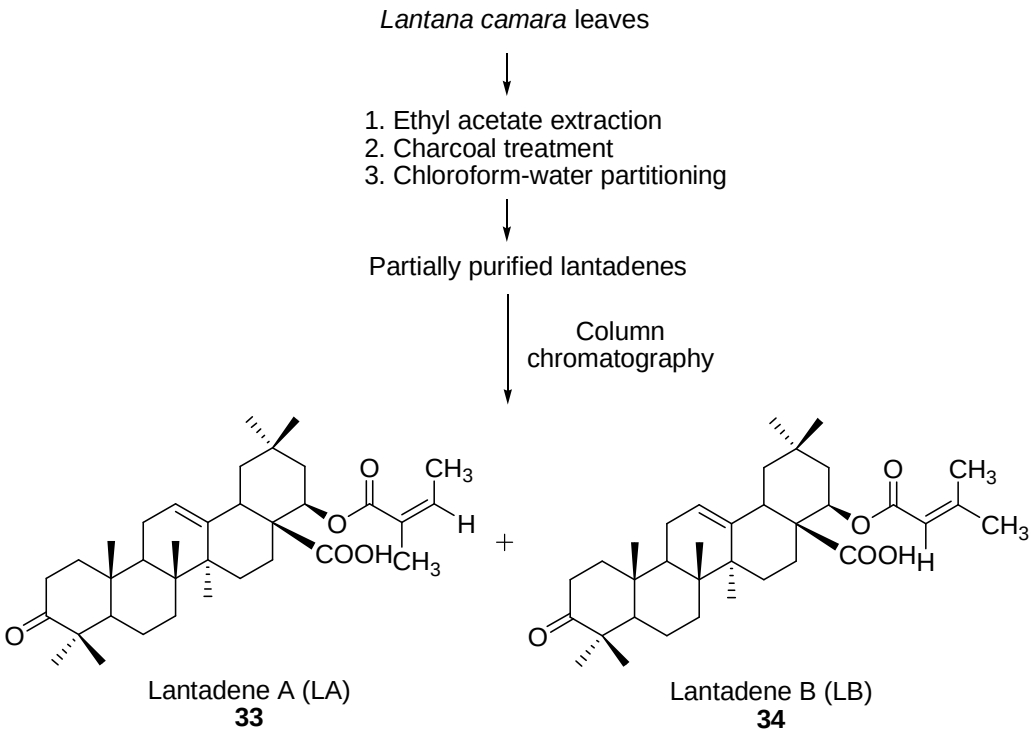

Figure 4.1. The sequence of steps involved in the isolation of lantadene A (**33**) and B (**34**)

4.2. Synthesis of lantadene congeners

The sequence of steps involved in synthesis of lantadene congeners (**33**–**79**) are summarized in the previous chapter 3 as **Schemes 3.1–3.5**. Lantadene A (**33**) and B (**34**) are pentacyclic triterpenoids present in the leaves of weed *Lantana camara* Linn. Structurally lantadene A (**33)** and lantadene B (**34**) both share an olean-12-ene-28-oic acid template, while differing from the each other at the C-22 position via an ester linkage. The structures of the isolated and synthesized compounds were confirmed by ^{1}H NMR, ^{13}C NMR, FT-IR, and Mass spectroscopic techniques. The ^{1}H NMR spectrum of the isolated compound **33** showed peaks characteristic to the C-12-H, C-22-H, C-18-H, and C-2-H. The C-12 and C-22 hydrogens were appeared at 5.3816 and 5.0911 ppm, respectively. The signal of C-18-H was observed as a double doublet between 3.0321 and 3.0734 ppm. Two protons of C-2 were observed as a multiplet (ddd) with C-2-Ha appearing downfield between 2.5175 and 2.6028 ppm, while C-2-Hb appeared upfield between 2.3396 and 2.4033 ppm. In the ^{13}C NMR analysis, the C-3-keto group appeared at 217.70 ppm, while the C-28 carbonyl carbon (of COOH) was observed at 179.28 ppm. The peaks at 166.27, 127.59, and 139.07 ppm were assigned to the C-31, C-32, and C-33, respectively, of the side chain carbons of compound **33**. The signals of C-12 and C-13 were detected at 122.50 and 143.11 ppm, respectively. The FT-IR spectrum of the isolated compound **33** showed O–H (COOH) stretching at 3308.77 cm^{-1}, while the stretchings at 1736.06, 1715.85, and 1702.14 cm^{-1} were assigned to the C=O (keto), C=O (ester), and C=O (acid) groups, respectively. The ESI-MS spectrum of **33** showed a molecular ion peak at 553.40 (*m/z*) (mol. mass 552.38).

The ^{1}H NMR spectrum of the isolated compound **34** showed peaks at 5.3785, 5.0404, 3.0072–3.0488 (dd), 2.5190–2.6039 (m), and 2.3417–2.4022 (m) ppm characteristic to the C-12-H, C-22-H, C-18-H, C-2-Ha, and C-2-Hb, respectively. The ^{13}C NMR spectrum of **34** indicated the presence of C-3-keto group at 217.77 ppm, while the C-28 carbonyl carbon (of COOH) was observed

at 178.84 ppm. The peaks at 127.37 and 143.09 ppm indicated the presence of C-12 and C-13, respectively.

The isolated compounds **33** and **34** differ only in the arrangement of atoms in the side chain with *E* conformation present in the side chain of **33**, while the side chain of compound **34** possesses *Z* conformation. Hence, in the compound **33,** the olefinic C-33-H appeared at 5.9759–6.0295 ppm as multiplet, while in the compound **34**, the olefinic-H was present at C-32 position and appeared as a singlet at 5.5577 ppm. The ^{13}C NMR of the compound **33** showed C-32 and C-33 peaks at 127.59 and 139.07 ppm, while in the compound **34**, C-32 and C-33 peaks were observed at 115.96 and 157.16 ppm, respectively. The C-35 of **33** appeared at 20.59 ppm, while it appeared downfield at 27.46 ppm in the compound **34**. In the FT-IR, the O–H (COOH) stretching of the compound **34** was observed at 3289.29 cm^{-1}. The stretchings at the 1738.61, 1712.29, and 1693.62 cm^{-1} were assigned to the C=O (keto), C=O (ester), and C=O (acid) groups, respectively. The molecular ion peak of the compound **34** was appeared at 553.50 (*m/z*) (mol. mass 552.38). Therefore, interpretation of the ^{1}H and ^{13}C NMR along with the FT-IR and mass spectra indicates the successful isolation of the compounds **33** and **34** as lantadene A (22*β*-angeloyloxy-3-oxo-olean-12-en-28-oic acid) and lantadene B (22*β*-senecioyloxy-3-oxo-olean-12-en-28-oic acid), respectively.

The isolated compounds **33** and **34** were reduced into the corresponding compounds **35** and **36**, respectively, using $NaBH_4$ as a selective reducing agent and MeOH–THF mixture as the solvent. Our isolated compounds **33** and **34** were only sparingly soluble in MeOH and therefore, the use of MeOH–THF mixture as the solvent alleviated the solubility problem, as **33** and **34** were freely soluble in the THF. $NaBH_4$ reduces carbonyl groups more rapidly in the polar solvents, as $NaBH_4$ must be ionized in the polar solvent to transfer the hydride ion (H^-) to the carbonyl group and because of this reason, MeOH–THF mixture was used as the solvent instead of using the THF alone as the solvent. The ^{1}H NMR spectra

of the reduced compounds **35** and **36** showed the appearance of the new double doublet peak of C-3-H at 3.2080–3.2430 and 3.1349–3.1725 ppm, respectively. The signals of C-2-Ha and C-2-Hb protons were shifted upfield on a reduction of **33** and **34** into the **35** and **36**, correspondingly. In the ^{13}C NMR, the C-3 peak appeared upfield at 79.02 and 79.01 ppm in **35** and **36**, respectively (217.70 and 217.77 ppm in **33** and **34**, respectively). On reduction, the C-2 and C-4 peaks also appeared upfield along with slight upfield shifting in the peak of C-1. In the FT-IR spectra, C=O (keto) stretching was disappeared on reduction, while the new O–H stretching was appeared at 3482.87 and 33480.79 cm^{-1} in **35** and **36**, respectively. The ESI-MS spectra of **35** and **36** showed the presence of peaks corresponding to their molecular weights.

Compound **37** was synthesized by alkali hydrolysis of **33** and **34** using 10% ethanolic KOH as a hydrolysis agent. On hydrolysis of **33** and **34** into the **37**, the side chain peaks (C-31-H/C-31 to C-35-H/C-35 of compounds **33** and **34**) were disappeared in the ^{1}H and ^{13}C NMR spectra of compound **37**. The C-22-H appeared upfield as triplet at 3.7501–3.7670 ppm (5.0911 and 5.0404 ppm in **33** and **34**, respectively), while in the ^{13}C NMR, the C-22 peak was observed downfield at 77.23 ppm (75.85 and 75.20 ppm in **33** and **34**, respectively). The FT-IR spectrum of **37** showed two O–H stretchings at 3439.83 and 3261.69 ppm, characteristic to the C-22-OH and 28-COOH groups, respectively. The ESI-MS spectra of **37** signified the presence of the molecular ion peak.

Compound **38** was synthesized by selective reduction of the C-3 carbonyl group of compound **37** into the hydroxyl group by using $NaBH_4$. On the generation of the hydroxyl group, the C-3-H of **38** appeared as a triplet between 3.0544 and 3.0934 ppm, while the newly generated C-3-OH appeared as a broad signal at 3.5768 ppm. The C-2-H signals were also moved upfield on a reduction of **37** into **38**. The ^{13}C NMR spectrum of **38** showed upfield shifting of the C-3-H and it emerged at 77.16 ppm, while it was present at 216.41 ppm in **37**. The FT-IR spectrum of compound **38** showed a peak characteristic to the hydroxyl group,

while the ESI-MS spectrum of the compound **38** exhibited the corresponding molecular ion peak.

Compound **39** was synthesized from compound **37** by esterification of the C-28 carboxylic group using dimethyl sulfate. On methylation of the carboxylic group, the newly created C-31-H (i.e. CH_3 protons) appeared as a singlet at 3.6702 ppm, while in the ^{13}C NMR, a signal of C-31 (COO–$\underline{CH_3}$) was detected at 52.43 ppm. However, no noticeable change in the shift was observed for C-28 (O–C=O) and it was appeared at 176.14 ppm, while in the ^{13}C NMR spectrum of the compound **37**, C-28 was also observed at 176.33 ppm. The ESI-MS spectrum of the compound **39** showed the characteristic $(M+Na)^+$ and $(2M+Na)^+$ peaks.

Compound **40** was synthesized from compound **39** by reduction of the C-3 carbonyl group into the hydroxyl group by employing the selective reducing agent $NaBH_4$. The ^1H NMR spectrum of **40** indicated the appearance of new double doublet peak at 3.1955–3.2352 ppm, which was assigned to the C-3-H. The C-3 signal in the ^{13}C NMR appeared upfield at 78.99 ppm, while the same signal was observed at 217.83 ppm in **39**. The C-1, C-2, and C-4 signals in the ^{13}C NMR were also moved upfield on conversion of compound **39** into **40**. The FT-IR spectrum of **40** showed the presence of hydroxyl groups, while the ESI-MS spectrum indicated the presence of the distinctive molecular ion peak.

The 3-hydroxylimino substituted compounds **41** and **42** were synthesized from **33** and **34**, correspondingly by the reaction of hydroxylamine hydrochloride with the 3-oxo group of **33** and **34**. The ^{13}C NMR spectra of **41** and **42** indicated upfield shifting of the C-3 signal and it was appeared at 164.22 and 164.08 ppm, respectively (C-3 was appeared at 217.70 and 217.77 ppm in **33** and **34**, respectively). The signal of C-4 was also affected and it shifted upfield from 46.87–46.88 ppm in **33** and **34** to 39.48–39.50 ppm in **41** and **42**. The FT-IR spectra of **41** and **42** showed peaks distinctive to the hydroxyl groups, while the ESI-MS spectra showed peaks analogous of the molecular weights.

The 3β,22β-diacetoyloxy substituted compound **43** was synthesized from the 3β,22β-dihydroxy substituted compound **38** by the reaction of acetyl chloride with the hydroxyl groups of **38** in the presence of 4-DMAP. Refluxing in pyridine for 10 h at 92–95 °C yielded compound **43**. On formation, C-3-H signal appeared downfield from 3.0544–3.0934 ppm in **38** to 4.4800–4.5196 ppm in **43** and it was observed as a triplet. The C-22-H signal also appeared downfield as a triplet at 5.0028–5.0172 ppm, while it was present at 3.7499–3.7654 ppm in **38**. The sharp singlet peaks at 2.0498 and 1.9411 ppm were assigned to the methyl groups of C-2′ (COO$\underline{CH_3}$) and C-4′ (COO$\underline{CH_3}$), respectively. In the ^{13}C NMR, the newly generated C=O of the ester group (C-1′ or $\underline{CO}OCH_3$) was observed at 171.08 ppm, while C=O of the newly formed ester group (C-3′ or $\underline{CO}OCH_3$) was detected at 169.70 ppm. The C-2 signal was discovered upfield at 23.44 ppm, while it was present at 27.96 ppm in **38**. The C-2′ and C-4′ signals of the methyl groups were observed at 21.31 and 21.10 ppm, respectively. The C-3 signal in the ^{13}C NMR remained unaffected from acetylation and it was appeared at 80.85 ppm. The presence of stretching at 1731.60 cm^{-1} in the FT-IR spectrum was assigned to the C=O stretching of the ester group. The molecular ion peak distinctive to the molecular weight was also present in the ESI-MS spectrum of **43**.

Compounds **44**–**47** and **52** were synthesized in a single step process by the reaction of carbonyl chlorides with the hydroxyl group of the compounds **35**, **36**, and **37**. Compounds **35**, **36**, and **37** with appropriate carbonyl chlorides were refluxed in pyridine, in the presence of 4-DMAP at 92–95 °C for 10–14 h to yield the compounds **44**–**47** and **52**. Compounds **48**–**51** and **53**–**54** were synthesized in a two step process. In step 1, the acidic function of the compounds was converted into the anhydride function by reacting it with acetyl chloride in the presence of pyridine. In the step 2, the anhydride function of the respective derivatives (anhydride derivatives) was reacted with the hydroxyl

group of the compounds **35**, **36**, and **37** in the presence of 4-DMAP to yield the compounds **48**–**51** and **53**–**54**.

On synthesis of 3*β*-substituted compounds **44**–**51**, the distinguishing C-3-H peak appeared downfield between 4.4113 and 4.8085 ppm either as a triplet or as a multiplet (3.2080–3.2430 and 3.1349–3.1725 ppm in **35** and **36**, respectively). In ^{13}C NMR, the carbonyl carbon of the newly generated ester group (C-1′) was observed at 165.28–171.14 ppm. The C-2 peak was detected upfield at 22.41–23.51 ppm (28.10–28.11 ppm in **35** and **36**, respectively). Also, the C-3 signal appeared between 79.89 and 82.63 ppm and no observable change in the shift was observed in it, when compared to the C-3 signal of **35** and **36**. The respective aromatic protons and the carbons were also observed in the ^{1}H NMR and ^{13}C NMR spectra of the compounds **46**–**51**. The FT-IR spectra of the compounds **44**–**51** indicated the presence of C=O stretching of the newly generated ester group. The ESI-MS spectra confirmed peaks related to the molecular weights of the compounds **44**–**51**.

On chemical synthesis of 22*β*-substituted compounds **52**–**54** from the compound **37**, the distinguishing C-22-H appeared downfield at 5.0958–5.2206 ppm (3.7501–3.7670 ppm in **37**), while in the ^{13}C NMR spectra of the compounds **52**–**54**, the C-22 peak appeared between 76.52 and 77.37 ppm. The carbonyl carbon of the ester group (C-1′) generated on esterification at the C-22 position appeared between 165.12 and 170.27 ppm. The C=O stretching of the ester group and the respective molecular ion peaks were also observed in the FT-IR and ESI-MS (negative-ion mode) spectra of the compounds **52**–**54**, correspondingly.

Compounds **55–69** were synthesized in a two step process. In step 1, the acidic function of the NSAIDs was converted into the anhydride function by the reaction with acetyl chloride in the presence of pyridine. In step 2, the anhydride function of the respective NSAIDs was reacted with compounds **35**,

36, and **37** in the presence of 4-DMAP, in pyridine. Refluxing at 92–95 °C, for 10–14 h, produced the compounds **55**–**69**. Attempts were also made to synthesize the esters by converting the acidic group of the NSAIDs into the halide and then into the esters by conjugation of the halide and alcohol groups, and also by direct hybridization of acid and alcohol in the presence of *N*,*N*'-dicyclohexylcarbodiimide (DCC) and 4-DMAP, as the Steglich esterification; though, couldn't met with success. The stability of the NSAID halides and the presence of free acidic group in compounds **35**, **36**, and **37** might have hindered the chances of the reactions, in these unsuccessful methods, respectively. In the synthesis of compounds **55**–**69**, the ^{1}H NMR spectra showed the presence of aromatic protons, while the aromatic carbons were observed in the ^{13}C NMR spectra. On the synthesis of compounds **55**–**64**, the C-3-H appeared downfield between 4.3784 and 4.5025 ppm, as a triplet (3.2080–3.2430 and 3.1349–3.1725 ppm in **35** and **36**, respectively). In the ^{13}C NMR spectra, the carbonyl carbon (C-1′) of the newly generated ester group was observed between 173.61 and 175.71 ppm. The C-2 peak was shifted to upfield at 23.41–23.72 ppm (28.10 and 28.11 ppm in **35** and **36**, respectively). The FT-IR spectra of the compounds **55**–**64** exhibited the C=O stretching of the newly generated ester group. The ESI-MS negative-ion mode spectra showed the peaks, corresponding to the molecular weights of the compounds **55–64**.

In the synthesis of compounds **65**–**69**, the C-22-H appeared downfield at 4.9015–5.0388 ppm (3.7501–3.7670 ppm in **37**), while in the ^{13}C NMR, no distinct change in the shift was observed for the C-22. The carbonyl carbon (C-1′) of the ester group created on esterification in compounds **65–69**, appeared between 172.33 and 173.77 ppm in the ^{13}C NMR spectra. The C=O stretching of the ester group and the respective molecular ion peaks were also observed in the FT-IR and ESI-MS (negative-ion mode) spectra of the compounds **65**–**69**, respectively.

The compounds **70**–**79** are ester conjugates of 3β,22β-dihydroxy-olean-12-en-28-oic acid (**38)** with different NSAIDs, and were synthesized via a two step

process. In step 1, the reaction was carried out at a carboxylic group of the NSAIDs to convert it into the anhydride function, by reacting it with acetyl chloride in the presence of pyridine as a base. In the subsequent step, the anhydride derivatives of the respective NSAIDs were refluxed for 10–14 h in pyridine with compound **38** in the presence of 4-DMAP to yield the mixture of 3*β*-substituted and 3*β*,22*β*-disubstituted derivatives, which were separated by means of column chromatography using silica gel of 100–200 mesh as an adsorbent and varying ratios of hexane and ethyl acetate as a mobile phase to yield the isolated *β*-substituted (**70**, **72**, **74**, **76**, and **78**) and 3*β*,22*β*-disubstituted (**71**, **73**, **75**, **77**, and **79**) compounds in the pure form.

On the synthesis of compounds **70**–**79**, the C-3-H shifted downfield from 3.0544–3.0934 ppm in **38** to 4.3275–4.5198 in **70**–**79**, while in the disubstituted compounds, the C-22-H signal was also detected downfield at 4.9055–5.0228 ppm (it was detected at 3.7499–3.7654 ppm in **38**). In the ^{13}C NMR analyses, the carbonyl carbon of the newly created ester group (C-1′) was detected between 169.81 and 174.30 ppm. The C-3 signal of 3*β*-substituted compounds remained unaffected on esterification and it appeared at 79.10−81.01 ppm, while it was detected at 77.16 ppm in compound **38**. The FT-IR spectra displayed C=O stretching, distinctive to the ester group of the compounds **70**–**79**, while the ESI-MS spectra of the compounds showed molecular ion peaks corresponding to the molecular weights of the compounds **70**−**79**.

4.3. Biological evaluations

4.3.1. *In vitro* cytotoxicity assay

All the isolated and synthesized lantadene congeners were evaluated for their *in vitro* cytotoxicity against lung cancer cells A549. The parent pentacyclic triterpenoids **33**, **34**, **35**, and **36** showed cytotoxicity against A549 lung cancer cells with IC_{50} values of 2.84, 1.19, 0.79, and 0.43 µmol, respectively, whereas the other parent compounds **37** and **38** along with lantadene congeners **39**–**43**,

and various NSAIDs (aspirin, ibuprofen, ketoprofen, naproxen, and diclofenac) showed IC_{50}s >10 µmol. Among all the compounds (**33**–**79**) screened, the hybrids of compounds **35** and **36** with cinnamic acid, *i.e.* **50** and **51** showed the highest cytotoxicity with IC_{50}s of 0.12 and 0.08 µmol, respectively.

The ester conjugates of **35** and **36** with various NSAIDs at C-3 position (**55**–**64**) also showed the marked cytotoxicity in the range of 1.31 to 0.15 µmol, with diclofenac–lantadene conjugates **63** and **64** being the most active, while showing IC_{50}s of 0.15 and 0.42 µmol, correspondingly. Conversely, the hybrids of compound **37** with various NSAIDs at C-22 position (**65**–**69**) were less active and exhibited decreased activity.

The ester conjugates of compound **38** with various NSAIDs with at C-3 and C-22 positions (**70**–**79**) displayed appreciable cytotoxicity (IC_{50}s) in the range of 6.74 to 0.42 µmol. Among the ester conjugates **70**–**79**, the diclofenac moiety bearing compounds **78** and **79** showed the most promising cytotoxicity against A549 cells with IC_{50} values of 0.84 and 0.42 µmol, respectively. The reference drug cisplatin showed IC_{50} of 21.30 µmol.

In brief, the cinnamic acid conjugates **50** and **51** demonstrated the highest cytotoxicity followed by diclofenac conjugates **63**, **64**, and **79**. Further, compounds **50**, **51**, **63**, **64**, and **79** inhibited proliferation of lung adenocarcinoma A549 cells in a dose dependent manner. From the cytotoxicity profiles of compounds **33**–**79**, it was evident that the removal of the ester side chain at C-22 position led to a decrease in the activity. The α,β-unsaturated carbonyl group of the ester side chain is strongly electrophilic and seems to play an important role in binding of the compounds to the receptor site. The cytotoxicity profile of the parent compounds **(33–38)** and lantadene congeners **(39–79)** are reported in **Table 4.2**.

Table 4.2. The *in vitro* cytotoxicity profile of the parent compounds **(33–38)**, lantadene congeners **(39–79)**, NSAIDs, and cisplatin against A549 cell line

Compound	IC_{50} (µmol)	Compound	IC_{50} (µmol)
33	2.84±0.72	60	1.23±0.12
34	1.19±0.28	61	0.90±0.05
35	**0.79±0.01**	62	0.91±0.03
36	**0.43±0.03**	**63**	**0.15±0.01**
37	>10	**64**	**0.42±0.04**
38	>10	65	>10
39	>10	66	2.95±0.75
40	>10	67	>10
41	>10	68	3.45±0.45
42	>10	69	1.65±0.45
43	>10	70	5.64±1.32
44	5.42±1.24	71	3.40±1.20
45	4.90±1.20	72	1.74±0.24
46	7.36±1.06	73	0.92±0.02
47	7.20±1.20	74	6.74±2.24
48	6.80±2.40	75	5.60±2.20
49	6.52±2.32	76	2.68±0.18
50	**0.12±0.02**	77	1.92±0.02
51	**0.08±0.02**	78	0.84±0.04
52	>10	**79**	**0.42±0.02**
53	>10	Aspirin	>10
54	3.64±1.24	Ibuprofen	>10
55	0.77±0.07	Ketoprofen	>10
56	1.10±0.20	Naproxen	>10
57	0.75±0.05	Diclofenac	>10
58	1.13±0.21	**Cisplatin**	**21.3±3.62**
59	1.31±0.10		

Results presented are the mean ± S.E.M of three values

4.3.2. The inhibition of TNF-α-induced NF-κB activation

The human lung adenocarcinoma cell line A549, transiently co-transfected with NF-κB-luc was used to monitor the effects of lantadene congeners on TNF-α induced NF-κB activation. The compounds (**33**–**79**) were evaluated in a dose-dependent manner to determine the concentration needed to inhibit 50% of TNF-α-induced NF-κB activation (IC_{50}s). The parent compounds **33**–**37** showed inhibition of TNF-α-induced NF-κB activation in the range of 6.42 to 0.98 µmol. The reduction of a C-3 keto group of compounds **33** and **34** into the C-3 hydroxyl group of compounds **35** and **36** led to an increase in the activity, whereas hydrolysis of a C-22 ester side chain of compound **33** and **34** into the compound **37** led to a decrease in the activity. The parent compound **38**, lantadene congeners **39**–**43**, and various NSAIDs (aspirin, ibuprofen, ketoprofen, naproxen, and diclofenac) showed IC_{50}s >10 µmol.

The conjugates of **35** and **36** with aliphatic (**44**–**45**) or aromatic acids (**46**–**51**) showed inhibition of TNF-α-induced NF-κB activation in the range between 5.04 and 0.42 µmol, with cinnamic acid conjugates **50** and **51** displaying the notable IC_{50}s of 0.56 and 0.42 µmol, respectively. On the contrary, the conjugates of **37** with aromatic acids (**52**–**53**) showed IC_{50}s >10 µmol, excluding the cinnamic acid conjugate (**54**) that showed IC_{50} of 2.42 µmol.

The hybrid compounds of **35** and **36** with various NSAIDs (**55**–**64**) showed inhibition of TNF-α-induced NF-κB activation in the range of 1.32 to 0.62 µmol, whereas the conjugates of compound **37** with various NSAIDs (**65**–**69**) showed IC_{50}s >10 µmol. The diclofenac conjugates **63** and **64** demonstrated the marked inhibition of NF-κB with IC_{50}s of 0.62 and 0.89 µmol, respectively.

The conjugates of compound **38** with various NSAIDs (**70**–**79**) were less active' yet, the conjugates of compound **38** with diclofenac showed the noteworthy activity, with diclofenac moiety bearing compounds **78** and **79** displaying IC_{50} values of 0.96 and 0.64 µmol, respectively.

Table 4.3. The *in vitro* inhibition of TNF-α-induced NF-κB activation by parent compounds **(33–38)**, lantadene congeners **(39–79)**, and NSAIDs

Compound	IC_{50} (µmol)	Compound	IC_{50} (µmol)
33	1.06±0.46	59	1.32±0.68
34	1.56±0.04	60	1.24±0.32
35	**0.98±0.02**	61	1.02±0.01
36	**1.02±0.62**	62	1.05±0.25
37	6.42±1.24	**63**	**0.62±0.02**
38	>10	**64**	**0.89±0.09**
39	>10	65	>10
40	>10	66	>10
41	>10	67	>10
42	>10	68	>10
43	>10	69	>10
44	2.80±0.24	70	4.20±1.20
45	2.32±0.01	71	3.92±0.42
46	5.04±1.02	72	2.60±0.30
47	4.64±1.76	73	1.92±0.62
48	4.18±1.68	74	>10
49	3.70±0.32	75	>10
50	**0.56±0.06**	76	>10
51	**0.42±0.01**	77	>10
52	>10	78	0.96±0.06
53	>10	**79**	**0.64±0.02**
54	2.42±0.24	Aspirin	>100
55	0.78±0.01	Ibuprofen	>100
56	1.20±0.02	Ketoprofen	>100
57	0.92±0.02	Naproxen	>100
58	1.18±0.76	Diclofenac	>100

Results presented are the mean ± S.E.M of three values.

Taken together, the introduction of the C-3 cinnamoyloxy functionality in the parent compounds **35**, **36**, and **37** led to an increase in the activity, highlighting the importance of the strongly electrophilic *α,β*-unsaturated carbonyl functionality at the C-3 and C-22 positions and their role in binding of compounds to the receptor site. Apart from cinnamic acid conjugates **50** and **51**, the diclofenac conjugates **63**, **64**, and **79** significantly inhibited the TNF-α-induced NF-κB activation. The hydrolysis of the C-22 ester functionality in lantadenes led to a significant reduction in the activity, supporting the notion that the mechanism of inhibition is likely through a covalent Michael addition of nucleophiles (such as SH from cysteine) from protein candidate(s) to lantadenes (**Fig. 4.2**). The results of inhibition of TNF-α-induced NF-κB activation in A549 lung adenocarcinoma cell line by compounds **33**–**79** are shown in **Table 4.3**.

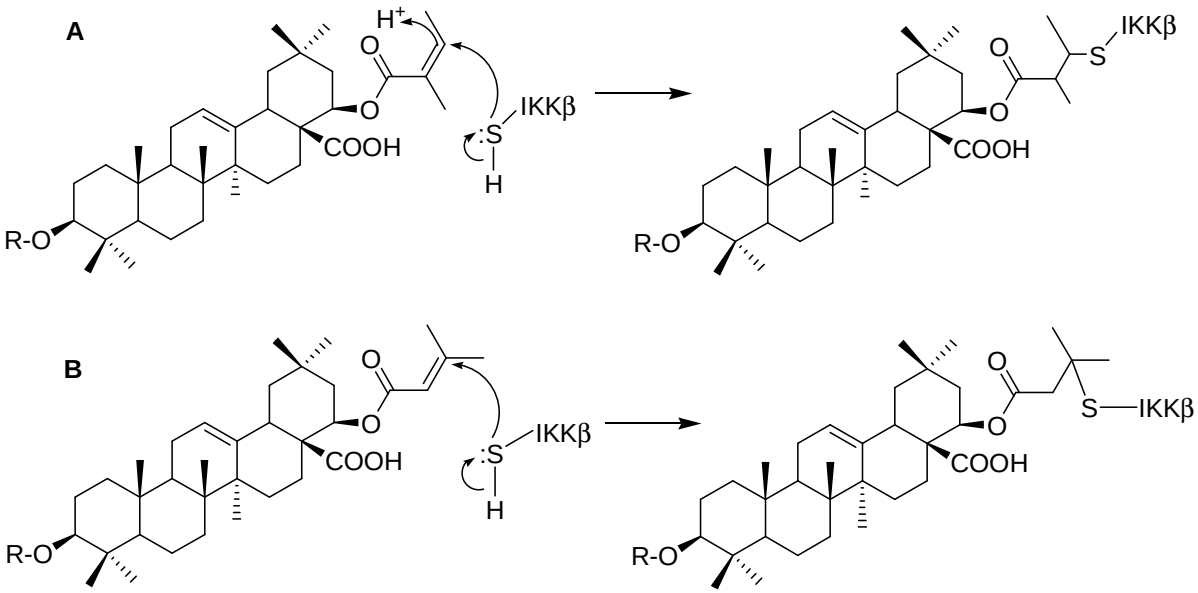

Figure 4.2. The proposed covalent Michael addition of lantadene A (**33**) and B (**34**) congeners (Fig. A & B, respectively) with the Cys-99 residue of the IKK*β* that subsequently leads to inhibition of NF-κB.

4.3.3. *In vitro* IKK*β* inhibition assay

The NF-κB can be activated by various signaling pathways and mostly through upstream IKK based phosphorylation of IκBα. The phosphorylation and subsequent degradation of IκBα leads to transmigration of NF-κB from the cytoplasm into the nucleus, where it binds with the DNA and transcripts the proteins responsible for the oncogenesis. As the compounds **50**, **51**, **63**, **64**, and **79** showed the potent inhibition of NF-κB; therefore, we decided to evaluate the effect of these compounds along with the most active parent compounds **35** and **36** against the upstream kinase IKK*β*, which is responsible for the activation of the NF-κB pathway. The results of *in vitro* IKK*β* inhibition assay revealed that along with the parent compounds **35** and **36**, lantadene congeners **50**, **51**, **63**, **64**, and **79** suppressed the activity of IKK*β* to an appreciable degree, with IC_{50} values of 2.62, 4.24, 1.20, 0.94, 1.56, 1.98, and 1.65 µmol, respectively (**Table 4.4**).

Table 4.4. The *in vitro* IKK*β* inhibition by parent compounds (**35–36**) and lantadene congeners (**50–51**, **63–64**, and **79**)

Compound	IC_{50} (µmol)
35	2.62±0.82
36	4.24±0.94
50	1.20 ±0.42
51	0.94±0.04
63	1.56 ±0.42
64	1.98±0.62
79	1.65±0.52

Results presented are the mean ± S.E.M of three values.

4.3.4. The evaluation of COX-2 activity by quantification of PGE_2

The COX-2 inhibitory potential of the lantadene–NSAID hybrid compounds (**55**–**79**) and their parent compounds (**33**–**38)** was determined by measuring the concentration of PGE_2, a product of the COX-2 reaction. The parent compounds (**33**–**38**) showed IC_{50}s >100 µmol. The hybrids of compounds **35** and **36** with various NSAIDs (**55**–**62**) showed inhibition of COX-2 with IC_{50}s ≥9.64 µmol, except diclofenac conjugates **63** and **64**, which revealed IC_{50}s of 0.68 and 0.84 µmol, respectively. The hybrids of compound **37** with various NSAIDs (**65**–**69**) exhibited inhibition of COX-2 with IC_{50}s ≥16.80 µmol.

Among the hybrids of compound **38** with various NSAIDs, the diclofenac conjugates **78** and **79** showed IC_{50}s of 1.20 and 0.56 µmol, respectively. The selected NSAIDs (aspirin, ibuprofen, ketoprofen, naproxen, and diclofenac) exhibited varying degrees of COX-2 inhibition, wherein aspirin showing the least COX-2 inhibition with IC_{50} of >100 µmol, whereas diclofenac displayed the most promising COX-2 inhibitory potential with IC_{50} of 0.038 µmol.

In brief, conjugates of diclofenac with NSAIDs, such as **63**, **64**, **78**, and **79** were the most potent inhibitors of COX-2 activity, with compound **79** displaying the highest COX-2 inhibitory potential. The lantadene congeners **39**–**54** did not bear any COX inhibitory or NSAID scaffold; hence, they were not tested for COX-2 inhibitory activity. The results of COX-2 inhibitory activity by parent compounds (**33**–**38**) and lantadene–NSAID hybrid compounds (**55**–**79**) are shown in **Table 4.5**.

Table 4.5. The COX-2 inhibitory activities of the parent compounds **(33–38)**, lantadene–NSAID ester conjugates **(55–79)**, and NSAIDs

Compound	IC_{50} (µmol)	Compound	IC_{50} (µmol)
33	>100	67	44.4±8.60
34	>100	68	>100
35	>100	69	16.8±8.20
36	>100	70	>100
37	>100	71	>100
38	>100	72	7.20±2.20
55	>100	73	5.60±2.60
56	>100	74	9.64±1.64
57	9.64±3.44	75	8.42±2.62
58	10.80±2.40	76	15.62±4.42
59	12.2±2.60	77	12.40±6.20
60	14.6±4.20	**78**	**1.20±0.20**
61	42.2±12.6	**79**	**0.56±0.06**
62	48.4±16.4	Aspirin	>100
63	**0.68±0.20**	Ibuprofen	7.60±2.30
64	**0.84±0.42**	Ketoprofen	9.20±3.40
65	>100	Naproxen	28.2±8.24
66	28.2±6.20	**Diclofenac**	**0.038±0.02**

Results presented are the mean ± S.E.M of three values.

4.3.5. The inhibition of TNF-α-induced PGE_2 secretion

The PGE_2 is formed via the COX-mediated conversion of arachidonic acid [90]. Further, we examined whether the suppression of COX-2 activity by the most active compound **79** correlates with the suppression of PGE_2 synthesis. The mouse macrophages were pretreated with the different concentrations of **79** for 4 h, followed by stimulation with 1 nmol TNF-α for 12 h. Thereafter, culture media were collected and analyzed for PGE_2 secretion. The results showed that TNF-α induced the PGE_2 secretion, while compound **79** suppressed it in a dose-dependent manner (**Fig. 4.3**).

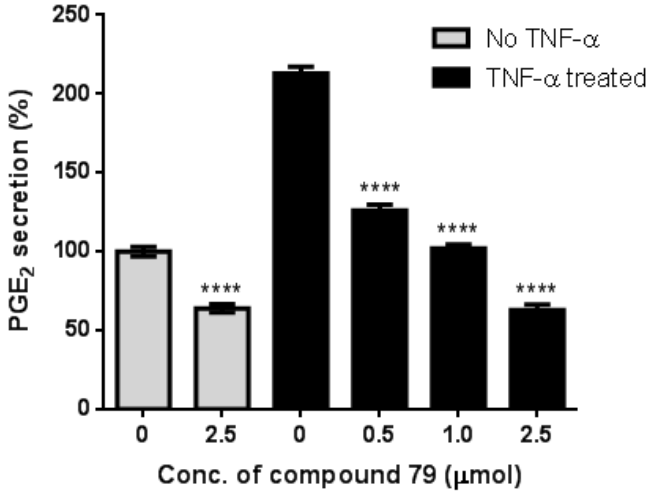

Figure 4.3. The effect of compound **79** on TNF-α-induced PGE_2 secretion. The results shown are the average ± SEM of three separate experiments. A *P* value < 0.05 was considered significant. ****P < 0.0001, 2.5 *vs*. 0; ****P < 0.0001, 0.5 TNF-α treated *vs*. 0 TNF-α treated, ****P < 0.0001, 1.0 TNF-α treated *vs*. 0 TNF-α treated; ****P < 0.0001, 2.5 TNF-α treated *vs*. 0 TNF-α treated.

4.3.6. The Western blot analysis of IκBα, cyclin D1, and COX-2

Compound **79** that not only showed the marked inhibition of TNF-α-induced NF-κB activation in A549 lung adenocarcinoma cells, but also displayed the distinguished activity against the COX-2, was selected for further studies. The activation of NF-κB requires the phosphorylation and degradation of IκBα, the natural inhibitor of NF-κB [91]. To determine whether the inhibition of TNF-α-induced NF-κB activation was due to the inhibition of IκBα phosphorylation and subsequent degradation, the cells were treated with various concentrations of **79** for 8 h and then exposed to 0.1 nmol TNF-α for 30 min. The cell extracts were then examined for IκBα status in the cytoplasm by Western blot analysis. The TNF-α induced the IκBα degradation in the control cells, whereas in the cells pretreated with compound **79**, TNF-α failed to induce the degradation of IκBα (**Fig. 4.4**)

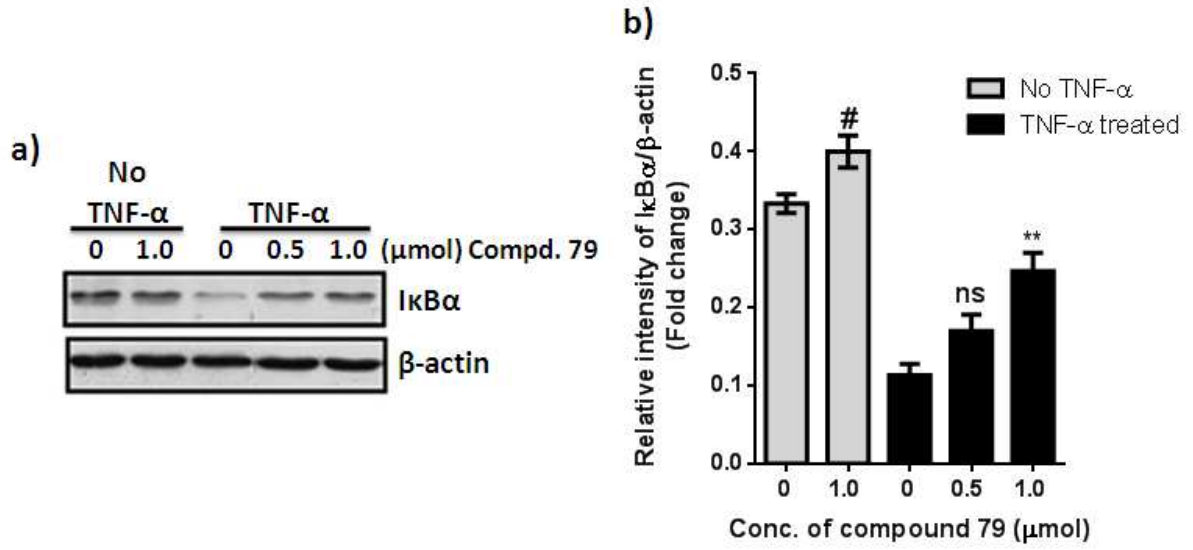

Figure 4.4. The effect of compound **79** on TNF-α-induced IκBα degradation. **a)** Western blot analysis describing the effect of compound **79** on TNF-α-induced IκBα degradation; **b)** The densitometry analysis of the Western blots shows the relative intensity of IκBα/β-actin. The results shown are the average ± SEM of three separate experiments. $^{\#}P$ > 0.05 or not significant, 1.0 *vs*. 0; ^{ns}P > 0.05 or not significant, 0.5 TNF-α treated *vs*. 0 TNF-α treated; $^{**}P$ < 0.01, 1.0 TNF-α treated *vs*. 0 TNF-α treated.

TNF-α induced NF-κB activation is necessary for the initiation of cyclin D1, which possess NF-κB-binding sites in their promoters [92–94]. The suppression of COX-2 is essential for anti-inflammatory effects, whereas the suppression of cyclin D1 is responsible for the antiproliferative properties of NSAIDs [92–94]. To determine whether the compound **79** inhibited the TNF-α-induced cyclin D1 and COX-2 expression, the cells were pretreated with **79**, and were then exposed to TNF-α. The results indicated that TNF-α induced the cyclin D1 expression, while compound **79** blocked the TNF-α-induced expression of this gene product in a dose-dependent manner (**Fig. 4.5a** and **4.5b**). Similarly, TNF-α also up-regulated the COX-2 protein expression, whereas the compound **79** down-regulated the expression of TNF-α-induced COX-2 protein in a dose-dependent manner (**Fig. 4.5c** and **4.5d**).

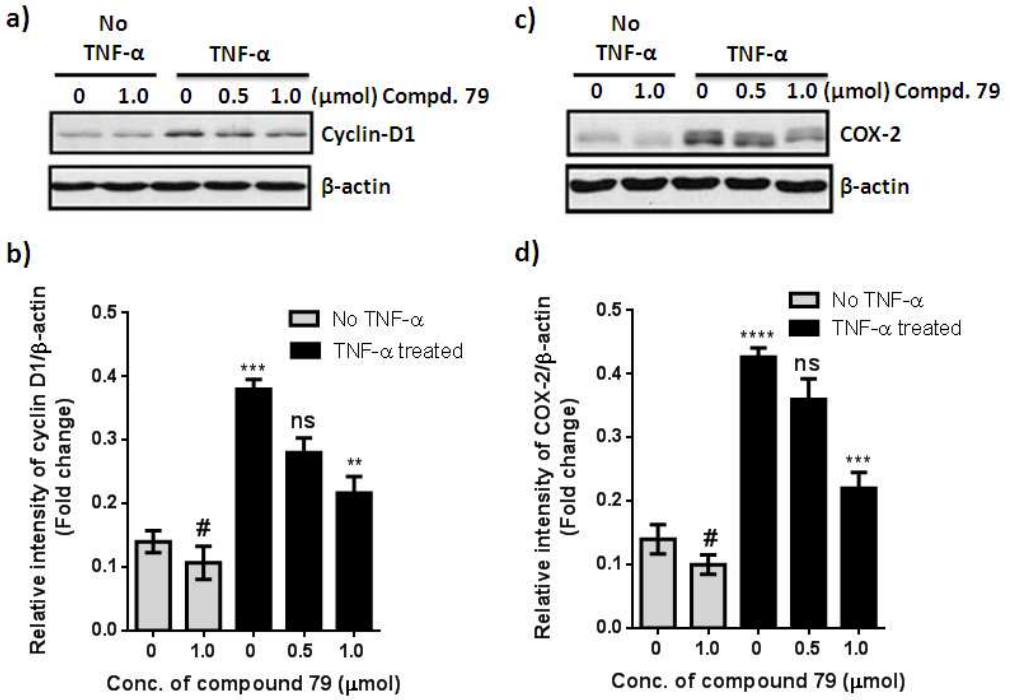

Figure 4.5. The effect of compound **79** on TNF-α-induced cyclin D1 and COX-2 expressions. The results shown are the average ± SEM of three separate experiments. A *P* value < 0.05 was considered significant. **a)** The effect of compound **79** on TNF-α-induced cyclin D1 expression; **b)** The densitometry analysis of the Western blots shows the quantification of the cyclin D1 levels. $^{\#}P$ > 0.05 or not significant, 1 *vs*. 0; $^{***}P$ < 0.001, 0 TNF-α treated *vs*. 0; ^{ns}P > 0.05 or not significant, 0.5 TNF-α treated *vs*. 0 TNF-α treated, $^{**}P$ < 0.01, 1.0 TNF-α treated *vs*. 0 TNF-α treated; **c)** The effect of compound **79** on TNF-α-induced COX-2 expression; **d)** The densitometry analysis of the Western blots shows the quantification of the COX-2 levels. $^{\#}P$ > 0.05 or not significant, 1 *vs*. 0; $^{****}P$ < 0.0001, 0 TNF-α treated *vs*. 0; ^{ns}P > 0.05 or not significant, 0.5 TNF-α treated *vs*. 0 TNF-α treated, $^{***}P$ < 0.001, 1.0 TNF-α treated *vs*. 0 TNF-α treated.

4.4. Chemical and plasma hydrolysis studies

4.4.1. The chemical stability of the lead lantadene congeners in simulated gastric fluid

One of the criteria of a successful prodrug is that it should be chemically stable in the acidic pH of the stomach. The compounds **50**, **51**, **63**, **64**, and **79** emerged as the lead lantadene congeners out of the synthesized series, were further studied for stability studies against chemical hydrolysis. Synthesized lantadene ester congeners **50**, **51**, **63**, **64**, and **79** were exposed to the simulated gastric fluid of pH 2 for 0, 2, 5, 8, and 12 h. Results of HPLC analysis of lantadene congeners exposed to the simulated gastric fluid of pH 2 showed that only 0.0, 3.57, 9.33, 15.26, and 23.42% of **50**, 0.0, 2.80, 7.52, 12.39, and 18.95% of **51**, 0.0, 5.29, 12.46, 21.74, and 29.67% of **63**, 0.0, 3.97, 9.75, 17.39, and 23.02% of **64**, and 0.0, 2.39, 6.76, 10.43, and 15.28% of **79** were hydrolyzed after the exposure time of 0, 2, 5, 8, and 12 h, respectively (**Table 4.6**). The chemical structures of lantadene congeners **50** and **51**, as well as of **63** and **64** differ from each other only at the ester side chain, present in the C-22 position. The 22β-angeloyloxy side chain is present in **50**, while 22β-senecioyloxy side chain is present in the congener **51**. Similarly, congener **63** possesses 22β-angeloyloxy side chain, while 22β-senecioyloxy side chain is present in the congener **64**. The lantadene congener **79** possesses diclofenac moiety at both the C-3 and C-22 positions. It can be inferred from the results of chemical hydrolysis studies that the lantadene congener **51** showed slightly higher resistances towards hydrolysis in comparison with the **50** and in the similar vein, congener **64** showed slightly more resistance towards hydrolysis in comparison with the **63**. Interestingly, all the lantadene ester congeners **50**, **51**, **63**, **64**, and **79** were sufficiently stable in the simulated gastric fluid and **s**uccessfully survived the stomach pH conditions.

Table 4.6. The chemical stability of the lead lantadene congeners (**50–51, 63–64**, and **79**) in simulated gastric fluid of pH 2

Time	% congeners remaining in simulated gastric fluid				
	Compd. **50**	Compd. **51**	Compd. **63**	Compd. **64**	Compd. **79**
0 h	100	100	100	100	100
2 h	96.43	97.20	94.71	96.03	97.61
5 h	90.67	92.48	87.54	90.25	93.24
8 h	84.74	87.61	78.26	82.61	89.57
12 h	76.58	81.05	70.33	76.98	84.72

4.4.2. The metabolic stability of the lead lantadene congeners in human blood plasma

To study plasma hydrolysis or susceptibility of lantadene ester congeners **50**, **51**, **63**, **64**, and **79** towards human blood plasma esterases, they were exposed to 80% human plasma for 0, 15, 30, 60, and 120 min and the extent of the hydrolysis was monitored by HPLC. On exposure to human plasma, lantadene ester congeners **50**, **51**, **63**, **64**, and **79** were hydrolyzed at a notably higher rate than the rate of their hydrolysis observed in the simulated gastric fluid. A level of lantadene ester congeners hydrolyzed was found to be 0.0, 25.84, 45.32, 53.19, and 63.25% of **50**, 0.0, 25.78, 44.50, 51.87, and 60.76% of **51**, 0.0, 27.86, 48.86, 56.71, and 70.10% of **63**, 0.0, 27.04, 47.38, 54.50, and 66.74% of **64**, 0.0, 19.13, 34.52, 43.91, and 55.65% of **79** after the exposure period of 0, 15, 30, 60, and 120 min, respectively (**Table 4.7**). Lantadene ester congener **51** showed a slightly lesser degree of hydrolysis than **50**, while congener **64** was hydrolyzed in slightly lesser extent than **63**. HPLC results indicated that lantadene congeners **50**, **51**, **63**, **64**, and **79** underwent rapid hydrolysis in the human blood plasma to liberate the parent drug molecules to reach the site of action, while in the simulated gastric fluid of pH 2, they survived the gastric conditions.

The stability of an ester depends on the reactivity of carbonyl carbon; because, it gets attacked by the reactive functional groups. In the synthesized lantadene ester congeners **50**, **51**, **63**, and **64**, the oxygen atom neighboring to the carbonyl carbon of the ester function is an electron withdrawing in nature and hence, it decreased the electron density on the carbonyl carbon. In this process, electron deficient carbonyl carbon would become more prone to suffer a nucleophilic attack and ultimately undergoes hydrolysis. The ester congener **51** and **64** showed a slower rate of hydrolysis than **50** and **63**, respectively; because, they possessed geminal methyl groups in the C-22 ester side chain. The geminal methyl groups would bear slightly higher ability to decrease the electrophilicity of the ester carbonyl carbon. On the contrary, methyl groups of the side chain of ester congener **50** and **63** were present in the vicinal position and therefore, **50** and **63** exhibited a slightly higher degree of hydrolysis than **51** and **64**, respectively.

In general, cinnamic acid–lantadene conjugates (**50** and **51**) displayed higher resistance towards chemical and plasma hydrolysis than diclofenac–lantadene conjugates (**63** and **64**) as α,β-unsaturated carbonyl carbon system is present in the 3-cinnamolyoxy substituted compounds **50** and **51**, which in turn would increase the electron density on the electron deficient ester carbonyl carbon to a greater extent than the 3-(2-(2-(2,6-dichlorophenylamino) phenyl)acetoyloxy substituted or diclofenac moiety bearing compounds **63** and **64**. Consequently, the ester carbonyl carbon of **50** and **51** would comparatively become less susceptible to the nucleophilic attack and thereby experienced a lesser degree of hydrolysis than **63** and **64**. The lantadene ester congener **79** showed the least hydrolysis among the compounds **50**, **51**, **63**, **64**, and **79**, as it bears diclofenac or aromatic moiety at both the C-3 and C-22 positions, while the rest of the compounds **50**, **51**, **63**, and **64** possess either a 22β-angeloyloxy or a 22β-senecioyloyloxy aliphatic side chain at C-22 position. As a result, the ester carbonyl carbon at both the C-3 and C-22 positions in **79** was relatively less

electron deficient than that of congeners **50**, **51**, **63**, and **64**. In other words, the lantadene ester congener **79** possessed a less cumulative chance (considering both the C-3 and C-22 ester bonds) to suffer a nucleophilic attack than the rest of the compounds **50**, **51**, **63**, and **64**. As a reason, the lantadene ester congener **79** demonstrated comparatively least hydrolysis.

Table 4.7. The metabolic stability of the lead lantadene congeners (**50–51, 63–64**, and **79**) in human blood plasma

Time	**% congeners remaining in human blood plasma**				
	Compd. **50**	Compd. **51**	Compd. **63**	Compd. **64**	Compd. **79**
0 min	100	100	100	100	100
15 min	74.16	74.72	72.14	72.96	80.87
30 min	54.68	55.50	51.14	52.62	65.48
60 min	46.81	48.13	43.29	45.50	56.09
120 min	36.75	39.24	29.90	33.26	44.35

4.5. Molecular docking studies

Molecular docking study was performed to rationalize the obtained biological results and to explain the possible interactions that might take place between the lead lantadene congeners **51**, **63**, **79** and IKK*β*. Before the discovery of the crystal structure of IKK*β* by Xu *et al*. in 2011 [14], molecular docking of ligands to the IKK*β* has been reported either by performing comparative modeling using the BLAST algorithm for template selection and the automated Modeler or by using the Swiss-Model server for model building [95]. During literature survey we did not come across any study that used the 3D crystal structure of IKK*β* for molecular docking analysis. Newly discovered crystal structure of IKK*β* revealed 8 chains, and the human IKK*β* kinase domain consisting of 15–312 residues [96]. Previous research revealed that Tyr-98 residue interacts with the adenine base of the ATP molecule by hydrophobic contact [95]. The NH of Cys-99 acts as a hydrogen bond donor to adenine base,

while carbonyl oxygen of Glu-97 acts as a hydrogen acceptor [95]. In our study, lantadene congeners were docked into the active site of IKK*β* (PDB ID: 3QA8) using AutoDock tools 1.5.4.

The lead lantadene congener **51** is a prodrug or hybrid compound of two potent anticancer moieties, *i.e.* reduced lantadene B and cinnamic acid, and at the site of action it is supposed to be hydrolyzed back into the parent moieties. Therefore, we docked both of the parent moieties, *i.e.* reduced lantadene B (**moiety A**) and cinnamic acid (**moiety B**) into the active site of IKK*β* (**Fig. 4.6a**–**4.6d**). The estimated free energy of binding of the docked prodrug **moiety A** was found to be –5.87 kcal/mol. Analyses of the docked complex (**Fig. 4.6a**–**4.6b**) indicated that 22*β*-senecioyloxy side chain and C-28 carboxylic group were critical for the IKK*β* inhibitory activity. Both the oxygens of the ester function of 22*β*-senecioyloxy side chain interacted with the amine hydrogens of Arg-31 by means of hydrogen bonding (O=C–O…H–N, 2.3 Å and O–C=O…H–N, 2.7 Å). Furthermore, the carbonyl oxygen of the ester group formed a hydrogen bond with the Gln-40 residue of the target protein (O–C=O…H–N, 2.2 Å). The hydroxyl oxygen of the C-28 carboxylic group showed a hydrogen bond with the hydroxyl hydrogen of Tyr-98 residue (O=C–O…H–O, 1.9 Å), whereas carbonyl oxygen of the acid function exhibited hydrogen bonding with the Gly-101 residue of the IKK*β* (O–C=O…H–N, 1.9 Å). Apart from hydrogen bondings, pentacyclic triterpenoid scaffold of the prodrug **moiety A** also showed hydrophobic and van der Waal interactions with the Leu-104, Val-152, Leu-153, Leu-160, and Ile-161 residues of the target protein, while the 22*β*-senecioyloxy side chain demonstrated hydrophobic and van der Waal interactions with the Leu-21 and Val-41 residues of the IKK*β* (**Fig. 4.6b**).

The estimated free energy of binding of the prodrug **moiety B** (cinnamic acid) of **51** to IKK*β* was found to be –4.65 kcal/mol. Analyses of the docked complex (**Fig. 4.6c**–**4.6d**) showed that the hydroxyl oxygen of the carboxylic function was hydrogen bonded to Tyr-98 (O=C–O…H–O, 2.0 Å), whereas carbonyl

oxygen of the carboxylic function formed a hydrogen with the Gly-102 residue of the IKKβ (O–C=O…H–N, 2.1 Å). In addition, carbonyl oxygen of the acid group exhibited hydrogen bonding with Asp-103 residue of the target protein with a distance of 2.2 Å (O–C=O…H–N). Furthermore, both the oxygens of the carboxylic acid function also interacted with Lys-106 residue of the target protein (O=C–O…H–N, 2.3 Å and O–C=O…H–N, 1.9 Å). The aromatic scaffold of the **moiety B** exhibited hydrophobic and van der Waal interactions with Met-96 and Ile-161 residues of the IKKβ protein (**Fig. 4.6d**).

The lead compound **63** is a prodrug or hybrid of anticancer and anti-inflammatory moieties and at the site of action, it is supposed to get hydrolyzed back into the parent moieties, *i.e.* reduced lantadene A (**moiety A**) and diclofenac (**moiety B**). The binding mechanism of **moiety B** to COX-2 is well established, as the carboxylic acid group of diclofenac forms hydrogen-bondings with the Ser-530 and Tyr-385 residues of the COX-2 [97]. The phenylacetic acid port of the **moiety B** is surrounded by Tyr-385, Trp-387, Leu-384, and Leu-352 residues, while the dichlorophenyl part is involved in van der Waals interactions with Val-349, Ala-527, Leu-531, and Val-523 residues of the COX-2 [97]. As the binding mechanism of the prodrug **moiety B** (diclofenac) to its target site (COX-2) is already known; hence, molecular docking analysis of prodrug **moiety A** to IKKβ was only performed.

The estimated free energy of binding of the docked complex of prodrug **moiety A** of **63** and IKKβ (**Fig. 4.7a**–**4.7d**) was found to be –4.67 kcal/mol. Further analysis of the docked complex showed that the prodrug **moiety A** interacted with the Arg-31, Tyr-98, and Gly-101 residues of the IKKβ via hydrogen bonding (**Fig. 4.7b** and **4.7c**). It was observed that 22β-angeloyloxy side chain was crucial for the IKKβ inhibitory activity. The ester group oxygen of the 22β-angeloyloxy side chain formed a hydrogen bond with the NH of Arg-31 residue (O…H–N, 2.6 Å). Another functionality that showed the paramount importance for IKKβ inhibitory activity was C-28 carboxylic group. Both the oxygens, as

well as hydrogen of the carboxylic group were involved in the hydrogen bond formation with the Arg-31, Tyr-98, and Gly-101 residues of the IKKβ. The carbonyl oxygen of C-28 carboxylic group exhibited hydrogen bondings with NH of Arg-31 and OH of Tyr-98, with a bond distance of 1.90 and 2.0 Å, respectively. The hydroxyl oxygen of C-28 carboxylic group showed hydrogen-bonding with the Gly-101 residue of the IKKβ (O=C–O…H–N, 2.1 Å), while the hydroxyl hydrogen of carboxylic group formed a hydrogen bond with the Tyr-98 (O=C–O–H…O, 2.1 Å) residue of the protein. Apart from hydrogen bondings, hydrophobic and van der Waal interactions were also observed between the prodrug **moiety A** of **63** and the target IKKβ (**Fig. 4.7d**). The stereoview of the docked complex showed that the non-polar amino acids Leu-21, Val-41, Val-74, and Met-96 were encircling the aliphatic side chain of the prodrug **moiety A**; indicating the strong possibility of interactions between these residues and side chain. Strong hydrophobic or van der Waal interaction was observed between the ring A of the **moiety A** and the Pro-155 residue of the target protein. The pentacyclic triterpenoid scaffold of the prodrug **moiety A** also showed weak hydrophobic and van der Waal interactions with the Leu-153, Leu-160, and Ile-161 residues of the target IKKβ.

Besides hydrogen, hydrophobic, and van der Waal interactions, the SH group of Cys-99 residue of the IKKβ that acts as a nucleophile was projected towards the β-carbon of the 22β-senecioyloxy side chain of **moiety A** (reduced lantadene B) of **51** (**Fig. 4.6b**) and 22β-angeloyloxy side chain of **moiety A** (reduced lantadene A) of **63** (**Fig. 4.7d**). This indicates possible covalent Michael addition reaction between the Cys-99 and the β-carbon of the C-22 side chains that might have played a central role in the IKKβ inhibitory potency of the lead lantadene congeners **51** and **63**.

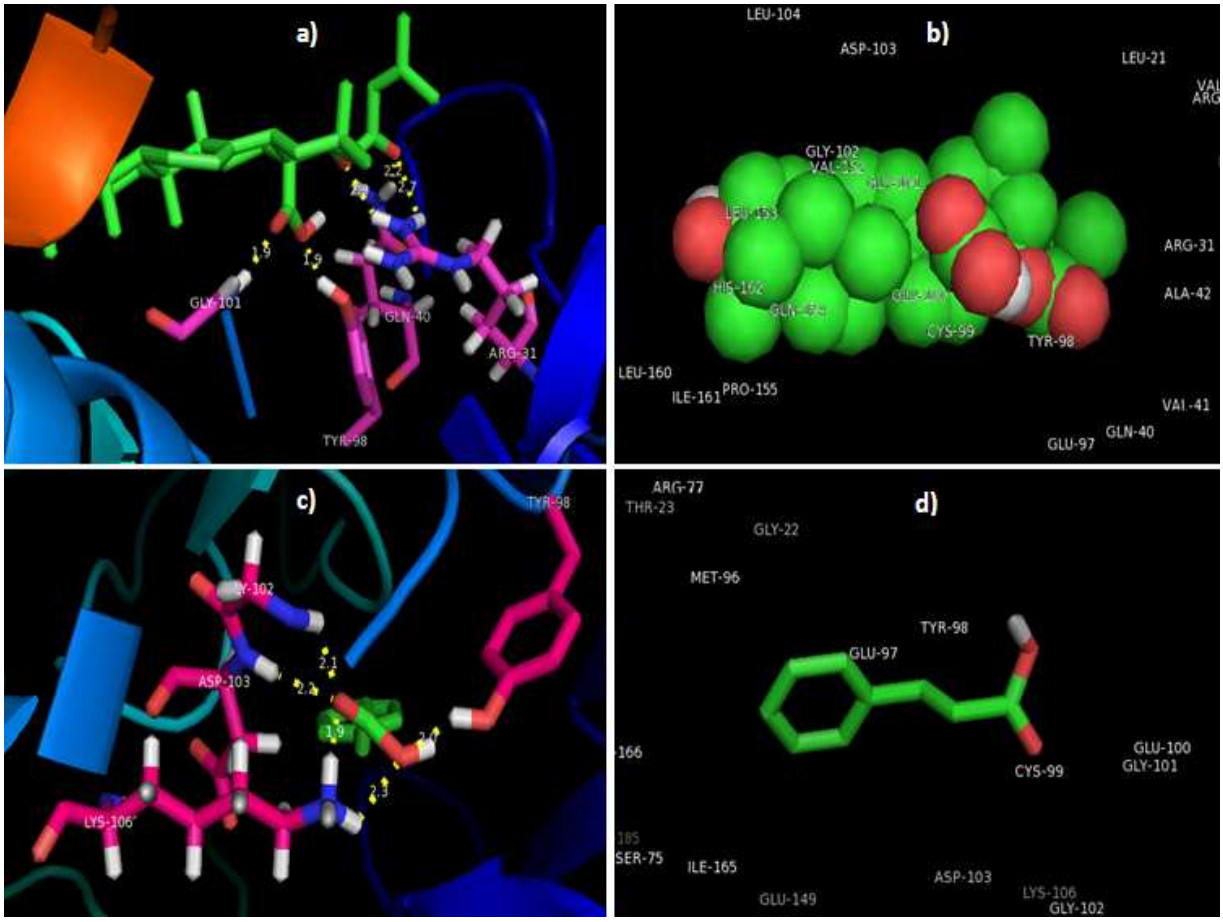

Figure 4.6. Molecular docking of the lead lantadene–cinnamic acid ester conjugate **51** (prodrug **moieties A** and **B**) into the active site of IKKβ. **a**) Binding of prodrug **moiety A** of **51** into the active site of IKKβ. The amino acids Arg-31, Gln-40, Tyr-98, and Gly-101 involved in the hydrogen bond interactions with the prodrug **moiety A**, are highlighted; **b**) Stereoview of the docked structure of prodrug **moiety A** of **51** into the active site of IKKβ. The amino acid residues involved in hydrogen, hydrophobic, and van der Waal interactions with prodrug **moiety A**, are highlighted; **c**) Binding of prodrug **moiety B** of **51** within the active site of IKKβ. The amino acid residues Tyr-98, Gly-102, Asp-103, and Lys-106 involved in the hydrogen bond interactions with the prodrug **moiety B**, are highlighted; **d**) Docking of prodrug **moiety B** of **51** into the active site of IKKβ. The amino acid residues engaged in hydrogen, hydrophobic, and van der Waal interactions with the prodrug **moiety B**, are highlighted.

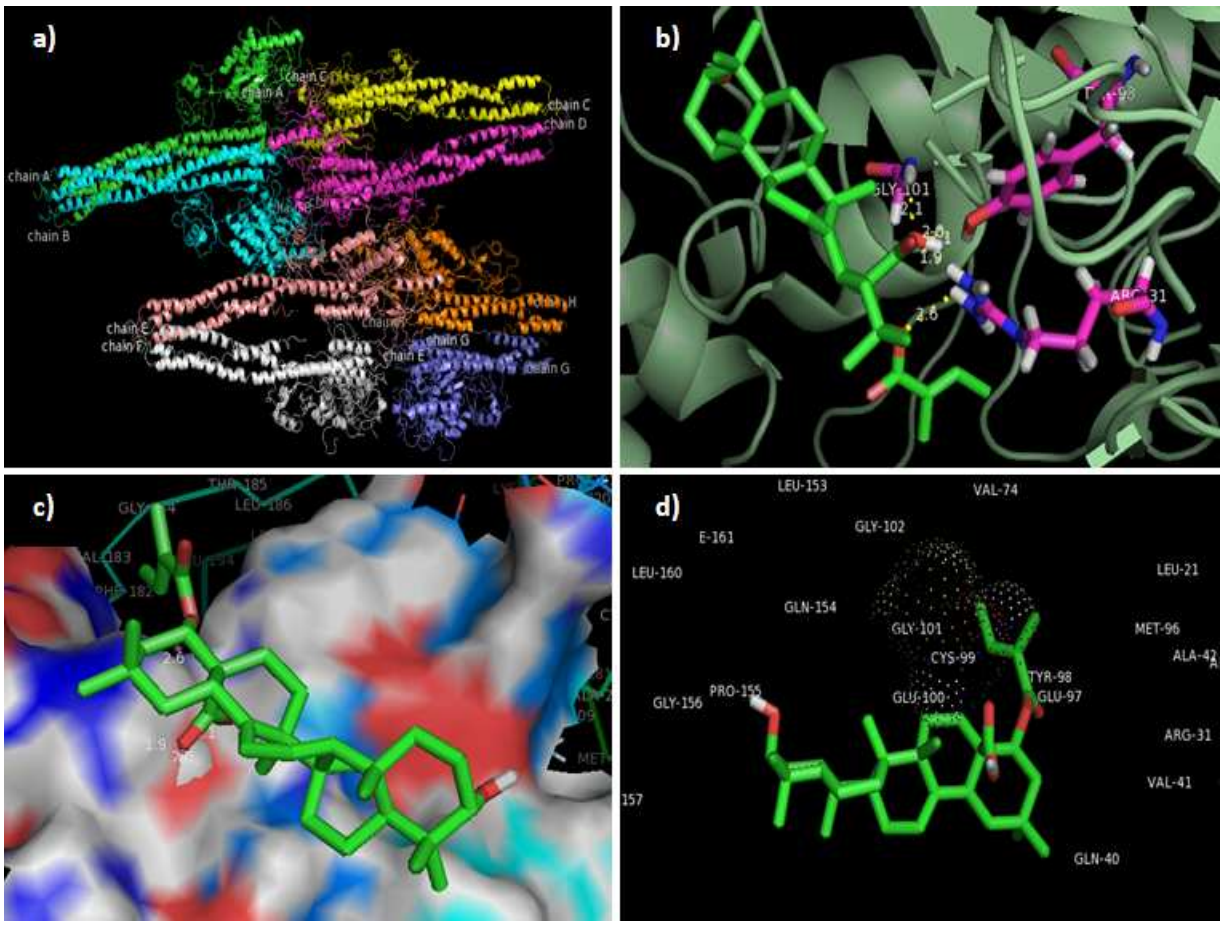

Figure 4.7. Molecular docking of the prodrug **moiety A** of the lead lantadene–diclofenac ester conjugate **63** into the active site of IKK*β*. **a)** 3D crystal structure of IKK*β* (PDB ID: 3QA8); **b)** Docking of prodrug **moiety A** of **63** into the active site of IKK*β*. The amino acids Arg-31, Tyr-98, and Gly-101 involved in the hydrogen bond interactions with prodrug **moiety A**, are highlighted; **c)** Binding orientation of prodrug **moiety A** of **63** within the active site of IKK*β*; **d)** Docking of prodrug **moiety A** of **63** into the binding site of IKK*β*. The amino acid residues of IKK*β* present around the docked structure of prodrug **moiety A** of **63**, are highlighted. The Cys-99 residue of IKK*β* involved in covalent binding with the side chain carbon (*β*-carbon) of the prodrug **moiety A** is highlighted in dot surface with red dots indicating the SH group of Cys-99 projected towards side chain carbon (*β*-carbon) of prodrug **moiety A** of **63**.

Another lead lantadene ester congener **79** is a conjugate of anticancer moiety 22*β*-hydroxy-oleanolic acid or 3*β*,22*β*-dihydroxy-olean-12-en-28-oic acid (**moiety A**) and anti-inflammatory moiety diclofenac (**moiety B**). The peculiar thing about this conjugate is that it bears two diclofenac scaffolds, one at C-3 position, whiles another at C-22 position, and it was found to be the most potent inhibitor of COX-2, among all the tested compounds. This conjugate also displayed considerable degree of inhibitions of NF-κB and IKK*β* with IC_{50}s in a single digit micro-molar range. Though, the binding of diclofenac (**moiety B**) with the COX-2 is extensively researched and already accounted, and we too have discussed it in the previous section; therefore, we only docked NF-κB and IKK*β* inhibitory **moiety A** into the active site of IKK*β*, which is shown in **Fig. 4.8a**–**4.8b**. The estimated free energy of binding of **moiety A** of **79** to IKK*β* was found to be –3.89 kcal/mol. The closer analysis of the docked complex showed that the C-28 carboxylic group of the **moiety A** showed three hydrogen bond interactions with the Arg-31 and Tyr-98 residues of the IKK*β* (**Fig. 4.8a**). The carbonyl oxygen of the carboxylic group of **moiety A** exhibited two hydrogen bonds, as i) HO–C=O…H–O-Tyr-98, 2.6 Å and ii) HO–C=O…H–N-Arg-31, 2.8 Å. The remaining oxygen of the carboxylic group was also hydrogen bonded with the Arg-31 residue of the IKK*β* (O=C–O…H–N, 2.8 Å). Aside from hydrogen bond interactions, rings A, B, and C part of the **moiety A** was projected into the hydrophobic cavity created by the Ile-151, Val-152, Leu-153, Pro-155, Leu-160, and Ile-161 residues, while rings D and E demonstrated hydrophobic and van der Waals contacts with the Lys-18, Leu-21, Leu-30, and Val-41 residues of the IKK*β*. In brief, the C-28 carboxylic acid group of the **moiety A** and its protrusion into the hydrophobic cavity as defined earlier along with the other hydrophobic and van der Waals contacts were accountable for the IKK*β* inhibitory activity of the lead prodrug **79**.

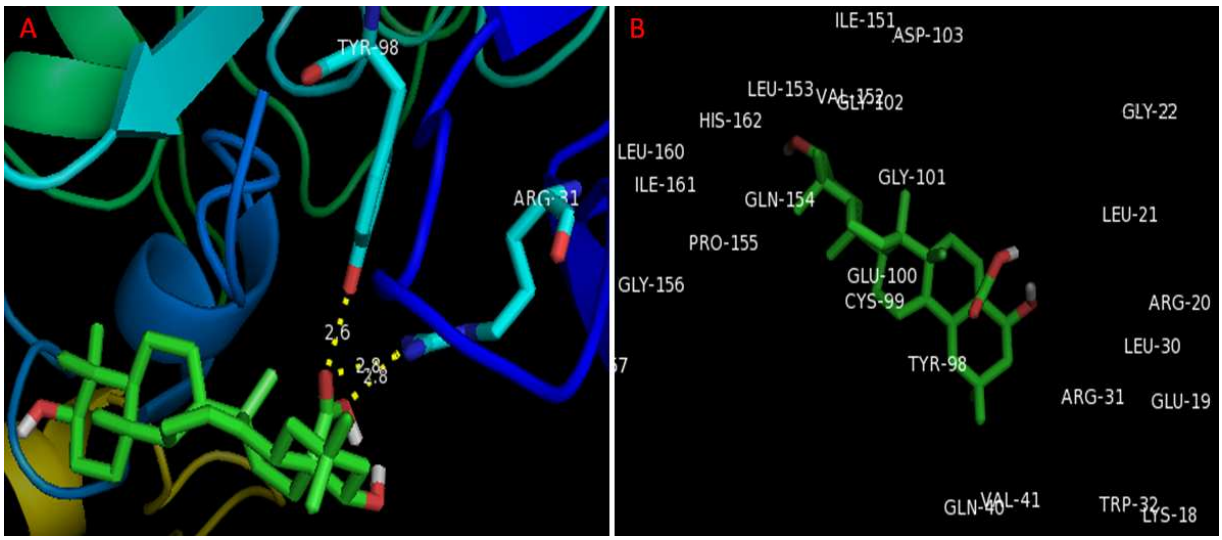

Figure 4.8. Molecular docking of the prodrug **moiety A** of the lead 22*β*-hydroxy-oleanolic acid–diclofenac ester conjugate **79** into the active site of IKK*β*. **A)** The amino acid residues Arg-31 and Tyr-98 of IKK*β* involved in the hydrogen bond interactions with the **moiety A** (22*β*-hydroxy-oleanolic acid), are highlighted; **B)** The amino acid residues of the IKK*β* present in the surroundings of the **moiety A** and also involved in the hydrogen, hydrophobic, and van der Waals interactions with the **moiety A** of **79**, are highlighted.

CHAPTER 5

CONCLUSIONS

The combination therapy in recent years, is increasingly finding a place among the principal strategies to combat the issues pertaining to drug's bioavailability, toxicity, and resistance. Moreover, the double-edged sword, an approach capable of targeting the two proteins at a time, is a novel and highly promising tactic, with several research groups around the globe are actively working in this direction. Taking consideration of this fact, lantadene–NSAID ester conjugates along with other lantadene congeners were synthesized as the cancer therapeutics, simultaneously inhibiting both the NF-κB and COX-2.

Our developed lantadene–NSAID and other lantadene congeners were highly effective against the IKK and IκBα mediated actions of NF-κB and inflammatory regulators COX-2 and PGE_2. These agents further showed distinct cytotoxicity against A549 lung cancer cells with the majority of the lantadene congeners displaying activity superior to the clinically used drug cisplatin. In advance study, the lead lantadene–diclofenac conjugate **79** further suppressed the NF-κB regulated protein cyclin D1, responsible for proliferation and differentiation of cancerous cells. Additionally, the lead lantadene ester congeners survived the gastric pH conditions, whereas hydrolyzed to a greater extent in the human blood plasma to release the active moieties to reach the site of action.

Currently, efforts are being made to *in vivo* evaluate these lead lantadene ester congeners, namely **50**, **51**, **63**, **64**, and **79** in the hollow fiber assay and a xenograft mouse model. On the whole, while considering the highly active biological profile of our developed lantadene ester congeners, these agents could be therapeutically exploited as novel dual acting anticancer and anti-inflammatory agents. At last but not least, transforming these vital findings

from NF-κB and COX-2 domains into fruitful cancer therapeutics in the coming years should be an attainable target. Much work is, however warranted to further develop these lantadene congeners as potential anticancer and anti-inflammatory agents with improved tumor selectivity and increased potency.

CHAPTER 6

REFERENCES

1. World Health Organization, ‘‘*Cancer*’’, http://www.who.int/cancer/en/, 2014. (Accessed on March 10, 2014).
2. International Agency for Research on Cancer, ‘‘*Cancer stats cancer worldwide*’’, http://publications.cancerresearchuk.org/downloads/product/CS_CS_WORLD.pdf, pp. 2–8, 2011. (Accessed on March 10, 2014).
3. American Cancer Society, ‘‘*Cancer facts & figures 2012*’’ http://www.cancer.org/acs/groups/content/@epidemiologysurveilance/documents/document/acspc-031941.pdf, pp. 1–68, 2012. (Accessed on March 10, 2014).
4. National Institute of Health and Family Welfare, ‘‘*National cancer control programme*’’, http://nihfw.nic.in/ndcnihfw/html/Programmes/NationalCancerControlProgramme.htm, 2014. (Accessed on March 10, 2014).
5. Ruiz F.M., Gil-Redondo R., Morreale A., Ortiz A.R., Fábrega C., Bravo J., ‘‘*Structure-based discovery of novel non-nucleosidic DNA alkyltransferase inhibitors: virtual screening and in vitro and in vivo activities*’’, J. Chem. Inf. Model, vol. 48, pp. 844–854, 2008.
6. Rayburn E.R., Ezell S.J., Zhang R., ‘‘*Anti-inflammatory agents for cancer therapy*’’, Mol. Cell. Pharmacol., vol. 1, pp. 29–43, 2009.
7. Arias J.I., Aller M.A., Arias J., ‘‘*Cancer cell: using inflammation to invade the host*’’, Mol. Cancer, vol. 6, pp. 29, 2007.
8. Coussens L.M., Werb Z., ‘‘*Inflammation and cancer*’’, Nature, vol. 420, pp. 860–867, 2002.
9. Lu Y., Cai Z., Galson D.L., Xiao G., Liu Y., George D.E., Melhem M.F., Yao Z., Zhang J., ‘‘*Monocyte chemotactic protein-1 (MCP-1) acts as a*

paracrine and autocrine factor for prostate cancer growth and invasion'', Prostate, vol. 66, pp. 1311–1318, 2006.

10. Balkwill F., Mantovani A., *''Inflammation and cancer: back to Virchow?''*, Lancet, vol. 357, pp. 539–545, 2001.
11. Hussain S.P., Harris C.C., *''Inflammation and cancer: an ancient link with novel potentials''*, Int. J. Cancer, vol. 121, pp. 2373–2380, 2007.
12. Bharti A.C., Aggarwal B.B., *''Nuclear factor-kappa B and cancer: its role in prevention and therapy''*, Biochem. Pharmacol., vol. 64, pp. 883–888, 2002.
13. Karin M., Ben-Neriah Y., *''Phosphorylation meets ubiquitination: the control of NF-[kappa]B activity''*, Annu. Rev. Immunol., vol. 18, pp. 621–663, 2000.
14. Xu G., Lo Y.C., Li Q., Napolitano G., Wu X., Jiang X., Dreano M., Karin M., Wu H., *''Crystal structure of inhibitor of κB kinase β''*, Nature, vol. 472, pp. 325–330, 2011.
15. DiDonato J.A., Mercurio F., Karin M., *''NF-κB and the link between inflammation and cancer''*, Immunol. Rev., vol. 246, pp. 379–400, 2012.
16. Li F., Sethi G., *''Targeting transcription factor NF-kappaB to overcome chemoresistance and radioresistance in cancer therapy''*, Biochim. Biophys. Acta, vol. 1805, pp. 167–180, 2010.
17. Aggarwal B.B., Shishodia S., Sandur S.K., Pandey M.K., Sethi G., *''Inflammation and cancer: how hot is the link?''*, Biochem. Pharmacol., vol. 2, pp. 1605–1621, 2006.
18. Surh Y.J., Chun K.S., Cha H.H., Han S.S., Keum Y.S., Park K.K., Lee S. S., *''Molecular mechanisms underlying chemopreventive activities of anti-inflammatory phytochemicals: down-regulation of COX-2 and iNOS through suppression of NF-kappa B activation''*, Mutat. Res., vol. 480–481, pp. 243–268, 2001.
19. Wang D., Dubois R.N., *''Prostaglandins and cancer''*, Gut, vol. 55, pp. 115–122, 2006.

20. Cha Y.I., DuBois R.N., ‘‘*NSAIDs and cancer prevention: targets downstream of COX-2*’’, Annu. Rev. Med., vol. 58, pp. 239–252, 2007.
21. Zhang G., Tu C., Zhang G., Zhou G., Zheng W., ‘‘*Indomethacin induces apoptosis and inhibits proliferation in chronic myeloid leukemia cells*’’, Leuk. Res., vol. 24, pp. 385–392, 2000.
22. Maguire A.R., Plunkett S.J., Papot S., Clynes M., O'Connor R., Touhey S., ‘‘*Synthesis of indomethacin analogues for evaluation as modulators of MRP activity*’’, Bioorg. Med. Chem., vol. 9, pp. 745–762, 2001.
23. Gobec S., Brožič P., Rižner T.L., ‘‘*Nonsteroidal anti-inflammatory drugs and their analogues as inhibitors of aldo-keto reductase AKR1C3: new lead compounds for the development of anticancer agents*’’, Bioorg. Med. Chem. Lett., Vol. 15, pp. 5170–5175, 2005.
24. Su B., Chen S., ‘‘*Lead optimization of COX-2 inhibitor nimesulide analogs to overcome aromatase inhibitor resistance in breast cancer cells*’’, Bioorg. Med. Chem. Lett., vol. 19, pp. 6733–6735, 2009.
25. Schmeltzer R.C., Schmalenberg K.E., Uhrich K.E., ‘‘*Synthesis and cytotoxicity of salicylate-based poly(anhydride esters)*’’, Biomacromolecules, vol. 6, pp. 359–367, 2005.
26. Congiu C., Cocco M.T., Lilliu V., Onnis V., ‘‘*New potential anticancer agents based on the anthranilic acid scaffold: synthesis and evaluation of biological activity*’’, J. Med. Chem., vol. 48, pp. 8245–8252, 2005.
27. Banekovich C., Ott I., Koch T., Matuszczaka B., Gust R., ‘‘*Synthesis and biological activities of novel dexibuprofen tetraacetylriboflavin conjugates*’’, Bioorg. Med. Chem. Lett., vol. 17, pp. 683–687, 2007.
28. Barbarić M., Kralj M., Marjanović M., Husnjak I., Pavelić K., Filipović-Grčić J., Zorc D., Zorc B., ‘‘*Synthesis and in vitro antitumor effect of diclofenac and fenoprofen thiolated and nonthiolated polyaspartamide-drug conjugates*’’, Eur. J. Med. Chem., vol. 42, pp. 20−29, 2007.
29. Romeiro N.C., Sant’Anna C.M., Lima L.M., Fraga C.A., Barreiro E.J., ‘‘*NSAIDs revisited: putative molecular basis of their interactions with*

peroxisome proliferator-activated gamma receptor (PPARγ)'', Eur. J. Med. Chem., vol. 43, pp. 1918–1925, 2008.

30. Bass S.E., Sienkiewicz P., MacDonald C.J., Cheng R.Y., Sparatore A., Del Soldato P., Roberts D.D., Moody T.W., Wink D.A., Yeh G.C., ‘‘*Novel dithiolethione-modified nonsteroidal anti-inflammatory drugs in human hepatoma HepG2 and Colon LS180 cells*’’, Clin. Cancer Res., vol. 15, pp.1964–1972, 2009.
31. Wittine K., Benci K., Rajić Z., Zorc B., Kralj M., Marjanović M., Pavelić K., De Clercq E., Andrei G., Snoeck R., Balzarini J., Mintas M., ‘‘*The novel phosphoramidate derivatives of NSAID 3-hydroxypropylamides: synthesis, cytostatic and antiviral activity evaluations*’’, Eur. J. Med. Chem., vol. 44, pp. 143−151, 2009.
32. Zawidlak-Wegrzyńska B., Kawalec M., Bosek I., Łuczyk-Juzwa M., Adamus G., Rusin A., Filipczak P., Głowala-Kosińska M., Wolańska K., Krawczyk Z., Kurcok P., ‘‘*Synthesis and antiproliferative properties of ibuprofen–oligo(3-hydroxybutyrate) conjugates*’’, Eur. J. Med. Chem., vol. 45, pp. 1833–1842, 2010.
33. Fogli S., Banti I., Stefanelli F., Picchianti L., Digiacomo M., Macchia M., Breschi M.C., Lapucci A., ‘‘*Therapeutic potential of sulindac hydroxamic acid against human pancreatic and colonic cancer cells*’’, Eur. J. Med. Chem. vol. 45, pp. 5100−5107, 2010.
34. Kapadia G.J., Azuine M.A., Shigeta Y., Suzuki N., Tokuda H., ‘‘*Chemopreventive activities of etodolac and oxyphenbutazone against mouse skin carcinogenesis*’’, Bioorg. Med. Chem. Lett., vol. 20, pp. 2546–2548, 2010.
35. Desai D., Sinha I., Null K., Wolter W., Suckow M.A., King T., Amin S., Sinha R., ‘‘*Synthesis and antitumor properties of selenocoxib-1 against rat prostate adenocarcinoma cells*’’, Int. J. Cancer, vol. 127, pp. 230–238, 2010.

36. Liu M., Yuan M., Li Z., Cheng Y.K., Luo H.B., Hu X., ‘‘*Structural investigation into the inhibitory mechanisms of indomethacin and its analogues towards human glyoxalase I’’*, Bioorg. Med. Chem. Lett., vol. 21, pp. 4243–4247, 2011.
37. Su Y.H., Chiang L.W., Jeng K.C., Huang H.L., Chen J.T., Lin W.J., Huang C.W., Yu C.S., ‘‘*Solution-phase parallel synthesis and screening of anti-tumor activities from fenbufen and ethacrynic acid libraries*’’, Bioorg. Med. Chem. Lett., vol. 21, pp. 1320–1324, 2011.
38. Chennamaneni S., Zhong B., Lama R., Su B., ‘‘*COX inhibitors Indomethacin and sulindac derivatives as antiproliferative agents: synthesis, biological evaluation, and mechanism investigation*’’, Eur. J. Med. Chem., vol. 56, pp. 17−29, 2012.
39. Rosenbaum C., Röhrs S., Müller O., Waldmann H., ‘‘*Modulation of MRP-1-mediated multidrug resistance by indomethacin analogues*’’, J. Med. Chem., vol. 48, pp. 1179–1187, 2005.
40. Bernardi A., Jacques-Silva M.C., Delgado-Cañedo A., Lenz G., Battastini A.M., ‘‘*Nonsteroidal anti-inflammatory drugs inhibit the growth of C6 and U138-MG glioma cell lines*’’, Eur. J. Pharmacol., vol. 532, pp. 214–222, 2006.
41. Lee B.S., Yoon C.W., Osipov A., Moghavem N., Nwachokor D., Amatya R., Na R., Pantoja J.L., Pham M.D., Black K.L., Yu J.S., ‘‘*Nanoprodrugs of NSAIDs: Preparation and characterization of flufenamic acid nanoprodrugs*’’, J. Drug Deliv., vol. 980720, pp. 1−13, 2011.
42. Yeh R.K., Chen J., Williams J.L., Baluch M., Hundley T.R., Rosenbaum R.E., Kalala S., Traganos F., Benardini F., del Soldato P., Kashfi K., Rigas B., ‘‘*NO-donating nonsteroidal antiinflammatory drugs (NSAIDs) inhibit colon cancer cell growth more potently than traditional NSAIDs: a general pharmacological property?*’’, Biochem. Pharmacol., vol. 67, pp. 2197–2205, 2004.

43. Bézière N., Goossens L., Pommery J., Vezin H., Touati N., Hénichart J.P., Pommery N., ‘‘*New NSAIDs-NO hybrid molecules with antiproliferative properties on human prostatic cancer cell lines*’’, Bioorg. Med. Chem. Lett., vol. 18, pp. 4655–4657, 2008.
44. Stewart G.D., Nanda J., Brown D.J., Riddick A.C., Ross J.A., Habib F.K., ‘‘*NO-sulindac inhibits the hypoxia response of PC-3 prostate cancer cells via the Akt signalling pathway*’’, Int. J. Cancer, vol. 124, pp. 223–232, 2009.
45. Kodela R., Chattopadhyay M., Kashfi K., ‘‘*NOSH-aspirin: a novel nitric oxide–hydrogen sulfide-releasing hybrid: a new class of anti-inflammatory pharmaceuticals*’’, ACS Med. Chem. Lett., vol. 3, pp. 257–262, 2012.
46. Cheng H., Mollica M.Y., Lee S.H., Wang L., Velázquez-Martínez C.A., Wu S., ‘‘*Effects of nitric oxide-releasing nonsteroidal anti-inflammatory drugs (NONO-NSAIDs) on melanoma cell adhesion*’’, Toxicol. Appl. Pharmacol., vol. 264, pp. 161–166, 2012.
47. Ott I., Schmidt K., Kircher B., Schumacher P., Wiglenda T., Gust R., ‘‘*Antitumor-active cobalt-alkyne complexes derived from acetylsalicylic acid: studies on the mode of drug action*’’, J. Med. Chem., vol. 48, pp. 622−629, 2005.
48. Rubner G., Bensdorf K., Wellner A., Kircher B., Bergemann S., Ott I., Gust R., ‘‘*Synthesis and biological activities of transition metal complexes based on acetylsalicylic acid as neo-anticancer agents*’’, J. Med. Chem., vol. 53, pp. 6889–6898, 2010.
49. Rubner G., Bensdorf K., Wellner A., Bergemann S., Ott I., Gust R., ‘‘*[Cyclopentadienyl]metalcarbonyl complexes of acetylsalicylic acid as neo-anticancer agents*’’, Eur. J. Med. Chem., vol. 45, pp. 5157−5163, 2010.
50. O’Connor M., Kellett A., McCann M., Rosair G., McNamara M., Howe O., Creaven B.S., McClean S., Kia A.F., O’Shea D., Devereux M.,

‘‘*Copper(II) Complexes of salicylic acid combining superoxide dismutase mimetic properties with DNA binding and cleaving capabilities display promising chemotherapeutic potential with fast acting in vitro cytotoxicity against cisplatin sensitive and resistant cancer cell lines*’’, J. Med. Chem., vol. 55, pp. 1957−1968, 2012.

51. Patrono C., Rocca B., ‘‘*Nonsteroidal antiinflammatory drugs: past, present and future*’’, Pharmacol. Res., Vol. 59, pp. 285–289, 2009.
52. Rayburn E.R., Ezell S.J., Zhang R., ‘‘*Anti-Inflammatory agents for cancer therapy*’’, Mol. Cell. Pharmacol., vol. 1, pp. 29–43, 2009.
53. Arun B., Goss P., ‘‘*The role of COX-2 inhibition in breast cancer treatment and prevention*’’, Semin. Oncol., vol. 31, pp. 22–29, 2014.
54. Hwang D.H., Fung V., ‘‘Dannenberg A,J., ‘‘*National Cancer Institute workshop on chemopreventive properties of nonsteroidal anti-inflammatory drugs: role of COX-dependent and -independent mechanisms*’’, Neoplasia, vol. 4, pp. 91–97, 2002.
55. Achiwa H., Yatabe Y., Hida T., Kuroishi T., Kozaki K., Nakamura S., Ogawa M., Sugiura T., Mitsudomi T., Takahashi T., ‘‘*Prognostic significance of elevated cyclooxygenase 2 expression in primary, resected lung adenocarcinomas*’’, Clin. Cancer Res. vol. 5, pp. 1001–1005, 1999.
56. Sheehan K.M., Sheahan K., O’Donoghue D.P., MacSweeney F., Conroy R.M., Fitzgerald D.J., Murray F.E., ‘‘*The relationship between cyclooxygenase-2 expression and colorectal cancer*’’, JAMA, vol. 282, pp. 1254–1257, 1999.
57. Flossmann E., Rothwell P.M., ‘‘*British doctors aspirin trial and the UK-TIA aspirin trial. Effect of aspirin on long-term risk of colorectal cancer: consistent evidence from randomised and observational studies*’’, Lancet, vol. 369, pp. 1603–1613, 2007.
58. Bardia A., Ebbert J.O., Vierkant R.A., Limburg P.J., Anderson K., Wang A.H., Olson J.E., Vachon C.M., Cerhan J.R., ‘‘*Association of aspirin and*

nonaspirin nonsteroidal anti-inflammatory drugs with cancer incidence and mortality'', J. Natl. Cancer Inst., vol. 99, pp. 881–889, 2007.

59. Cruz-Correa M., Hylind L.M., Romans K.E., Booker S.V., Giardiello F.M., ''*Long-term treatment with sulindac in familial adenomatous polyposis: a prospective cohort study*'', Gastroenterology, vol. 122, pp. 641–645, 2002.
60. Gill S., Sinicrope F.A., ''*Colorectal cancer prevention: is an ounce of prevention worth a pound of cure?*'', Semin. Oncol., vol. 32, pp. 24–34, 2005.
61. Harris R.E., Chlebowski R.T., Jackson R.D., Frid D.J., Ascenseo J.L., Anderson G., Loar A., Rodabough R.J., White E., McTiernan A., ''*Breast cancer and nonsteroidal anti-inflammatory drugs: prospective results from the Women's Health Initiative*'', Cancer Res., vol. 63, pp. 6096–6101, 2003.
62. Calaluce R., Earnest D.L., Heddens D., Einspahr J.G., Roe D., Bogert C.L., Marshall J.R, Alberts D.S., ''*Effects of piroxicam on prostaglandin E2 levels in rectal mucosa of adenomatous polyp patients: a randomized phase IIb trial*'', Cancer Epidemiol. Biomarkers Prev., vol. 9, pp. 1287–1292, 2009
63. A service of the U.S. National Institute of Health, ''*ClinicalTrials.gov*'', www.clinicaltrials.gov, 2014. (accessed on April 29, 2014)
64. North G.L., ''*Celecoxib as adjunctive therapy for treatment of colorectal cancer*'', Ann. Pharmacother., vol. 35, pp. 1638–1643, 2001.
65. Casanova I., Parreño M., Farré L., Guerrero S., Céspedes M.V., Pavon M.A., Sancho F.J., Marcuello E., Trias M., Mangues R., ''*Celecoxib induces anoikis in human colon carcinoma cells associated with the deregulation of focal adhesions and nuclear translocation of p130Cas*'', Int. J. Cancer, vol. 118, pp. 2381–2389, 2006.

66. Ulrich C.M., Bigler J., Potter J.D., ‘‘*Non-steroidal anti-inflammatory drugs for cancer prevention: promise, perils and pharmacogenetics*’’, Nat. Rev. Cancer, vol. 6, pp. 130–140, 2006.
67. Phillips C., ‘‘*Advisory panel weighs COX-2 inhibitors’ fate*’’, NCI Cancer Bull., vol. 2, pp. 1–2, 2005.
68. Bresalier R.S., Sandler R.S., Quan H., Bolognese J.A., Oxenius B., Horgan K., Lines C., Riddell R., Morton D., Lanas A., Konstam M.A., Baron J.A., ‘‘*Adenomatous polyp prevention on Vioxx (APPROVe) trial investigators. Cardiovascular events associated with rofecoxib in a colorectal adenoma chemoprevention trial*’’, N. Engl. J. Med., vol. 352, pp. 1092–1102, 2005.
69. Wallace J.L., Viappiani S., Bolla M., ‘‘*Cyclooxygenase-inhibiting nitric oxide donators for osteoarthritis*’’, Trends Pharmacol. Sci., vol. 30, pp. 112–117, 2009.
70. Kashfi K., ‘‘*Anti-inflammatory agents as cancer therapeutics*’’, Adv. Pharmacol., vol. 57, pp. 31–89, 2009.
71. Cragg G.M., Newman D.J., ‘‘*Natural products: a continuing source of novel drug leads*’’, Biochim. Biophys. Acta, vol. 1830, pp. 3670–3695, 2013.
72. Molinari G., ‘‘*Natural products in drug discovery: present status and perspectives*’’, Adv. Exp. Med. Biol., vol. 655, pp. 13–27, 2009.
73. Mehta G., Singh V., ‘‘*Hybrid systems through natural product leads: an approach towards new molecular entities*’’, Chem. Soc. Rev., vol. 31, pp. 324–334, 2002.
74. Floss H.G., ‘‘*Natural products derived from unusual variants of the shikimate pathway*’’, Nat. Prod. Rep., vol. 14, pp. 433–452, 1997.
75. Newman D.J., Cragg G.M., ‘‘*Natural products as sources of new drugs over the 30 years from 1981 to 2010*’’, J. Nat. Prod., vol. 75, pp. 311–335, 2012.

76. Kaur J., Sharma M., Sharma P.D., Bansal M.P., ‘‘*Chemopreventive activity of lantadenes on two-stage carcinogenesis model in Swiss albino mice: AP-1 (c-jun), NF κB (p65) and p55 expression by ELISA and immunohistochemical localization*’’, Mol. Cell. Biochem., vol. 314, pp. 1–8, 2008.
77. Kaur J., Sharma M., Sharma P.D., Bansal M.P., ‘‘*Antitumor activity of Lantadenes in DMBA/TPA induced skin tumors in mice: expression of transcription factors*’’, Am. J .Biomed. Sci., vol. 2, pp. 79–90, 2010.
78. Sharma M., Sharma P.D., Bansal M.P., Singh J., ‘‘*Lantadene A-induced apoptosis in human leukemia HL-60 cells*’’, Ind. J. Pharmacol., vol. 39, pp. 140–144, 2007.
79. Sharma M., Sharma P.D., Bansal M.P., ‘‘*Lantadenes and their esters as potential antitumor agents*’’, J. Nat. Prod., vol. 71, pp. 1222–1227, 2008.
80. Tailor N.K., Lee H.B., Sharma M., ‘‘*Synthesis and in vitro anticancer studies of novel C-2 arylidene congeners of lantadenes*’’, Eur. J. Med. Chem., vol. 64, pp. 285–291, 2013.
81. Tailor N.K., Jaiswal V., Lan S.S., Lee H.B., Sharma M., ‘‘*Synthesis, selective cancer cytotoxicity and mechanistic studies of novel analogs of lantadenes*’’, Anticancer Agents Med. Chem., vol. 13, pp. 957–966, 2013.
82. Heynekamp J.J., Weber W.M., Hunsaker L.A., Gonzales A.M., Orlando R.A., Deck L.M., Jagt D.L., ‘‘*Substituted trans-stilbenes, including analogues of the natural product resveratrol, inhibit the human tumor necrosis factor alpha-induced activation of transcription factor nuclear factor kappaB*’’, J. Med. Chem., vol. 49, pp. 7182–7189, 2006.
83. Lorenzo P., Alvarez R., Ortiz M.A., Alvarez S., Piedrafita F.J., de Lera A.R., ‘‘*Inhibition of IkappaB kinase-beta and anticancer activities of novel chalcone adamantyl arotinoids*’’, J. Med. Chem., vol. 51, pp. 5431–5440, 2008.

84. Waffo-Teguo P., Lee D., Cuendet M., Mérillon J., Pezzuto J.M., Kinghorn A.D., ‘‘*Two new stilbene dimer glucosides from grape (Vitis vinifera) cell cultures*’’, J. Nat. Prod., vol. 64, pp. 136–138, 2001.
85. Kim K.S., Cui X., Lee D.S., Sohn J.H., Yim J.H., Kim Y.C., Oh H., ‘‘*Anti-inflammatory effect of neoechinulin a from the marine fungus Eurotium sp. SF-5989 through the suppression of NF-κB and p38 MAPK pathways in lipopolysaccharide-stimulated RAW264.7 macrophages*’’, Molecules, vol. 18, pp. 13245–13259, 2013.
86. Ashikawa K., Majumdar S., Banerjee S., Bharti A.C., Shishodia S., Aggarwal B.B., ‘‘*Piceatannol inhibits TNF-induced NF-kappaB activation and NF-kappaB-mediated gene expression through suppression of IkappaBalpha kinase and p65 phosphorylation*’’, J. Immunol., vol. 169, pp. 6490–6497, 2002.
87. Takada Y., Khuri F.R., Aggarwal B.B., ‘‘*Protein farnesyltransferase inhibitor (SCH 66336) abolishes NF-kappaB activation induced by various carcinogens and inflammatory stimuli leading to suppression of NF-kappaB-regulated gene expression and up-regulation of apoptosis*’’, J. Biol. Chem., vol. 279, pp. 26287–26299, 2004.
88. Bandgar B.P., Sarangdhar R.J., Viswakarma S., Ahamed F.A., ‘‘*Synthesis and biological evaluation of orally active prodrugs of indomethacin*’’, J. Med. Chem., vol. 54, pp. 1191–1201, 2011.
89. Bandgar B.P., Sarangdhar R.J., Ahamed F.A., Viswakarma S., ‘‘*Synthesis, characterization, and biological evaluation of novel diclofenac prodrugs*’’, J. Med. Chem., vol. 54, pp. 1202–1210, 2011.
90. Lawrence T., Willoughby D.A., Gilroy D.W., ‘‘*Anti-inflammatory lipid mediators and insights into the resolution of inflammation*’’, Nat. Rev. Immunol., vol. 2, pp. 787–795, 2002.
91. Ghosh S., Karin M., ‘‘*Missing pieces in the NF-kappaB puzzle*’’, Cell, vol. 109, pp. S81–96, 2002.

92. Guttridge D.C., Albanese C., Reuther J.Y., Pestell R.G., Baldwin Jr A.S., ‘‘*NF-kappaB controls cell growth and differentiation through transcriptional regulation of cyclin D1*’’, Mol. Cell. Biol., vol. 19, pp. 5785–5599, 1999.
93. Hinz M., Krappmann D., Eichten A., Heder A., Scheidereit C., Strauss M., ‘‘*NF-kappaB function in growth control: regulation of cyclin D1 expression and G0/G1-to-S-phase transition*’’, Mol. Cell. Biol., vol. 19, pp. 2690–2698, 1999.
94. Yamamoto K., Arakawa T., Ueda N., Yamamoto S., ‘‘*Transcriptional roles of nuclear factor kappa B and nuclear factor-interleukin-6 in the tumor necrosis factor alpha-dependent induction of cyclooxygenase-2 in MC3T3-E1 cells*’’, J. Biol. Chem., vol. 270, pp. 31315–31320, 1995.
95. Kalia M., Kukol A., ‘‘*Structure and dynamics of the kinase IKK-β – A key regulator of the NF-kappa B transcription factor*’’, J. Struct. Biol., vol. 176, pp. 133–142, 2011.
96. Mercurio F., Zhu H., Murray B.W., Shevchenko A., Bennett B.L., Li J., Young D.B., Barbosa M., Mann M., Manning A., Rao A., ‘‘*IKK-1 and IKK-2: cytokine-activated IkappaB kinases essential for NF-kappaB activation*’’, Science, vol. 278, pp. 860–866, 1997.
97. Blobaum A.L., Marnett L.J., ‘‘*Structural and functional basis of cyclooxygenase inhibition*’’, J. Med. Chem., vol. 50, pp. 1425–1441, 2007.

LIST OF PUBLICATIONS

PATENTS

1. Sharma M., Suthar S.K., ‘‘*An improved process of conversion of Lantadene A & B to reduced Lantadene A & B*’’, Application No. 2867/DEL/2011. (Published).
2. Sharma M., Suthar S.K., ‘‘*An economical and improved process of isolation of antitumor pentacyclic triterpenoid Lantadene B from leaves of weeds Lantana camara L. (pink-edged red flowering variety)*’’, Application No. 1940/DEL/2012. (Published).

RESEARCH PAPERS

1. Suthar S.K., Boon H.L., Sharma M., ‘‘*Novel lung adenocarcinoma and nuclear factor-kappa B (NF-κB) inhibitors: synthesis and evaluation of lantadene congeners*’’, Eur. J. Med. Chem., vol. 74, pp. 135–144, 2014. (Impact factor: 3.432).
2. Suthar S.K., Sharma N., Lee H.B., Nongalleima K., Sharma M., ‘‘*Novel dual inhibitors of nuclear factor-kappa B (NF-κB) and cyclooxygenase-2 (COX-2): synthesis, in vitro anticancer activity and stability studies of lantadene–non steroidal anti-inflammatory drug (NSAIDs) conjugates*’’, Curr. Top. Med. Chem., vol. 14, pp. 991–1004, 2014. (Impact factor: 3.453).
3. Suthar S.K., Lee H.B., Sharma M., ‘‘*The synthesis of non-steroidal anti-inflammatory drug (NSAID)–lantadene prodrugs as novel lung adenocarcinoma inhibitors via the inhibition of cyclooxygenase-2 (COX-2), cyclin D1 and TNF-α-induced NF-κB activation*’’, RSC Adv., vol. 4, pp. 19283–19293, 2014. (Impact factor: 3.708).

4. Suthar S.K., Tailor N., Lee H.B., Sharma M., ‘‘*Reduced lantadenes A and B: semi-synthetic synthesis, selective cytotoxicity, apoptosis induction and inhibition of NO, TNF-α production in HL-60 cells*’’, Med. Chem. Res., vol. 22, pp. 3379–3388, 2013. (Impact factor: 1.612).

REVIEW PAPERS

1. Suthar S.K., Sharma M., ‘‘*Recent developments in chimeric NSAIDs as safer anti-inflammatory agents*’’, Med. Res. Rev., DOI: 10.1002/med.21331. (Impact factor: 8.131).
2. Suthar S.K., Sharma M., ‘‘*Recent developments in chimeric NSAIDs as anticancer agents: Teaching an old dog a new trick*’’, Manuscript under review with Mini-Rev. Med. Chem., 2014. (Impact factor: 3.186).

CONFERENCE PAPER

1. Suthar S.K., Tailor N., Lee H.B., Sharma M., ‘‘*Synthesis of lantadene A and B congeners: Cytotoxicity, apoptosis induction and expression of transcription factors in HL-60 cells*’’, 12th International Congress of Ethnopharmacology, SNPSJU0150, February 17−19, 2012, Kolkata, India.